TESIS DE LA UNIVERSIDAD DE ZARAGOZA

2020 1

Iván Raúl Cristóbal Monreal

Optimización de sistemas híbridos aislados alimentados con fuentes renovables de energía

Departamento

Centro de Investigación de Recursos y Consumos Energéticos (CIRCE)

Director/es

Yusta Loyo, José María
Dufo López, Rodolfo

ISSN 2254-7606

Prensas de la Universidad Universidad Zaragoza

ISSN 2254-7606

Universidad Zaragoza
1542

Tesis Doctoral

OPTIMIZACIÓN DE SISTEMAS HÍBRIDOS AISLADOS ALIMENTADOS CON FUENTES RENOVABLES DE ENERGÍA

Autor

Iván Raúl Cristóbal Monreal

Director/es

Yusta Loyo, José María
Dufo López, Rodolfo

UNIVERSIDAD DE ZARAGOZA

Centro de Investigación de Recursos y Consumos Energéticos (CIRCE)

2017

Universidad Zaragoza

Tesis Doctoral

Optimización de Sistemas Híbridos Aislados Alimentados con Fuentes Renovables de Energía

Autor

D. Iván Raúl Cristóbal Monreal

Directores

Dr. D. José María Yusta Loyo

Dr. D. Rodolfo Dufo López

Departamento de Ingeniería Eléctrica

Universidad Zaragoza

Septiembre de 2017

Esta tesis se presenta en la modalidad de compendio de publicaciones.

Artículos presentados en congresos internacionales:

1. Iván R. Cristóbal Monreal, Rodolfo Dufo López, José María Yusta Loyo. Influence of the battery model in the optimisation of stand-alone renewable systems. ***International Conference on Renewable Energies and Power Quality*** (ICREPQ 2016), ISBN 978-84-608-5473-9. ***Renewable Energy and Power Quality Journal*****,** No.14, May 2016, 185-189, ISSN 2172-038X.

Artículos publicados en revistas incluidas en el *Journal Citation Reports* (JCR):

2. Iván R. Cristóbal Monreal, Rodolfo Dufo López. Optimisation of photovoltaic–diesel–battery stand-alone systems minimising system weight. ***Energy Conversion and Management*** 119 (2016) 279–288.

3. Rodolfo Dufo López, Iván R. Cristóbal Monreal, José María Yusta Loyo. Optimisation of PV-wind-diesel-battery stand-alone systems to minimise cost and maximise human development index and job creation. ***Renewable Energy*** 94 (2016) 280-293.

4. Rodolfo Dufo López, Iván R. Cristóbal Monreal, José María Yusta Loyo. Stochastic-heuristic methodology for the optimisation of components and control variables of PV-wind-diesel-battery stand-alone systems. ***Renewable Energy*** 99 (2016) 919-935.

Informe favorable de los directores de tesis:

Los directores de la presente tesis, el Dr. D. José María Yusta Loyo y el Dr. D. Rodolfo Dufo López, ingenieros industriales y profesores titulares del Departamento de Ingeniería Eléctrica de la Universidad de Zaragoza, hacen constar:

Que D. Iván Raúl Cristóbal Monreal, ingeniero Industrial por la Universidad de Zaragoza, ha realizado bajo su dirección y supervisión la presente tesis doctoral, que lleva por título:

"Optimización de Sistemas Híbridos Aislados Alimentados con Fuentes Renovables de Energía"

y autorizan su presentación en la modalidad de compendio de publicaciones.

Y para que así conste a los efectos oportunos, se firma la presente autorización.

En Zaragoza, Septiembre de 2017

Fdo: Dr. D. José María Yusta Loyo

Fdo: Dr. D. Rodolfo Dufo López

Agradecimientos:

En primer lugar, deseo expresar mi más sincero agradecimiento a mis directores de tesis, D. José María Yusta Loyo y D. Rodolfo Dufo López, por su dedicación, por la confianza ofrecida y por el continuo apoyo que me han brindado durante el desarrollo de este trabajo.

Pero, sobre todo, gracias a mi esposa y a mi hija, por su paciencia, comprensión y solidaridad con este proyecto, por el tiempo que me han concedido, un tiempo robado a nuestra historia familiar. Sin su apoyo nunca hubiera sido posible y, por eso, esta tesis es también suya.

ÍNDICE

1. INTRODUCCIÓN

La producción de energía eléctrica mundial no cesa de aumentar, si bien ha experimentado una desaceleración en los últimos dos años (Figura 1). La mayoría de esta energía eléctrica es transportada mediante las redes de distribución eléctricas desde el lugar de producción hasta el lugar de consumo.

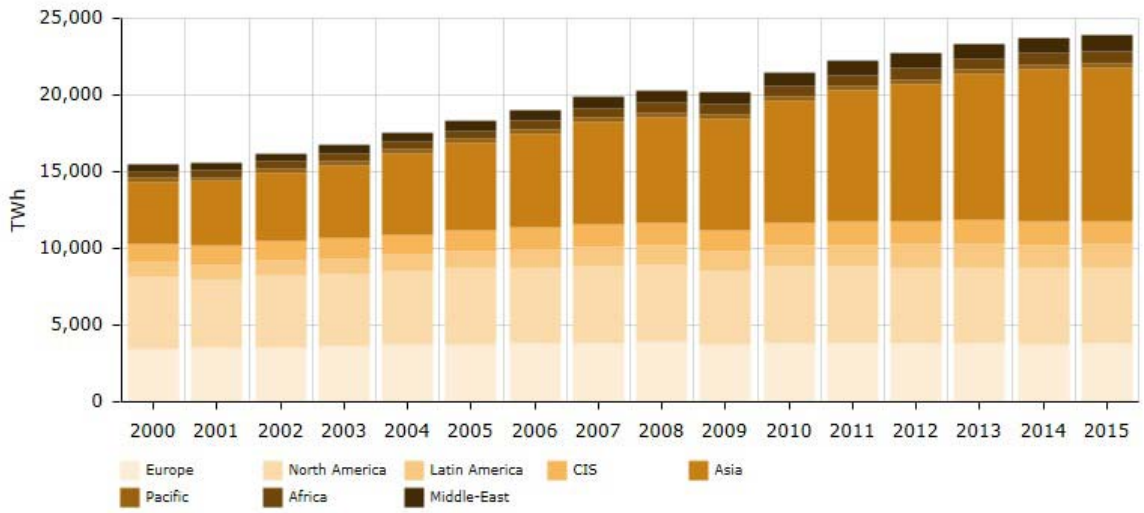

Figura 1. Producción de energía eléctrica mundial [1].

Sin embargo, hay lugares, debido a que el pequeño consumo no lo justifica o cuando la extensión de dichas redes es demasiado costosa (ya que son zonas remotas o existen limitaciones geográficas para los trazados), donde estas redes de distribución no llegan. En estos casos, la alternativa a la red eléctrica es generar “in situ” la propia energía eléctrica que ha de ser consumida. Este tipo de sistemas son los llamados sistemas aislados.

La solución más habitual hasta hace unos años era satisfacer la demanda eléctrica en estos emplazamientos aislados mediante sistemas basados en grupos generadores de corriente alterna. Normalmente, y sobre todo a partir de cierta potencia, los motores se suelen alimentar con combustible diésel.

Pero la inestabilidad del precio de los combustibles fósiles (normalmente en aumento), unido a la necesidad creciente de generar energía de forma limpia y

sostenible, hizo que se orientaran estos sistemas hacia las energías renovables. La mejora de las distintas tecnologías relacionadas con estas fuentes de energía y el descenso de los costes de generación (principalmente de energía fotovoltaica y eólica) ha hecho que desde hace algunos años haya sido una solución muy demanda para satisfacer el consumo energético en muchos lugares aislados. En la siguiente figura se muestra el crecimiento y proyección de la generación de energía eléctrica mediante fuentes renovables.

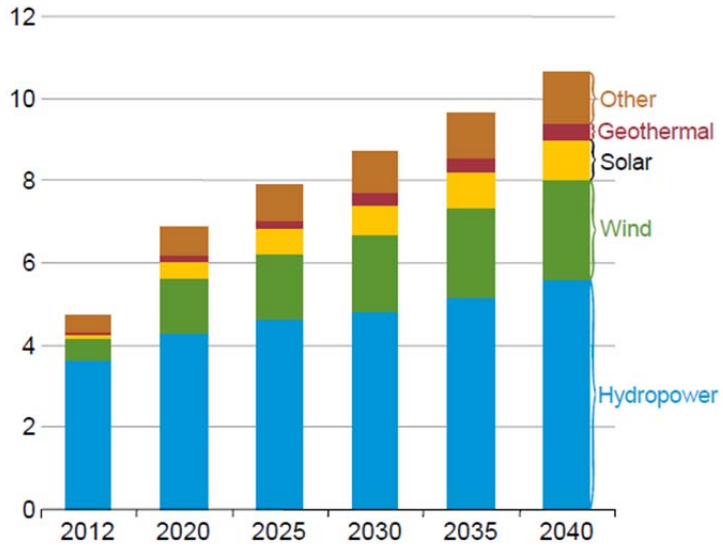

Figura 2. Generación de energía eléctrica mundial mediante fuentes renovables, en miles de TWh [2].

El principal problema de los sistemas basados exclusivamente en un tipo de energía renovable es la variabilidad de la climatología y por lo tanto su carácter intermitente. Ello hace que si se quiere asegurar el suministro, se deba sobredimensionar el sistema de generación, o el sistema de almacenamiento, o ambos; lo que incurre en un encarecimiento global de la instalación.

Una solución al problema anterior son los sistemas híbridos de energías renovables. Estos sistemas de generación emplean dos o más fuentes diferentes de energía para transformarla en energía eléctrica. Gracias a ello, se consigue aumentar la fiabilidad del suministro eléctrico, al estar basado en más de una fuente de energía. Además, al ser sistemas más fiables, se puede disminuir la

capacidad del necesario sistema de almacenamiento de energía (normalmente un banco de baterías de tipo plomo-ácido).

Sin embargo, la tendencia actual, en sistemas de cierta envergadura, es la generación mediante sistemas híbridos entre energías renovables y generadores diésel. Frente a sistemas basados exclusivamente por generadores diésel o frente a sistemas basados en una única fuente de energía renovable, los sistemas híbridos renovables-diésel presentan numerosas ventajas:

a) Suministro eléctrico más fiable, ya que la generación se basa en más de una fuente.
b) Reducción de la capacidad de almacenamiento de energía del sistema debido a que las fuentes de generación son complementarias.
c) Reducción en los costes de mantenimiento y operación al disminuir la capacidad necesaria de almacenamiento del sistema.
d) Menor efecto medioambiental frente a los generadores diésel.
e) No están tan afectados por la evolución de los precios de los combustibles fósiles.
f) El coste de generación de la energía eléctrica es normalmente menor a lo largo de la vida útil del sistema.

Por otro lado, también presentan una serie de desventajas:

a) El coste inicial del sistema suele ser más elevado frente a los generadores diésel, aunque a lo largo de la vida útil el coste de generación pueda ser menor.
b) Al estar compuestos por distintas fuentes de energía y tecnologías, son sistemas en los que su control, mantenimiento y operación resultan más complejos que en otro tipo de sistemas.
c) El empleo de sistemas de almacenamiento (baterías plomo-ácido) y generadores diésel reduce la sostenibilidad medioambiental del sistema.

El continuo aumento de la demanda de energía eléctrica y la inestabilidad de precios de los combustibles fósiles, unido a la reducción de costos y las mejoras

en las distintas tecnologías relacionadas con las fuentes de energía renovables, las mejoras en los sistemas de almacenamiento de energía y en los sistemas de control han hecho que los sistemas híbridos aislados renovables-diésel hayan visto ampliada su difusión para distintas aplicaciones en los últimos años.

Como todo sistema de generación de energía eléctrica, estos sistemas deben cumplir con dos objetivos primordiales: garantizar el suministro de energía eléctrica y reducir al máximo el coste del mismo y de su operación. Ambos objetivos influyen decisivamente en el dimensionado óptimo de cada una de las partes del sistema. En cualquier condición de recursos energéticos y de carga a suministrar, el sobredimensionamiento del sistema aumenta su confiabilidad a expensas del costo, mientras que un dimensionamiento insuficiente sacrifica la confiabilidad para disminuir el costo del sistema. Por tanto, conseguir el tamaño óptimo para un sistema, no solo mejora su fiabilidad, sino que también reduce su coste.

La experiencia demuestra que el proceso de optimización de sistemas híbridos aislados es más complejo que en los sistemas no híbridos, y no se logra de manera fácil utilizando los procedimientos clásicos de optimización [3], ya que el problema que debe resolverse tiene multitud de soluciones posibles (distintas combinaciones de paneles fotovoltaicos, aerogeneradores, generadores diésel, baterías de almacenamiento, distintas estrategias de gestión del sistema, etc.), unido al alto grado de variabilidad que presentan los recursos renovables y a que algunos de los componentes de los sistemas presentan características no lineales hacen que exista un gran número de variables que pueden influir en este proceso de optimización [4].

La práctica totalidad de los sistemas híbridos aislados, por el hecho de estar aislados, disponen de un banco de baterías como sistema de almacenamiento de energía. Por ello, en el primer artículo, se ha estudiado la influencia del modelo utilizado para la estimación de la vida útil de las baterías en la optimización de este tipo de sistemas. En el segundo artículo se presenta la optimización de sistemas híbridos aislados temporales desde el punto de vista del peso del sistema. En algunos casos, donde el transporte de los sistemas (ida y vuelta)

hasta zonas remotas o aisladas puede resultar difícil y/o peligroso, además de suponer un coste elevado, la minimización del peso del mismo puede ser un factor determinante. Se presenta en el tercer artículo una nueva metodología para optimizar sistemas híbridos aislados (zonas rurales sin acceso a la red eléctrica) que minimiza el coste del sistema y maximiza al mismo tiempo el índice de desarrollo humano y la creación de empleo. El último artículo se presenta una nueva metodología para la optimización estocástico-heurística de sistemas híbridos aislados con alimentación renovable, considerando las incertidumbres de distintas variables de entrada teniendo en cuenta sus correlaciones. Al obtenerse las funciones de probabilidad de las distintas variables de los resultados, se dispondrá de mucha más información (que utilizando solamente un enfoque determinista) a la hora de diseñar estos sistemas, que al estar aislados, no disponen de una red que respalde el abastecimiento de energía eléctrica.

1.1 PRESENTACIÓN DE LOS TRABAJOS PUBLICADOS

Los trabajos publicados que conforman esta tesis son:

1. Iván R. Cristóbal Monreal, Rodolfo Dufo López, José María Yusta Loyo. Influence of the battery model in the optimisation of stand-alone renewable systems. *International Conference on Renewable Energies and Power Quality* (ICREPQ 2016), ISBN 978-84-608-5473-9. *Renewable Energy and Power Quality Journal*, No.14, May 2016, 185-189, ISSN 2172-038X. http://www.icrepq.com/icrepq'16/262-16-cristobal.pdf

2. Iván R. Cristóbal Monreal, Rodolfo Dufo López. Optimisation of photovoltaic–diesel–battery stand-alone systems minimising system weight. *Energy Conversion and Management* 119 (2016) 279–288. http://dx.doi.org/10.1016/j.enconman.2016.04.050

3. Rodolfo Dufo López, Iván R. Cristóbal Monreal, José María Yusta Loyo. Optimisation of PV-wind-diesel-battery stand-alone systems to minimise cost and maximise human development index and job creation. *Renewable Energy* 94 (2016) 280-293. http://dx.doi.org/10.1016/j.renene.2016.03.065

4. Rodolfo Dufo López, Iván R. Cristóbal Monreal, José María Yusta Loyo. Stochastic-heuristic methodology for the optimisation of components and control variables of PV-wind-diesel-battery stand-alone systems. *Renewable Energy* 99 (2016) 919-935. http://dx.doi.org/10.1016/j.renene.2016.07.069

1.1.1 *Influence of the battery model in the optimisation of stand-alone renewable systems*.

En los sistemas híbridos aislados con alimentación renovable, el componente con un mayor coste es normalmente el banco de baterías, considerando su coste de adquisición, el coste de operación y mantenimiento (O&M) y la reposición de los componentes cuando alcanzan su vida útil, durante toda la vida útil del sistema en su conjunto. La correcta estimación de la vida útil de las baterías es muy importante, ya que determina el número de reposiciones del banco de baterías durante la vida útil del sistema (que normalmente se considera entre 20 y 25 años, la misma que la vida útil de los paneles fotovoltaicos). Por ejemplo, si la estimación de la vida de las baterías es de 5 años y la vida del sistema es de 25 años, se esperará reponer el banco de baterías 5 veces. Sin embargo, si la vida real de las baterías es de 2,5 años, se deberán reponer 10 veces, y el coste actual neto del sistema (*Net Present Cost*, NPC) y el coste normalizado de la energía (*Levelised Cost of Energy*, LCE) serán mucho mayores que los esperados.

Por tanto, el modelo de las baterías utilizado en las simulaciones y optimizaciones de estos sistemas, tiene gran importancia, ya que es la herramienta que permite estimar la vida de las baterías. Los modelos clásicos como “Ciclos completos equivalentes hasta el fallo” y el “Conteo de ciclos Rainflow”, ampliamente utilizados para estimar la vida útil de las baterías en herramientas de simulación y de optimización [5], solamente consideran la cantidad de energía ciclada por las baterías, sin tener en cuenta las condiciones de operación.

Estas condiciones de operación influyen mucho en la estimación de vida útil de las baterías de tipo plomo-ácido, haciendo que esta sea una tarea compleja. Esta estimación es propensa a errores, y en muchos trabajos de investigación se obtienen valores más altos que los reales. Los procesos más importantes que causan el envejecimiento (pérdida de capacidad) de las baterías son la corrosión anódica y la degradación de la masa activa, incluyendo la pérdida de adherencia

a la rejilla, la sulfatación o formación irreversible de sulfato de plomo en la masa activa, el cortocircuito, la pérdida de agua y la estratificación del electrolito [6].
La pérdida de capacidad por *degradación de la masa activa* se ve principalmente influenciada por el estado de carga de la batería (State Of Charge, SOC), por el tiempo en el que las baterías se encuentran en un estado de carga bajo, por el tiempo desde la última carga completa, por la corriente, por la estratificación del electrolito,… La pérdida de capacidad por *corrosión*, se ve influenciada por la tensión de las celdas, por la temperatura y otros factores [7].

Las baterías sujetas a regímenes de descarga profundos envejecen usualmente por degradación de la estructura de la masa activa positiva. Los ciclos de vida útil de las baterías, mostrados en las hojas de características de los fabricantes (varios cientos de ciclos completos), se obtienen en los laboratorios bajo condiciones standard. A menudo, las condiciones reales son muy diferentes de las condiciones standard. En estos casos, el envejecimiento por degradación de la masa activa, y por lo tanto la vida útil de las mismas puede ser muy diferente (normalmente menor) que la esperada.

En el caso de las baterías estacionarias (operando en condiciones de flotación/carga), el mecanismo más importante de envejecimiento es la corrosión de la rejilla positiva. Las condiciones reales de las baterías estacionarias pueden ser muy diferentes de las condiciones de los test de laboratorio, de tal manera que la vida en flotación puede ser muy diferente (normalmente menor) que la vida en flotación mostrada en las hojas de características (a 20 ó 25 ºC), ya que el efecto de la temperatura en la vida en flotación es aproximadamente un 50% de reducción de la misma por cada 8,3 ºC de incremento en la temperatura media para las baterías de plomo-ácido.

Los modelos clásicos usados para estimar la vida útil de las baterías son simples, sin embargo en muchos casos pueden incurrir en errores grandes. Modelos mucho más complejos como el “Criterio ponderado del flujo de Ah” pueden aportar resultados mucho más precisos [7]. Se comparan en este artículo distintos modelos de baterías de plomo-ácido, donde se realiza la simulación

(hora a hora durante toda la vida útil del sistema) y la optimización de diferentes sistemas híbridos aislados con distintos perfiles de consumo.

1.1.2. *Optimisation of photovoltaic–diesel–battery stand-alone systems minimising system weight*.

El suministro eléctrico de instalaciones temporales aisladas (no conectadas a la red eléctrica), como pueden ser los hospitales de las organizaciones no gubernamentales, los campamentos civiles o militares, las bases militares en zonas de conflicto y cualquier otra instalación situada en zonas remotas, suele realizarse mediante generadores diésel (en muchos casos con baterías para suministrar las cargas críticas durante unas pocas horas o en el caso de mantenimiento o reparación del generador). Este tipo de suministro suele darse a menudo en países en desarrollo, zonas de guerra o zonas donde se produce un desastre humanitario (huracanes, terremotos, hambrunas, etc.) en los que deben instalarse hospitales, campamentos (civiles o militares) u otras instalaciones temporales, lejos de la red eléctrica y, en algunos casos, con acceso difícil o peligroso.

Una vez que se han instalado en un determinado lugar, este tipo de instalaciones, y después de cierto tiempo (varios días, semanas, meses o incluso años), se desmontan y más adelante se instalan en otro lugar o se almacenan en la sede de la ONG correspondiente o del ejército, esperando para otra emergencia. En muchos casos, el transporte de los componentes y el combustible desde la sede es una tarea difícil y peligrosa, y el costo del transporte es muy caro, por lo que el peso del sistema puede ser la variable más importante a minimizar (siempre asegurando el suministro de la carga eléctrica). En algunos casos, el coste del sistema también puede ser una variable importante a la hora de ser optimizada.

En este trabajo se presenta por primera vez un nuevo modelo para la optimización de sistemas híbridos aislados con alimentación renovable (fotovoltaica y/o diésel, con o sin acumulación de baterías) para suministrar la

carga eléctrica durante un periodo de tiempo específico, mientras la instalación temporal (hospital, campamento, etc.) está instalada en un área remota o peligrosa. Solamente se considera la energía solar fotovoltaica como fuente renovable porque la radiación solar de un período relativamente largo (un mes o un período más alto) puede predecirse con facilidad, y es similar de un año a otro. Además, en zonas relativamente próximas al ecuador (la mayoría de los países de África, Asia y América del Sur), la radiación no varía mucho durante los meses del año y es similar de un lugar a otro, incluso a una distancia de cientos de kilómetros. Sin embargo, la energía eólica es mucho más impredecible; depende en gran medida de la orografía, por lo que puede ser muy diferente de un lugar a otro, incluso si están a pocos kilómetros de distancia, y puede diferir significativamente de un mes a otro, incluso de un día para otro. Debido a estas razones, los aerogeneradores no son considerados en el sistema híbrido.

En función del periodo de tiempo que el sistema vaya a estar instalado, un sistema fotovoltaico-diésel-baterías puede tener menor peso y/o coste. Se han considerado tres tipos de optimizaciones:

a) Minimización del peso total: peso de los componentes (que se transportará desde la sede de almacenamiento al punto donde se instalará y regreso a la sede al final del período) más el peso del combustible utilizado durante el período de tiempo considerado.
b) Minimización del coste total: costo del combustible utilizado más el costo de operación y mantenimiento (O&M), más el costo de transporte del peso total (ida y vuelta), más el costo del envejecimiento de los paneles fotovoltaicos, el generador diésel, las baterías y el inversor/cargador durante el período considerado.
c) Minimización de ambos factores: peso y costo.

Cada uno de los componentes (paneles fotovoltaicos, generadores diésel, banco de baterías y el inversor/cargador) pueden presentar distintos tamaños y tecnologías. Si se consideran por ejemplo tres tipos distintos de paneles fotovoltaicos y 20 tamaños distintos, obtendremos un total de 60 tipos posibles de generador fotovoltaico. Lo mismo ocurre con los otros componentes del sistema.

Además, para cada combinación de componentes, se pueden utilizar muchas combinaciones de estrategias de control de los mismos. En general, el número de posibles combinaciones de componentes y de estrategias de control puede ser muy elevado, y la evaluación de todos ellos puede implicar un tiempo inadmisible de computación. Por lo tanto, se aplican técnicas heurísticas en aras de conseguir tiempos de cálculo aceptables. Los casos a) y b) se realizan mediante algoritmos genéticos, mientras que el caso c) se realiza aplicando algoritmos evolutivos multiobjetivo.

1.1.3. *Optimisation of PV-wind-diesel-battery stand-alone systems to minimise cost and maximise human development index and job creation*.

Se presenta por primera vez en este trabajo una nueva metodología para optimizar sistemas híbridos aislados con fuentes renovables que suministren energía eléctrica a un área rural, sin acceso a la red eléctrica, y minimizando el *coste actual neto* del sistema a la vez que se maximiza el *índice de desarrollo humano* y la *creación de empleo*.

El sistema estudiado consiste en una carga AC, que es la que debe ser obligatoriamente satisfecha por el sistema híbrido. El exceso de energía producida por los paneles fotovoltaicos y los aerogeneradores (cuando la carga AC está totalmente cubierta y el banco de baterías está totalmente cargado) puede ser usado por nuevos negocios o servicios (carga AC extra, con su propio banco de baterías de almacenamiento), incrementando la carga total consumida por la comunidad e incrementando por lo tanto el *índice de desarrollo humano*. Se utiliza una carga de “vertido” para consumir la energía eléctrica producida por los aerogeneradores cuando la carga AC y la carga AC extra están cubiertas y las baterías están a plena carga.

El *índice de* desarrollo *humano* (*Human Development Index*, HDI) es un indicador del desarrollo de un país, que tiene en cuenta la esperanza de vida al nacer, los años de escolarización esperados y la renta nacional bruta per cápita [8]. En 2014, el 17,8% de la población mundial no tenía acceso a la electricidad

(1285 millones de personas) [8,9]. El acceso a la energía eléctrica puede mejorar todos estos indicadores y por tanto, aumentar el HDI. Por ejemplo, la esperanza de vida se puede incrementar con el suministro de agua potable (que se puede extraer fácilmente mediante bombas eléctricas) y la conservación de los alimentos puede mejorarse mediante refrigeradores eléctricos, entre otros factores. La educación se puede mejorar con la electricidad, ya que permite el uso de ordenadores y la iluminación eléctrica. La renta nacional bruta per cápita también se mejora con el acceso a la electricidad, ya que se pueden desarrollar nuevos servicios y negocios.

Las Naciones Unidas [8] clasifican a los países con un índice de desarrollo humano bajo, medio, alto o muy alto. El HDI depende del uso de electricidad per cápita en una dependencia logarítmica que ha sido estudiada por varios autores en función de los datos de distintos países ofrecidos por los distintos Informes de Desarrollo Humano de las Naciones Unidas.

La *creación de empleo* (*Job Creation*, JC) de distintas tecnologías generadoras de electricidad ha sido estudiada por distintos autores [10-16]. Ramanathan y Gadesh [10] estudiaron el número de empleos por GWh/año (energía suministrada durante un año) por las diferentes tecnologías en la India. La unidad empleos/(GWh/año) es adecuada para tecnologías de combustibles fósiles, como generadores diésel, ya que la vida útil de un generador (y también el costo de operación y mantenimiento) depende del número de horas de operación (y por lo tanto de la energía suministrada). El consumo de combustible también depende de la cantidad de energía suministrada, por lo que los empleos relacionados con este tipo de tecnología se miden correctamente en empleos/(GWh/año) de energía suministrada. Estos investigadores [10] informaron 0.17 empleos/(GWh/año) para la electricidad generada mediante diésel en la India en 1984-85. Este valor ha caído desde entonces debido a los avances tecnológicos y a la mejora de la productividad laboral; Rojas-Zerpa [17] proponen un valor de 0.14 empleos/(GWh/año) para la generación mediante diésel o gasolina.

Para otras tecnologías, como la generación fotovoltaica o los aerogeneradores, se utilizan diferentes unidades para la creación de empleo. Muchos estudios

utilizan unidades de empleo en la fabricación e instalación (actividades no continuas) de plantas fotovoltaicas y eólicas en términos de empleos·año por MW (donde MW significa potencia pico para la producción fotovoltaica y potencia máxima de salida para los aerogeneradores), denotado en muchos casos como empleos-año/MW o persona-año/MW. Un empleo·año significa un trabajo a tiempo completo para una persona durante un año. Sin embargo, los trabajos de operación y mantenimiento (actividades continuas, cuya duración es toda la vida útil del sistema) suelen medirse en empleos/MW. Por ejemplo, en una planta de 20 MW que requiere 50 personas durante 1 año para la fabricación de sus componentes y 25 personas durante 6 meses para su instalación, se calcula el número de empleos·año/MW como (50 empleos · 1 año + 25 empleos · 0,5 años) / 20 MW = 3,125 empleos·año/MW. Si la vida útil de la planta es de 25 años, podríamos normalizar los empleos promedio durante su vida, con lo que podríamos considerar que ha creado un número equivalente de empleos permanentes a tiempo completo (es decir, puestos de trabajo durante su vida) de 3,125 puestos de empleos·año/MW / 25 años = 0,125 empleos/MW. En el mismo ejemplo, si para la O&M de la central eléctrica de 20 MW se necesitan 5 personas, entonces 5 empleos / 20 MW = 0,25 empleos/MW en O&M durante su vida útil. Así, durante su vida útil, el número total equivalente de trabajos permanentes a tiempo completo será de 0,125 + 0,25 = 0,375 empleos/MW.

Existen diferentes trabajos obteniendo distintos valores y utilizando distintas unidades para medir este indicador. Cameron y Van der Zwaan [16] comparan diferentes estudios, incluyendo todas las fases (fabricación, instalación y O&M) y considerando tanto trabajos directos como indirectos, normalizando a la unidad de empleos/MW. En base a esos resultados se apoya este trabajo.

Al igual que en los trabajos presentados anteriormente, y debido al elevado número de combinaciones posibles entre componentes y estrategias de control, la evaluación de todas ellas resulta inadmisible en un tiempo de computación razonable. Por ello, se han utilizado técnicas heurísticas en la optimización. Se han utilizado algoritmos evolutivos multiobjetivo combinados con algoritmos genéticos.

1.1.4. *Stochastic-heuristic methodology for the optimisation of components and control variables of PV-wind-diesel-battery stand-alone systems.*

Normalmente, la optimización de este tipo de sistemas suele llevarse a cabo mediante un enfoque determinista, es decir, considerando que la carga eléctrica y los datos meteorológicos (irradiación, temperatura y velocidad del viento) no varían a lo largo de los años, es decir, el comportamiento de un año se puede extrapolar al resto de los años de vida útil del sistema (que generalmente se considera 25 años). El costo del combustible diésel se considera generalmente como un costo fijo durante la vida útil del sistema o, en el mejor de los casos, se tiene en cuenta una inflación anual fija para el precio del mismo.

Sin embargo, el comportamiento del sistema real es diferente de un año a otro, ya que la carga eléctrica y las variables meteorológicas son diferentes. Además, el costo del combustible diésel consumido cada año depende del precio real del combustible de cada año. Estas han sido las motivaciones para realizar con este trabajo una optimización probabilística de los sistemas híbridos aislados. El enfoque estocástico permitirá considerar los diferentes rendimientos del sistema durante los años de su vida, considerando las incertidumbres de las variables meteorológicas y la carga, y sus correlaciones, y también permitirá considerar la incertidumbre del precio del combustible diésel. Se obtendrán las funciones de probabilidad para las variables de los resultados (coste esperado, duración del banco de baterías, ...), conociendo la media, la desviación estándar, el mínimo y el máximo esperados para cada uno de los resultados y por lo tanto disponiendo de mucha más información que usando un enfoque determinista.

Después de un exhaustivo trabajo de revisión bibliográfica, se evaluaron los trabajos previos de distintos autores que utilizaban enfoques estocásticos y modelos probabilísticos. A menudo, algunos de ellos no calculan los costos (no realizan la optimización del sistema), la mayoría de ellos no consideran la correlación entre las variables de entrada, otros no consideran el almacenamiento mediante un banco de baterías y otros usan modelos clásicos simples para la estimación de la vida útil de las baterías. Además, ninguno de los estudios previos incluye el modelo PWM (modulación de anchura de pulso) del controlador de

carga de la batería o del inversor/cargador, y por lo tanto, ninguno considera la optimización de las variables de control que se pueden ajustar en el controlador de las baterías o en el inversor/cargador.

Se presenta en este trabajo una nueva metodología para la optimización estocástico-heurística de sistemas híbridos aislados con alimentación renovable, considerando las incertidumbres de las variables de entrada (carga, irradiación, temperatura y velocidad del viento), y teniendo en cuenta sus correlaciones. También se considera la incertidumbre de la inflación anual de los precios del combustible (ninguna de los trabajos anteriores considera esta variable, la cual tiene una gran influencia en el coste actual neto). En el modelo de optimización, se aplica el “Criterio ponderado del flujo de Ah” para las baterías de plomo-ácido, modelo que ha sido ya introducido en un artículo anterior (incluyendo la estimación precisa de la vida útil), lo que es mucho más realista que el enfoque utilizado en los estudios anteriores. Además, se modela un controlador de carga PWM (con carga en tres etapas: carga, absorción y flotación) con control del estado de carga mediante una compleja estrategia de control de ocho variables.

En general, las series de varios años (por ejemplo, 10 ó 20 años) de la irradiación diaria promedio durante un año completo varían de año a año, de modo que su función de densidad de probabilidad sigue aproximadamente una distribución normal o gaussiana, con una media y una desviación estándar. Lo mismo ocurre con la carga, la temperatura, la velocidad del viento y la tasa de interés del combustible diésel.

Se conocerán como datos para el presente trabajo las funciones de densidad de probabilidad de la carga media diaria de un año *E*, de la irradiación media diaria de un año sobre la superficie de los paneles fotovoltaicos *G*, de la temperatura media en un año *T*, de la velocidad media del viento de un año *W* y de la tasa anual de interés del combustible diésel *Int (%). E*, *G*, *T* y *W* son generalmente variables correlacionadas y su matriz varianza-covarianza es conocida.

También se conocerá la serie horaria de un año completo (8760 horas) de *E*, *G*, *T* y *W*, denominadas como $E_h(t)$, $G_h(t)$, $T_h(t)$, $W_h(t)$, con t = 1 ... 8760 h, con sus valores medios *Emean*, *Gmean*, *Tmean* y *Wmean*.

La optimización estocástica se desarrolla mediante la simulación de Monte Carlo, combinada con algoritmos genéticos (enfoque heurístico) para obtener la solución óptima o una solución cerca del óptimo en un tiempo razonable. Cada combinación de componentes *i* y estrategia de control *k* es evaluada MCS_{sample} veces (número de muestras de la simulación de Monte Carlo o hasta que se alcance una regla de parada), con lo que se obtiene una función de densidad de probabilidad para cada una de las variables que se obtienen como resultado (energía suministrada por los paneles fotovoltaicos, energía suministrada por los aerogeneradores, energía suministrada por el generador diésel, la energía no servida o insatisfecha, la energía ciclada por las baterías, la duración de las baterías, el consumo de combustible, los costos de O&M, los costos de reemplazo, el coste actual neto del sistema, el coste normalizado de la energía, etc.). En particular, se podrá obtener la media de la distribución del coste actual neto del sistema (variable que se quiere minimizar), y que es el resultado principal de la optimización. En función de esta media, se ordenarán de mejor a peor los individuos simulados.

1.2 JUSTIFICACIÓN DE LA UNIDAD TEMÁTICA

Los cuatro trabajos presentados anteriormente versan todos sobre optimización de sistemas híbridos aislados con energías renovables. En todos ellos el sistema híbrido puede incluir, entre otros, generador fotovoltaico y generador diésel (o gasolina), además de baterías de plomo-ácido. En tres de los cuatro artículos se utiliza, por primera vez en trabajos de simulación y optimización, el modelo avanzado de Schiffer et al. [20] de estimación de la vida de las baterías de plomo-ácido. A lo largo de los trabajos, se han comparado distintos modelos (utilizados en la literatura) para la simulación de algunos elementos de estos sistemas, se han introducido nuevas variables que no habían sido optimizadas antes (fijando un único o varios objetivos en la optimización), se han utilizado enfoques, que si bien habían sido utilizados anteriormente, nunca lo habían sido de la manera tan completa como han sido utilizados en estos trabajos. Queda entonces perfectamente justificada su unidad temática, lo cual es un requisito imprescindible para la presentación de una tesis como compendio de artículos.

2. TRABAJOS PUBLICADOS

Los trabajos publicados que conforman esta tesis son: Página

1. Iván R. Cristóbal Monreal, Rodolfo Dufo López, José María Yusta Loyo. Influence of the battery model in the optimisation of stand-alone renewable systems. *International Conference on Renewable Energies and Power Quality* (ICREPQ 2016), ISBN 978-84-608-5473-9. *Renewable Energy and Power Quality Journal*, No.14, May 2016, 185-189, ISSN 2172-038X. 19

2. Iván R. Cristóbal Monreal, Rodolfo Dufo López. Optimisation of photovoltaic–diesel–battery stand-alone systems minimising system weight. Energy Conversion and Management 119 (2016) 279–288. 24

3. Rodolfo Dufo López, Iván R. Cristóbal Monreal, José María Yusta Loyo. Optimisation of PV-wind-diesel-battery stand-alone systems to minimise cost and maximise human development index and job creation. Renewable Energy 94 (2016) 280-293. 34

4. Rodolfo Dufo López, Iván R. Cristóbal Monreal, José María Yusta Loyo. Stochastic-heuristic methodology for the optimisation of components and control variables of PV-wind-diesel-battery stand-alone systems. Renewable Energy 99 (2016) 919-935. 48

International Conference on Renewable Energies and Power Quality (ICREPQ'16)
Madrid (Spain), 4th to 6th May, 2016
Renewable Energy and Power Quality Journal (RE&PQJ)
ISSN 2172-038 X, No.14 May 2016

Influence of the battery model in the optimisation of stand-alone renewable systems

I.R. Cristóbal-Monreal[1], R. Dufo-López[2] and J. M. Yusta-Loyo[2]

[1] Centro Universitario de la Defensa
Academia General Militar. Ctra. de Huesca s/n. 50.090 Zaragoza (Spain)
Phone/Fax number:+0034 976 73 98 37, e-mail: icristob@unizar.es

[2] Electrical Engineering Department, University of Zaragoza
C/ María de Luna, 3. 50018 Zaragoza
Phone/Fax number: +0034 976 76 19 21, e-mail: rdufo@unizar.es, jmyusta@unizar.es

Abstract. Stand-alone (off-grid) renewable systems are usually composed by photovoltaic panels and/or wind turbines, with batteries (usually lead-acid) and in some cases including diesel generator. In many cases the total cost of the batteries (including replacement during the lifetime of the system) is the highest cost.

The model of batteries used in simulation and optimisation of stand-alone renewable systems has a great importance as it allows the estimation of the lifetime of the batteries, which is one of the most important variables to calculate the Net Present Cost of the system and also the Levelised Cost of Energy.

The lifetime estimation of lead-acid batteries is a complex task because it depends on the operating conditions of the batteries. In many engineering works and research studies, the estimation of battery lifetime is error-prone, obtaining values much higher than the real ones.

In this paper we compare different models of lead-acid batteries, used in the simulation and optimisation of different stand-alone systems. We conclude that in many cases we obtain good results by using a complex weighted Ah-throughput model for the batteries, however using the classical models the estimation of the batteries lifetime is too optimistic.

Key words

Renewable stand-alone systems, batteries models, optimisation.

1. Introduction

In stand-alone renewable systems, the component with highest cost is the battery bank, considering acquisition cost, operation and maintenance (O&M) cost and replacements of the component when it reaches its lifetime, during system lifetime. The correct estimation of the battery lifetime is very important as it determines the number of replacements of the battery bank during the lifetime of the system (which is usually considered as 20 or 25 years, same as the photovoltaic panels lifetime). For example, if the estimation of the lifetime of the batteries is 5 years and the system lifetime is 25 years, the battery bank will be expected to be replaced 5 times. However, if the real lifetime is 2.5 years, it will be replaced 10 times, and the real total Net Present Cost (NPC) of the system and the Levelised Cost of Energy (LCE) would be much higher than the expected ones.

Classical models like "Equivalent full cycles to failure" and "Rainflow cycle counting", widely used to estimate the lifetime of the batteries in simulation and optimisation tools [1] only consider the amount of energy cycled by the batteries, they do not take into account the operating conditions.

The most important ageing processes are anodic corrosion, positive active mass degradation and loss of adherence to the grid, irreversible formation of lead sulphate in the active mass, short-circuit, loss of water and electrolyte stratification [2].

Real batteries lifetime highly depends on the operating conditions, considering the capacity loss by degradation of the active mass (with the influence of the State Of Charge (SOC), the time that the batteries are in a low state of charge, the time since the last full charge, the current, acid stratification...) and the capacity loss by corrosion (with the influence of the cell voltage, temperature and other factors) [3].

Batteries subject to deep cycling regimes typically age by degradation of the structure of the positive active mass. The battery cycle lifetime shown in the datasheet of the batteries (several hundreds of full cycles) is obtained in laboratory tests under standard conditions. However, the real conditions can be very different from standard conditions. Then the ageing by degradation of the active mass and therefore the lifetime can be very different from the expected.

In the case of stationary batteries (operating under float-charge conditions), the most important ageing mechanism is corrosion of the positive grid. The real conditions of stationary batteries can be different from the laboratory tests, so the real floating life can be very different (usually lower) than floating life shown in the datasheet (which is at 20 or 25º C), as the effect of temperature on float life is around 50% reduction for each 8.3 °C increase in temperature for lead-acid batteries.

Classical models used to estimate the lifetime of the batteries are very simple but they can imply high errors. Much more complex models like weighted Ah-throughput approach can bring much more accurate results [3].

2. Battery ageing models

In this paper we compare three models of batteries:

1) *Equivalent full cycles to failure*
2) *Rainflow cycle counting*
3) *Weighted Ah-throughput model proposed by Schiffer et al. in 2007 [4]*

A. Equivalent full cycles to failure

This method is widely used by many simulation and optimisation tools [1]. The end of the battery lifetime is expected to be reached when a specified number of full charge-discharge cycles are reached, shown in the manufacturer's datasheet. This model only consider the amount of energy cycled by the batteries, it does not take into account the operating conditions.

B. Rainflow cycle counting

This model is known as "rainflow", based on Downing's algorithm [5] that is used by HYBRID2 software [6]. It is more complex than equivalent full cycles to failure. This model counts the charge/discharge cycles Z_i corresponding to each range of the Depth of Discharge (DOD), split in m intervals of DOD_i, for a year. For each interval there is a number of Cycles to Failure (CF_i) obtained from the manufacturer's datasheet (example shown in Fig. 1).

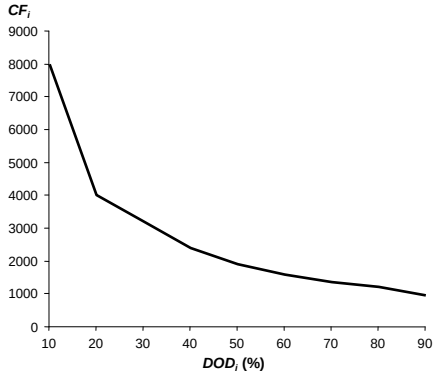

Fig. 1. Cycles to Failure vs. Depth of Discharge.

The battery expected lifetime, in years, can be calculated as follows:

$$Life_{bat} = \frac{1}{\sum_{i=1}^{m} \frac{Z_i}{CF_i}} \qquad (1)$$

This model considers the depth of discharge of the cycles, but it does not consider the rest of the operating conditions (time that batteries are in a low SOC, time since the last full charge, current, acid stratification, voltage, temperature...).

C. Schiffer weighted Ah-throughput model

This is a weighted Ah-throughput model proposed by Schiffer et al. [4]. It considers real operating conditions.

The actual Ah throughput is continuously multiplied by a weight factor that represents the actual operating conditions.

This model calculates the capacity loss by corrosion and the capacity loss by degradation. The remaining battery capacity is the normalised initial battery capacity minus the capacity loss by corrosion and degradation. The end of the battery lifetime is reached when its remaining capacity is 80% of the nominal capacity.

It takes into account the influence of the SOC, the time that the batteries are in a low state of charge, the time since the last full charge, the current, the acid stratification, the cell voltage, the temperature and other factors. By using this model, the effect of the voltage cut limits of the battery controller can be modelled, and also other parameters which can be set in the battery controller [3].

It is a complex model which uses many equations, detailed information can be seen in [4] and [3]. In [3] we demonstrated that this model is much more accurate and predicts batteries lifetime much better than the other models. Classical models (the equivalent full cycles model or the rainflow cycle counting model) do not correctly estimate the ageing of the batteries; in many cases, the predicted battery lifetime is two or three times higher than the lifetime obtained in the real system; however, using the Schiffer weighted Ah model, predictions are very similar to real lifetimes [3].

The Schiffer weighted Ah model has been added in iHOGA software [7], which is the only software for the simulation and optimisation of hybrid renewable systems which incorporates such an accurate model.

3. Stand-alone renewable system

Fig. 2 shows the system to be simulated and optimized. It will supply an AC load, and can be composed by photovoltaic (PV) array, a battery bank, a Diesel generator and a inverter/charger controller.

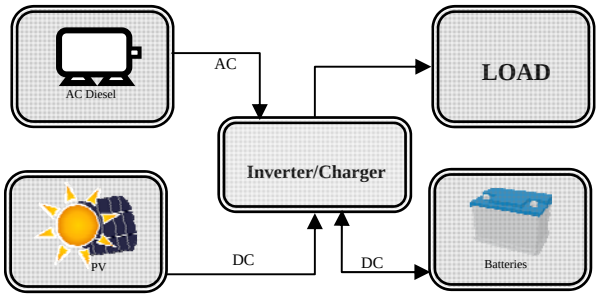

Fig. 2. PV-Diesel-battery system

We will consider three different configurations:

1) *PV-batteries system*
2) *PV-Diesel-batteries system*
3) *Diesel-batteries system (non-renewable system)*

The three configurations will be optimized in order to supply the load with the lowest cost. For the three cases of systems, we will use the three cases of battery ageing models, seeing the differences in the results.

A system located near Sabiñánigo (42.53ºN, 0.37ºW, close to Pyrenees mountains, in Aragon, Spain) has been evaluated. Two load profiles has been considered:

1) *AC Household load (3.63 kWh/day, following a typical hourly distribution shown in Fig. 3)*

2) *DC Telecom station load (2.88 kWh/day, continuous load of 120 W)*

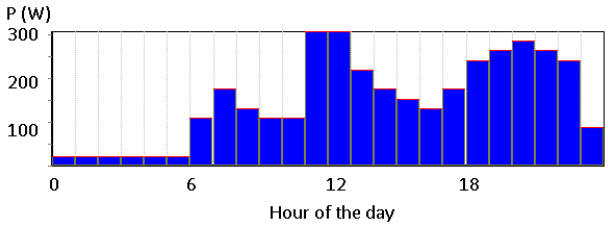

Fig. 3. Hourly distribution of AC household load

The irradiation for the location has been obtained by means of the web of PVGIS, JRC European Commission [8].

The PV panels used in the optimisation are of 100 Wp peak power, 17.7 V open voltage, 6.79 A shortcut current, 143 € acquisition cost (including support), O&M cost 1.43 €/year (1% of acquisition cost), expected lifetime 25 years. The selected slope for the PV panels is the optimal one (65º), with azimuth 0º.

The batteries used in the optimisation are a OPzS lead-acid batteries family, with 1,258 full cycles to failure and cycles to failure vs. DOD shown in Fig. 4 (red curve). Also in same figure the cycled energy during lifetime is shown in green. Floating life is 18 years. The capacity of the batteries of the family is from 180 to 3360 Ah. The nominal voltage is 2 V. The acquisition cost is around 190 €/kWh, and the O&M annual cost is 1% of the acquisition cost.

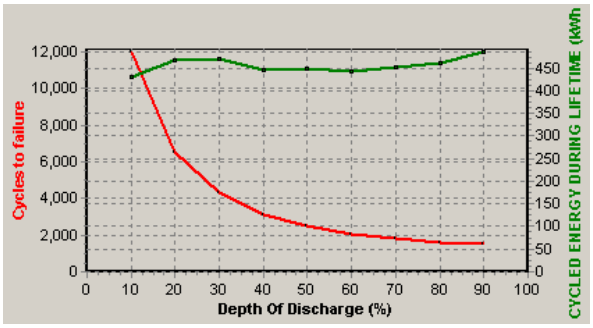

Fig. 4. Cycles to Failure vs. Depth of Discharge of the batteries used in the optimisations.

Three generators have been considered:
A diesel of 1.9 kVA, 1040 € of acquisition cost, and two gasoline generators, one of 0.5 kVA and another of 1 kVA (325 and 520 € of acquisition cost, respectively). Their O&M cost is 0.15 €/h for the Diesel and 0.23 €/h for the gasoline generators.

Also several inverter/chargers have been considered for the different cases.

For all the cases a DC bus voltage of 48 V has been considered. Also, for all the cases when there is a diesel (or gasoline) generator, the strategy "Cycle charging" is used [9]: whenever the load cannot be supplied by the PV nor the batteries, the diesel (or gasoline) runs at full power, charging batteries until 100% of SOC is reached. Also for all the cases interest annual rate of 2% and annual inflation of 4% have been taken into account to calculate NPC and LCE.

3. Computational results

The optimisation of each system to supply the load has been done three times, one for each battery ageing model.

A. Household load

Tables I, II and III show the optimal system found for the different configurations (PV-batteries, PV-Diesel-batteries and Diesel-batteries, respectively) using for each configuration the three battery ageing models.

Table I. – Results for Household load, PV-batteries.

Battery ageing model	Optimal system	Battery expected lifetime (years)	NPC (€)	LCE (€/kWh)
Equivalent full cycles to failure	PV 2000 Wp Batt. 18.72 kWh	18	21074	0.64
Rainflow cycle counting	PV 2000 Wp Batt. 18.72 kWh	18	21074	0.64
Schiffer Weighted Ah-throughput	PV 2000 Wp Batt. 18.72 kWh	8.12	25366	0.77

Table II. – Results for Household load, PV-Diesel-batteries.

Battery ageing model	Optimal system	Battery expected lifetime (years)	NPC (€)	LCE (€/kWh)
Equivalent full cycles to failure	PV 1600 Wp Diesel 1.9 kVA Batt. 8.64 kWh	13.61	19322	0.58
Rainflow cycle counting	PV 1600 Wp Diesel 1.9 kVA Batt. 8.64 kWh	15.8	18857	0.57
Schiffer Weighted Ah-throughput	PV 1600 Wp Diesel 1.9 kVA Batt. 8.64 kWh	8.92	21783	0.66

Table III. – Results for Household load, Diesel-batteries.

Battery ageing model	Optimal system	Battery expected lifetime (years)	NPC (€)	LCE (€/kWh)
Equivalent full cycles to failure	Diesel 1.9 kVA Batt. 18.72 kWh	16.76	47244	1.43
Rainflow cycle counting	Diesel 1.9 kVA Batt. 18.72 kWh	18	46902	1.42
Schiffer Weighted Ah-throughput	Diesel 1.9 kVA Batt. 8.64 kWh	4.8	55334	1.67

B. Telecom station

Tables IV, V and VI show the optimal system found for the different configurations (PV-batteries, PV-Diesel-batteries and Diesel-batteries, respectively) using for each configuration the three battery ageing models.

Table IV. – Results for Telecom load, PV-batteries.

Battery ageing model	Optimal system	Battery expected lifetime (years)	NPC (€)	LCE (€/kWh)
Equivalent full cycles to failure	PV 1200 Wp Batt. 18.72 kWh	18	13904	0.53
Rainflow cycle counting	PV 1200 Wp Batt. 18.72 kWh	18	13904	0.53
Schiffer Weighted Ah-throughput	PV 1200 Wp Batt. 18.72 kWh	7.68	18797	0.72

Table V. – Results for Telecom load, PV-Diesel-batteries.

Battery ageing model	Optimal system	Battery expected lifetime (years)	NPC (€)	LCE (€/kWh)
Equivalent full cycles to failure	PV 1600 Wp Gasoline 0.5 kVA Batt. 8.64 kWh	17.64	13931	0.53
Rainflow cycle counting	PV 1600 Wp Gasoline 0.5 kVA Batt. 8.64 kWh	17.68	13927	0.53
Schiffer Weighted Ah-throughput	PV 1600 Wp Gasoline 0.5 kVA Batt. 8.64 kWh	8.61	16828	0.64

Table VI. – Results for Telecom load, Diesel-batteries.

Battery ageing model	Optimal system	Battery expected lifetime (years)	NPC (€)	LCE (€/kWh)
Equivalent full cycles to failure	Diesel 1.9 kVA Batt. 18.72 kWh	18	34911	1.33
Rainflow cycle counting	Diesel 1.9 kVA Batt. 18.72 kWh	18	34911	1.33
Schiffer Weighted Ah-throughput	Diesel 1.9 kVA Batt. 8.64 kWh	5.23	42711	1.63

The results show that the three ageing models obtain same optimal system in PV-Diesel-batteries and in PV-batteries systems. However, in the case of Diesel-batteries system the Schiffer weighted Ah-throughput model obtains a optimal system with lower battery bank.

The classical models ("Equivalent full cycles to failure" and "Rainflow cycle counting") obtain very similar estimation for the battery lifetime and then very similar NPC and LCE. However, Schiffer weighted Ah-throughput model obtains more realistic results for the batteries expected lifetime (much lower than the values obtained with the classical models), then expected NPC and LCE are more realistic (higher than the values obtained with the other models).

4. Conclusion

In this paper we compare three different batteries ageing models to be used in the simulation and optimisation of hybrid renewable systems. Two models are simple and classical ones: "Equivalent full cycles to failure" and "Rainflow cycle counting", and the third model is a complex weighted Ah-throughput model proposed by Schiffer et al. in 2007 [4].

We optimize three types of systems: PV-batteries, PV-Diesel-batteries and Diesel-batteries. We use two different loads, a household AC load and a telecom station continuous DC load.

Comparing the results for the different optimisations, we conclude in the cases studied all the models obtain same optimal system (except for the case of Diesel-batteries, where Schiffer model obtains a lower battery bank in the optimal system).

However, in NPC and LCE the results are very different comparing the classical models to the Schiffer model. The Schiffer Ah-throughput model obtains more realistic results (lower battery lifetime and therefore higher NPC and LCE). Classical models obtain too optimistic results for the battery lifetime, in some cases two or three times higher than values obtained with Schiffer model.

References

[1] Bernal-Agustín JL, Dufo-López R. Simulation and optimization of stand-alone hybrid renewable energy systems. Renew Sustain Energy Rev 2009;13:2111–8.

[2] Ruetschi P. Aging mechanisms and service life of lead–acid batteries. J Power Sources 2004;127:33-44

[3] Dufo-López R, Lujano-Rojas JM, Bernal-Agustín JL. Comparison of different lead–acid battery lifetime prediction models for use in simulation of stand-alone photovoltaic systems. Appl Energy 2014;115:242–53. doi:10.1016/j.apenergy.2013.11.021.

[4] Schiffer J, Sauer DU, Bindner H, Cronin T, Lundsager P, Kaiser R. Model prediction for ranking lead-acid batteries according to expected lifetime in renewable energy systems and autonomous power-supply systems. J Power Sources 2007;168:66-78.

[5] Downing SD, Socie DF. Simple rainflow counting algorithms. Int J Fatigue 1982;4:31–40.

[6] Green HJ, Manwell J. HYBRID2 – A Versatile Model of the Performance of Hybrid Power Systems. Proceedings of WindPower'95, Washington DC, March 27-30, 1995.

[7] iHOGA software. Rodolfo Dufo-López. Free educational versión can be downloaded from: http://personal.unizar.es/rdufo/index.php?lang=en

[8] PVGIS, interactive maps. JCR European Commission: http://re.jrc.ec.europa.eu/pvgis/apps4/pvest.php#

[9] Dufo-López R, Bernal-Agustín JL. Design and control strategies of PV-Diesel systems using genetic algorithms. Sol Energy 2005;79:33–46. doi:10.1016/j.solener.2004.10.004.

Energy Conversion and Management 119 (2016) 279–288

Contents lists available at ScienceDirect

Energy Conversion and Management

journal homepage: www.elsevier.com/locate/enconman

Optimisation of photovoltaic–diesel–battery stand-alone systems minimising system weight

Iván R. Cristóbal-Monreal [a], Rodolfo Dufo-López [b,*]

[a] Centro Universitario de la Defensa, Academia General Militar, Ctra. de Huesca s/n, 50.090 Zaragoza, Spain
[b] Electrical Engineering Department, University of Zaragoza, Calle María de Luna, 3, 50018 Zaragoza, Spain

ARTICLE INFO

Article history:
Received 7 February 2016
Received in revised form 11 April 2016
Accepted 14 April 2016
Available online 20 April 2016

Keywords:
Renewable stand-alone systems
Weight minimisation
Genetic algorithms
Multi-objective evolutionary algorithms

ABSTRACT

This article shows a new method for the optimisation of stand-alone (off-grid) hybrid systems (photovoltaic–diesel–battery) to supply the electricity of mobile systems such as non-governmental organization hospitals, temporary camps or other mobile facilities to be placed temporally in remote or conflictive areas. If there is difficult or dangerous access, the most important objective to be minimised is the total weight of the system. Also, the cost is an important variable to minimise. Nowadays, the majority of these systems are diesel-only or diesel-battery systems. However, depending on the duration of the temporary system, a photovoltaic–diesel–battery system can have a lower weight and/or cost. Three types of optimisation are considered: (i) minimisation of the weight of the system; (ii) minimisation of the cost; and (iii) minimisation of both weight and cost. The two first are conducted by genetic algorithms, and the last one is performed using multi-objective evolutionary algorithms. An example of application of this method to a temporary hospital in Central African Republic is shown, concluding that in the cases of more than 90 days photovoltaic (flexible crystalline silicon panels) + diesel + battery is the solution which minimises weight. When minimising cost, all the cases include photovoltaic with high penetration.

1. Introduction

The electrical supply of stand-alone off-grid (far from the electrical grid) temporary facilities as non-governmental organization (NGO) hospitals, military, or civil camps or barracks in conflict areas and any other facilities installed in remote areas is usually done by diesel generators (in many cases with batteries to supply the critical loads during a few hours in the case of maintenance or reparation of the diesel). The application of this kind of system is in developing countries, war areas or areas where a humanitarian disaster (hurricanes, earthquakes, famines, etc.) occurs, where temporary hospitals, temporary camps (military or civilian) or other temporary facilities must be installed far from the electrical grid and, in some cases, with difficult or dangerous access.

This kind of facility is installed in a certain place, and, after a certain time (several days, weeks, months or even years), they are disassembled and then installed in another place or to be stored in the NGO or military headquarters, waiting for another emergency. In many cases, the transportation of the components and fuel from the headquarters is a difficult and dangerous task, and the transport cost is very expensive, so the weight of the system can be the most important variable to be minimised (ensuring the supply of the whole electrical load). In some cases, the cost of the system can also be an important variable to be optimised.

A study of costs and weight of PV panels, batteries, diesel generators and inverter/chargers has been done. For PV panels, from 1.1 to 1.5 €/Wp and around 0.085 kg/Wp are available in the market at the beginning of 2016 for mono or multi-crystalline silicon (c-Si), which is the most widely used technology. Including the aluminium support structure and the micro-inverters, prices from 1.6 to 2.2 €/Wp and weight around 0.1 kg/Wp are for c-Si. During the last few years, some manufacturers offered c-Si flexible panels, with a cost around 2.5 €/Wp but a much lower weight, around 0.015 kg/Wp (including the screws or fixing system and the micro-inverters, around 3.2 €/Wp and 0.025 kg/Wp). Also, new CIGS flexible panels, with a very competitive price (1.5 €/Wp) and low weight (0.026 kg/Wp), are reported; however, their availability in the market is limited. CdS–CdTe and amorphous silicon (a-Si) technologies have not been considered as their price and weight are similar or higher than c-Si. The cost and weight of diesel generators is quite variable, from 300 to more than 1000 €/kVA and from around 13 to 50 kg/kVA. OPzV batteries (gel and tubular technology) have been selected as they present excellent

* Corresponding author.
E-mail addresses: icristob@unizar.es (I.R. Cristóbal-Monreal), rdufo@unizar.es (R. Dufo-López).

http://dx.doi.org/10.1016/j.enconman.2016.04.050
0196-8904/

deep discharge recovery and cyclability, with immobilised electrolyte (gel) so that the transport is safe and easy and very low maintenance is required (no water addition). The cost of this kind of battery is from around 200 to 450 €/kW h and the weight from around 35 to 45 kg/kW h. The inverter/chargers vary from 500 to 700 €/kW and 10 to 14 kg/kW.

The transport cost by truck (in € per tonne and km) is different in each country, and it depends mainly on the type of road and on the fuel price. In Europe, Bina et al. [1] reported costs from 0.059 to 0.094 €/(t km), while an overview of the transport-related statistics is shown in [2]. In the United States of America, values around 0.1 €/(t km) are shown in [3]. In Africa, values from 0.036 (Kenya) to 0.109 €/(t km) (Republic of Congo) are reported for international corridors [4]. The transportation on domestic roads is usually more expensive; for example, in Ethiopia, Rancourt et al. [5] reported a mean of 0.109 €/(t km) while the international corridors present a mean of 0.089 €/(t km). Air cargo is much more expensive: in the USA, a value around 0.65 €/(t km) is reported [3]. In transport by helicopter, values of more than 2 €/(t km) can be observed. In dangerous areas, the transport cost can be much higher.

Previous studies show issues related to renewable energy and rural electrification in some geographical locations. Ahlborg and Hammar [6] show drivers and barriers to rural electrification by renewable energy in Tanzania and Mozambique. Borhanazad et al. [7] study the application of renewable sources for rural electrification in the poorest areas of Malaysia. Adaramola et al. [8] present an economic analysis of a hybrid PV-wind-diesel system for application in remote areas of southern Ghana. Ismail et al. [9] show a techno-economic analysis of a PV-microturbine hybrid system for a remote community located in Palestine; same authors present a similar analysis for a PV–diesel system to supply a small community in Malaysia [10]. Kumar and Manoharan [11] analyse the economic feasibility of hybrid PV–diesel systems in different areas of Tamil Nadu (India) with unstable grid connection.

Also previous studies show specific applications of renewable stand-alone systems. For example, Campana et al. show the economic optimisation of PV water pumping for irrigation [12]. Edwin and Sekhar study the use of biomass and biogas for cooling for milk preservation in India [13]. In a recent work Dufo-López et al. [14] present the stochastic optimisation of a PV–diesel system to supply an off-grid hospital located in Democratic Republic of the Congo.

Many previous works show the optimisation of stand-alone hybrid systems (PV and/or wind turbines and/or hydro and/or diesel, usually using batteries as storage) by minimising the net present cost of the system (including all the costs throughout the lifetime of the system, usually 25 years) or the levelised cost of energy. Comprehensive reviews of studies of stand-alone hybrid renewable systems are shown by many authors. Akikur et al. [15] present a review of PV systems and hybrid PV systems used to electrify off-grid locations. Mohammed et al. [16] show a review of drivers and benefits of hybrid systems (considering PV, wind, hydro and biomass), including the factors to be considered for their designing and implementation. Bajpai and Dash [17] show a review on the sizing, optimisation, management and modeling of the hybrid system components. Bernal-Agustín and Dufo-López [18] present a review of the most relevant previous works of simulation and optimisation of stand-alone hybrid renewable systems, including a review of the software tools. A review of the most relevant software tools for the simulation and/or optimisation of hybrid renewable systems is also shown by Sinha and Chandel [19].

In some cases, if the number of possible combinations of the hybrid renewable system implies an unacceptable computation time, some authors apply heuristic techniques like genetic algorithms (GA) [20] in the optimisation. For example, in [21] GA are applied in the optimisation of PV–diesel–battery systems while in [22] a PV–microturbine–battery system is optimised by means of GA. Most of the works consider only one variable to be optimised (the cost). However, in some cases, CO_2 emissions and/or unmet load or loss of power probability also are variables used in the optimisation, applying multi-objective evolutionary algorithms (MOEA) [23]. Fadaee and Radzi [24] show a review of the most important works of the optimisation of stand-alone hybrid renewable systems using MOEA.

The design and development of a hybrid renewable mobile medical clinic in Dominican Republic is shown in [25], composed by PV panels, wind turbines, batteries and a diesel generator. The authors show the performance of a complete day; however, no optimisation is performed.

This paper presents, for the first time, a new model for the optimisation of the hybrid system (PV and/or diesel, with or without batteries storage, Fig. 1) to supply the electrical load during a specified period of time when the temporary facility (hospital, camp, etc.) is installed in the remote or dangerous area. Only PV is considered as renewable source because the solar radiation of a relative long period (a month or a higher period) can be easily predicted, it is similar from one year to another, and, in areas relatively near the equator (most countries of Africa, Asia and South America), the radiation does not vary much during the months of the year and is similar from one place to another place even over a distance of hundreds of km. However, wind energy is much more unpredictable; it strongly depends on the orography, so it can be very different from one place to another, even if they are only a few km away, and it can differ significantly from one month to the next, even from one day to the next. Due to these reasons, wind turbines are not considered in the hybrid system.

Three types of optimisation are considered:

(a) Minimisation of total weight: weight of components (to be transported from the headquarters to the location and return to the headquarters at the end of the period) plus weight of fuel used during the period of time considered.
(b) Minimisation of total cost: cost of fuel used plus cost of operation and maintenance (O&M), plus cost of transportation of the total weight (go and return), plus cost of ageing of the PV generator, the batteries, the inverter/charger and the diesel during the period considered.
(c) Minimisation of both weight and cost.

Each component (PV generator, diesel generator, battery bank and inverter/charger) can present different sizes or technologies. For example, 3 types of PV panels with 20 different sizes can be considered, obtaining a total of 60 possible types of PV generator.

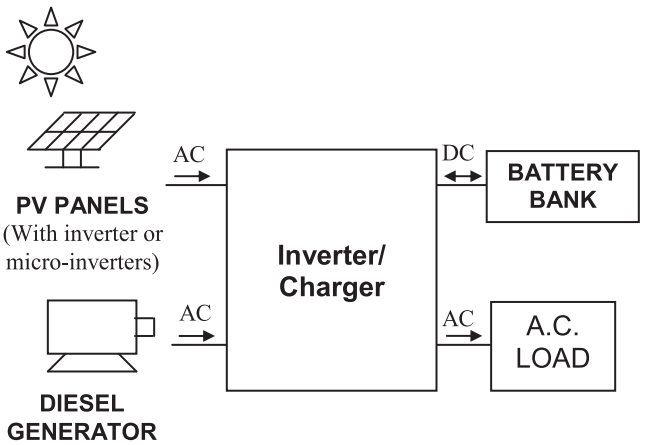

Fig. 1. PV–diesel–battery system.

The same occurs for the other components and also each combination of components can use many combinations of control strategies. In general, the number of possible combinations of components and control strategies is high, and the evaluation of all of them can imply inadmissible computation time, so heuristic techniques are applied to perform the optimisations in acceptable computation time. Cases (a) or (b) are conducted by GA, while (c) is performed using MOEA.

2. Methods

In this section, the mathematical model used for the simulation and evaluation of each combination of components and control strategy is shown. Then, the mono-objective optimisation (minimisation of just one objective, weight or cost) by GA is shown. Later, the different mono-objective optimisations are defined, and finally the multi-objective optimisation (minimisation of weight and cost by means of MOEA) is shown.

2.1. Mathematical model for the hourly simulation of the system

The evaluation of each combination of components and control strategy implies that the performance of that combination must be simulated during the period of time when the temporary facility (hospital, camp, etc.) is installed. After the simulation, it can be known if that combination can supply the whole load, and also the fuel consumed will be known and other variables as the number of hours the diesel runs, the battery charging/discharging energy, the capacity loss of the batteries, etc. With these results, it is possible to calculate the weight of the system (components + fuel) and the cost of the system (fuel + operation and maintenance + ageing of the components).

The simulation of the system is performed in hourly time steps, from the first hour ($t = 0$) until the last hour ($t = 24 \cdot N_{days}$), where N_{days} is the number of days the temporary facility is working in the place it has been installed. The mathematical models of the PV generator, diesel and battery bank are described below.

Each hour, the power balance must be satisfied:

- If the PV output power is higher than the load demand, the difference will be used to charge the batteries.
- If the PV output power is not enough to cover the load demand, the battery bank and/or the diesel must supply the rest. It depends on the state of charge (SOC) of the battery bank and on the control strategy, shown in Section 2.2 below.

2.1.1. PV generator

It has been considered that the PV inverter or micro-inverters include a maximum power point tracking (MPPT) system, so the output power (W) of the PV generator during hour t (0, 1, ..., $24 \cdot N_{days}$) is:

$$P_{PV}(t) = P_{STC} \cdot \frac{G_h(t)}{1\ \text{kW h/m}^2} \cdot \left[1 + \frac{\alpha}{100}(T_c(t) - 25)\right] \cdot F_{losses} \quad (1)$$

where P_{STC} (Wp) is the output power in standard test conditions; $G_h(t)$ (kW h/m^2) is the irradiation over the surface of the PV panels during hour t; F_{losses} (around 0.85–0.9) is a factor which takes into account the losses due to dirt, wires, module mismatch or power tolerance, efficiency of the micro-inverter, and other losses; α is the power temperature coefficient (%/°C); and $T_c(t)$ (°C) is the PV cell temperature, which can be calculated as:

$$T_c(t) = T_a(t) + \left(\frac{\text{NOCT} - 20}{0.8}\right) \cdot \frac{G_h(t)}{1\ \text{kW h/m}^2} \quad (2)$$

where $T_a(t)$ is the ambient temperature (°C) and $NOCT$ is the nominal operation cell temperature (°C).

2.1.2. Diesel generator

The diesel generator output power $P_{GEN}(t)$ depends on the output power of the PV generator, the load, the control strategy and the SOC of the battery bank. The diesel fuel consumption (l/kW h) during hour t is calculated as follows:

- If the diesel was running during the previous hour:

$$\text{Cons}_{fuel}(t) = B \cdot P_{GEN,rated} + A \cdot P_{GEN}(t) \quad (3)$$

- Else:

$$\text{Cons}_{fuel}(t) = B \cdot P_{GEN,rated} + A \cdot P_{GEN}(t) + F_{START}\left(B \cdot P_{GEN,rated} + A \cdot P_{GEN,rated}\right) \quad (4)$$

where $A = 0.246$ l/kW h and $B = 0.08415$ l/kW h are the fuel curve coefficients [26] and F_{START} is a factor which takes into account the extra fuel due to the start of the generator; if it was not working during the previous hour, it is usually lower than 0.0083, equivalent to 5 min at rated power [27].

2.1.3. Battery bank

The battery output current depends on the output power of the PV generator, the load, the control strategy and the SOC. If the battery is at SOC = 1 (per unit), it is fully charged and it does not accept any more charge; on the other hand, if it is at the lowest allowed SOC (depending on the battery technology, from 0.2 to 0.4 per unit), it cannot be discharged.

For the first hour the facility works, the state of charge SOC ($t = 0$) is known.

The SOC is calculated by adding the effective charge that comes into the battery to the SOC of the previous hour:

$$\begin{aligned} &\text{If } I_{bat}(t) > 0 \text{ (charge)}: \ \text{SOC}(t + \Delta t) = \text{SOC}(t) + I_{bat}(t) \cdot \eta_{ch} \cdot \Delta t / C_N \\ &\text{If } I_{bat}(t) < 0 \text{ (discharge)}: \text{SOC}(t + \Delta t) = \text{SOC}(t) - |I_{bat}(t)| / \eta_d \cdot \Delta t / C_N \end{aligned} \quad (5)$$

where $I_{bat}(t)$ (A) is the current that enters into the battery, η_{ch} is the charge efficiency, η_d is the discharge efficiency, C_N (A h) is the nominal capacity and Δt (h) is the time step (in this work 1 h).

The degradation of the battery must be considered so that when it finishes its lifetime, it must be replaced. The battery ageing is modelled considering that the battery can perform a specified number of full IEC cycles to failure (Z_{IEC}) [28] until the remaining capacity reaches 80% of its nominal capacity (when it is considered the end of its lifetime). If a battery of nominal capacity C_N (Ah) and nominal voltage V_{bat} (V) cycles an amount of energy E_{cycled} (kW h) during a specified period, the degradation of the battery Deg_{bat} during that period (in per unit: 1 is full degradation, i.e., the battery would consumes its whole lifetime) can be calculated as follows:

$$\text{Deg}_{bat} = E_{cycled} / (Z_{IEC} \cdot C_N \cdot V_{bat} / 1000) \quad (6)$$

2.1.4. Inverter/charger

The inverter/charger includes a charger that is modelled as a PWM controller with the charge in three stages (bulk, boost and float). The charger efficiency is usually considered as a fixed value. However, the inverter efficiency depends on the output power as shown in Fig. 2.

2.2. Mono-objective optimisation algorithm

Many combinations of components and control strategies can be considered. If the number of possible combinations of components and control strategies is too high, it would imply an inadmissible computation time. Then, GAs are used to perform the mono-objective optimisation (i.e., minimise one objective:

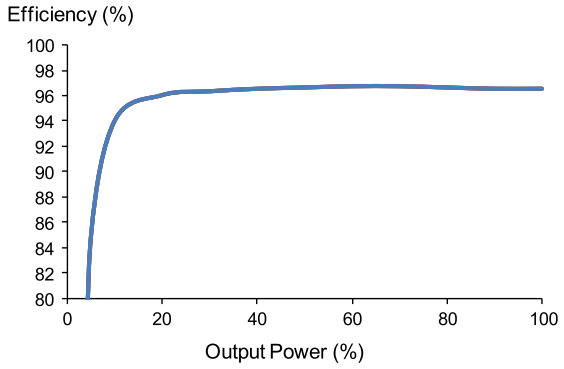

Fig. 2. Inverter efficiency.

weight or cost). Two GA are applied: the main algorithm for the optimisation of components and the second algorithm for the optimisation of the control strategy (for each combination of components).

The main GA uses an integer vector with the PV panel type code (a), the number of PV panels in parallel (b), the battery type code (c), the number of batteries in parallel (d), the diesel generator type code (e), and the inverter/charger type code (f):

$$|a|b|c|d|e|f|$$

The secondary GA also uses an integer vector, with four variables related to the control strategy:

$$|\text{Strategy}|P_{\text{min\_gen}}|\text{SOC}_{\text{min\_disconnect}}|\text{SOC}_{\text{stp\_gen}}|$$

Strategy: This variable has six possible values, as there are three general control strategies that can be applied [21] and also for each strategy there are two possibilities for the priority in supplying the load that cannot be covered by the PV, i.e., priority of battery bank or priority of diesel. The three general control strategies are:

- Load following strategy: when the diesel must work, it just runs to meet the load; it does not charge the batteries (unless its minimum output power was higher than the power required by the load).
- Cycle charging strategy: when the diesel must work, it will run at its rated power, not just to meet the demand but also to charge the batteries, just during that hour.
- Cycle charging strategy until setpoint: when the diesel must work, it will run at its rated power until the battery bank reaches a specified state of charge setpoint $\text{SOC}_{\text{stp\_gen}}$.

$P_{\text{min\_gen}}$: Minimum output power of the diesel generator. The specific consumption (l/kW h) for low output power is always higher than for high power [21], so the optimal $P_{\text{min\_gen}}$ could be higher than the value recommended by the manufacturer. This variable can vary from the value recommended by the manufacturer to the rated power, in a specified number of steps.

$\text{SOC}_{\text{min\_disconnect}}$: Minimum SOC of the battery. When the battery is discharging and reaches this value, the load is disconnected from the battery, preventing over-discharge. It can vary from the value recommended by the manufacturer to 80%, in a specified number of steps.

$\text{SOC}_{\text{stp\_gen}}$: When the Cycle charging strategy until setpoint is selected, the diesel runs at rated power, charging the battery bank until this SOC setpoint is reached. It can vary from $\text{SOC}_{\text{min\_disconnect}}$ to 100%, in a specified number of steps.

The flowchart of the mono-objective optimisation is shown in Fig. 3.

For each combination of components i that is evaluated by the main GA, a sub-algorithm (called the secondary GA) is used to obtain the optimal control strategy k and to minimise the objective variable (total weight or total cost). The main GA is used to obtain the optimal combination of components i (with the optimal combination of control variables obtained by the secondary algorithm), which minimises the objective variable (total weight or total cost).

For each GA, a population of N vectors (or individuals) is initially obtained randomly (first generation). Each vector of the secondary GA is evaluated by means of an hourly simulation of the system during the period of time the facility is working (a number of days N_{days}). At the end of the simulation of each individual (combination of components and control strategy), if the unmet load is higher than a specific value (for example, 0.01%), this individual is discarded. The set of vectors is sorted by the objective. The first (rank 1) is the best individual, whereas the last (rank N) is the worst. The fitness function of the individual with rank i is assigned as follows:

$$\text{fitness}_i = \frac{(N+1)-i}{\sum_j[(N+1)-j]} \quad j = 1 \ldots N \tag{7}$$

Then the reproduction, crossing and mutation occur, obtaining a new generation of individuals, and the process continues until a specified number of generations $N_{\text{gen\_max}}$ has been evaluated.

Two types of mono-objective optimisation have been considered: minimisation of total weight or minimisation of total cost.

2.2.1. Minimisation of total weight

The objective in this case is to minimise the total weight of the system, W_{TOTAL} (kg), calculated as the total weight of components and fuel used during the period of N_{days} to be transported:

- Weight of all the components to be placed in the location: weight of the PV panels, including the support and cables (W_{PV}), weight of the batteries, including the support and cables (W_{bat}), weight of the inverter/charger ($W_{\text{I/C}}$) and weight of the diesel generator ($W_{\text{D\_gen}}$).
- Same weight of all the components to return to the headquarters when the facility is disassembled.
- Weight of the diesel fuel used during the period considered:

$$W_{\text{fuel}} = \sum_{t=0}^{24\cdot N_{\text{days}}} \text{Cons}_{\text{fuel}}(t) \cdot \text{Dens}_{\text{fuel}} \tag{8}$$

where $\text{Dens}_{\text{fuel}}$ (kg/l) is the fuel density.

- If the fuel used is lower than a minimum number of litres (with weight $W_{\text{fuel\_min}}$, a minimum value decided by the designer which must be transported at the beginning so that the diesel itself can cover a percentage of the total load, in the case of any incidence in the PV or the battery bank, or in the case the solar radiation is lower than expected), the difference ($W_{\text{fuel\_min}} - W_{\text{fuel}}$) must be transported back to the headquarters when the facility is disassembled.

The total weight is:

$$W_{\text{total}} = 2 \cdot (W_{\text{PV}} + W_{\text{bat}} + W_{D\_\text{gen}} + W_{\text{I/C}}) + W_{\text{fuel}} + \min(0, W_{\text{fuel\_min}} - W_{\text{fuel}}) \tag{9}$$

The weight per kW h is calculated by dividing the total weight by the total load, L_{total} (kW h), consumed during the period.

$$W_{\text{per\_kW h}} = W_{\text{total}}/L_{\text{total}} \tag{10}$$

2.2.2. Minimisation of total cost

The objective in this case is to minimise the total cost of the system C_{total} (€) during the period considered (N_{days}), which includes:

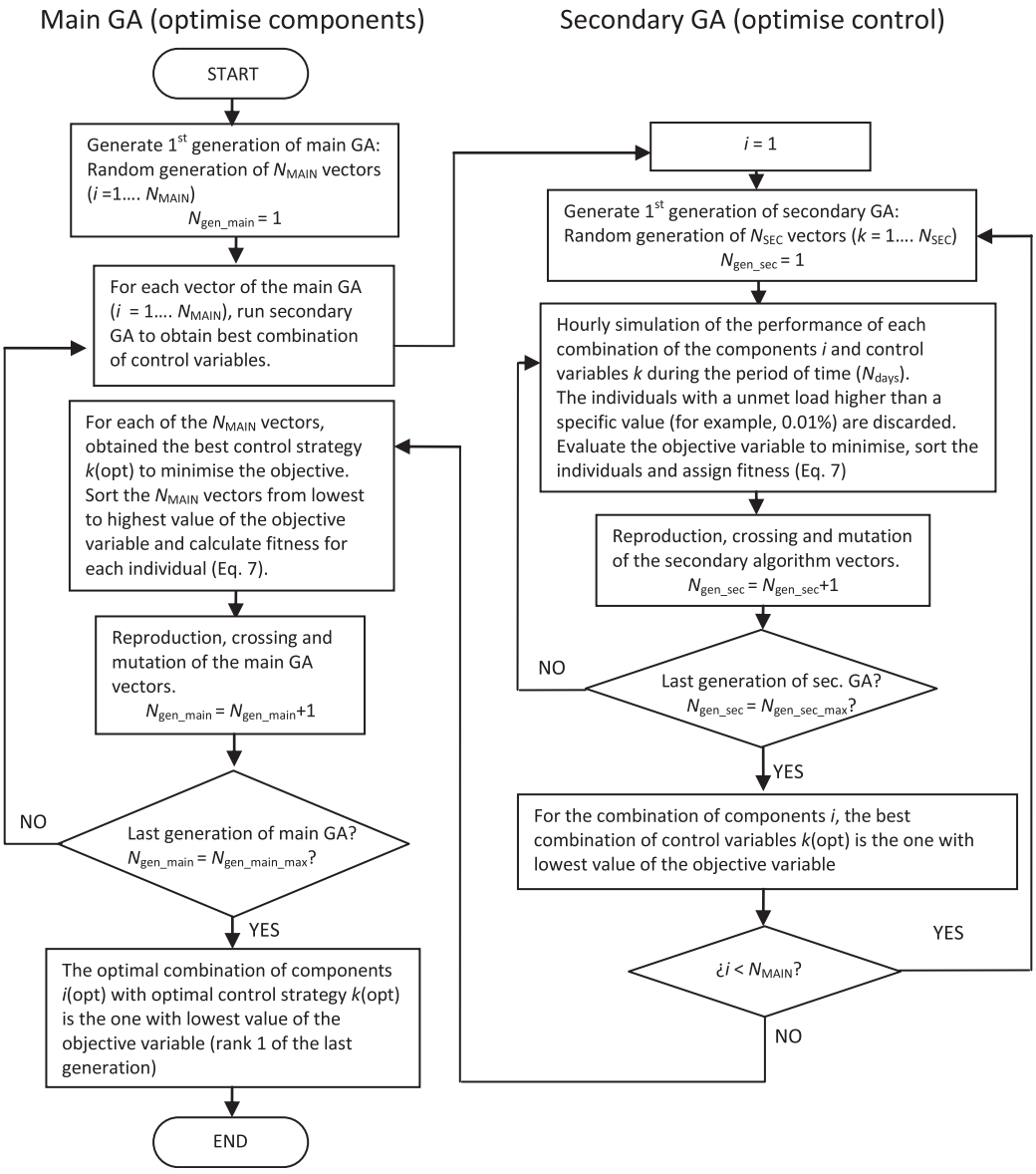

Fig. 3. Mono-objective optimisation by means of two GA.

- Cost of fuel used during the period considered:

$$C_{\text{fuel}} = \sum_{t=0}^{24 \cdot N_{\text{days}}} \text{Cons}_{\text{fuel}}(t) \cdot Pr_{\text{fuel}} \tag{11}$$

where Pr_{fuel} (€/l) is the diesel fuel price.

- Cost of O&M of the diesel during the period considered:

$$C_{\text{O\&M}} = h_{D_{\text{gen}}} \cdot Pr_{\text{O\&M}} \tag{12}$$

where $h_{\text{D\_gen}}$ (h) is the diesel number of hours of operation during the period considered and $Pr_{\text{O\&M}}$ (€/h) is the O&M cost per hour.

- Cost of transportation of the total weight:

$$C_{\text{weight}} = W_{\text{total}}/1000 \cdot C_{\text{transp}} \cdot \text{Dist} \tag{13}$$

where C_{transp} (€/(t km)) is the transportation cost per tonne and km and Dist (km) is the distance from the headquarters to the location of the facility.

- Cost of ageing of the PV generator during the period considered. The PV generator's expected lifetime Life_{PV} (yr) is usually considered as a fixed value, typically 25 years. So the ageing of the PV generator during the period considered (N_{days}) will be proportional to its lifetime, $N_{\text{days}}/(365 \cdot \text{Life}_{\text{PV}})$. The cost of ageing is calculated as follows:

$$C_{\text{PV}} = (1 + F_{\text{ageing\_PV}}) \cdot Pr_{\text{PV}} \cdot N_{\text{days}}/(365 \cdot \text{Life}_{\text{PV}}) \tag{14}$$

where Pr_{PV} (€) is the acquisition cost of the PV generator, and $F_{\text{ageing\_PV}}$ is the extra ageing factor to consider the premature ageing due to extreme conditions in the location (temperature, humidity, wild animals, etc.), the ageing due to transport, mounting and dissemblance, the ageing due to the non-optimal storage during the periods of time the PV generator is not used (i.e., the periods the system is stored in the headquarters), etc.

- Cost of ageing of the battery bank during the period considered. The battery bank's expected lifetime is not a fixed value in years: it depends on the operating conditions, mainly on the

energy cycled (degradation shown in Eq. (6) where Deg_{bat} is the degradation of the battery bank in per unit: 0 means no degradation during the period considered, while 1 means full degradation, i.e., the battery lifetime is the same as the period considered). Then, the cost of ageing of the battery bank can be calculated as follows:

$$C_{BAT} = (1 + F_{ageing\_bat}) \cdot Pr_{bat} \cdot Deg_{bat} \quad (15)$$

where Pr_{bat} (€) is the acquisition cost of the battery bank, Deg_{bat} (per unit) is the degradation of the battery due to the energy cycled during the period considered (Eq. (6)) and F_{ageing_bat} is the extra ageing factor to consider the periods of time the battery bank is stored (and periodically charged), the ageing due to the transport, mounting and dissemblance and for other ageing factors.

- Cost of ageing of the diesel generator during the period considered. The diesel generator's expected lifetime $Life_{D\_gen}$ (h) is usually considered the number of hours of operation (usually more than 10,000 h). Then, the ageing of the diesel during the period considered is proportional to its number of hours of operation during that period, $h_{D\_gen}/Life_{D\_gen}$. The cost of ageing of the diesel generator can be calculated as:

$$C_{D\_gen} = (1 + F_{ageing\_D\_gen}) \cdot Pr_{D\_gen} \cdot h_{D\_gen}/Life_{D\_gen} \quad (16)$$

where Pr_{D_gen} (€) is the acquisition cost of the diesel generator and $F_{ageing\_D\_gen}$ is the extra ageing factor due to the transport, mounting and dissemblance, and other ageing factors.

- Cost of ageing of the inverter/charger during the period considered. The inverter/charger's expected lifetime $Life_{I/C}$ (yr) is usually considered as a fixed value, usually 10 or 15 years. The cost of ageing is calculated as follows:

$$C_{I/C} = (1 + F_{ageing\_I/C}) \cdot Pr_{I/C} \cdot N_{days}/(365 \cdot Life_{I/C}) \quad (17)$$

where $Pr_{I/C}$ (€) is the acquisition cost of the inverter/charger and $F_{ageing\_I/C}$ is the extra ageing factor to consider the non-optimal conditions of storage during the periods of time the inverter/charger is not used and also the extra ageing due to the transport, mounting and dissemblance, and other ageing factors.

The total cost is:

$$C_{total} = C_{fuel} + C_{O\&M} + C_{weight} + C_{PV} + C_{BAT} + C_{D\_gen} + C_{I/C} \quad (18)$$

The cost per kW h is calculated by dividing the total cost by the total load consumed during the period.

$$C_{per\_kW\ h} = C_{total}/L_{total} \quad (19)$$

2.3. Multi-objective optimisation

When there are two objectives (minimisation of total cost and also minimisation of total weight), a Pareto-optimisation MOEA is applied for the main algorithm to optimise the components. Fig. 4 shows the Pareto front [29]: solutions "a" to "f" are non-dominated individuals (there is no other individual better in both objectives), and they compose the "Pareto front." At the final stage of the optimisation process, the non-dominated solutions constitute the Pareto Optimal Set. The solutions "1" to "3" are dominated solutions, as there is at least one non-dominated solution which is better in the two objectives.

The same GA as the one used for the mono-objective optimisation (Section 2.2) is applied for the secondary algorithm, but in this case the objective for the secondary GA is to minimise the fuel consumption (which is the variable which most affects both cost and weight). The MOEA used for the main algorithm is based on the one explained in [30].

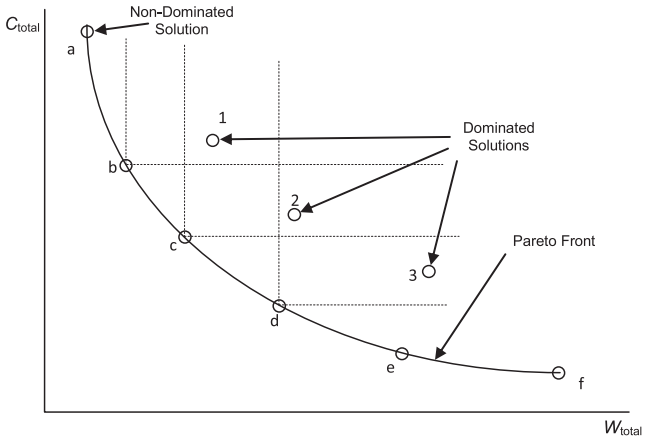

Fig. 4. Pareto front of the MOEA.

3. Example of application

Following the methods shown in Section 2, as an example it is shown the optimisation of a PV–diesel–batteries system to supply the load of a hypothetical hospital which will be installed due to any humanitarian emergency in a remote area of Central African Republic (latitude around 7.8°N, longitude around 23.2°E). The expected load is around 7 kW during daytime (with a maximum during one hour of 8 kW with 0.95 power factor) and around 2 kW during night time; total daily load is approximately 123 kW h/day. The fuel price in the country is 1.3 €/l. The hourly solar irradiation data are not usually available from measured values, but they can be synthetically generated from average monthly irradiation data (obtained in [31]) using the model of Graham and Hollands [32] which includes the randomness of cloudiness. The optimal slope for the PV panels is 0° (to optimise the irradiation of the worst month, which is July, with 4.96 kW h/m^2/day as average daily irradiation); however, usually a minimum of 10° or 15° is used to avoid excessive dirtiness. A value of 15° has been used so that 4.58 kW h/m^2/day is obtained for July as an average daily irradiation over the PV panel's surface. The average temperature for each month is also obtained in [31], being the average value for the whole year 25.3 °C.

Table 1 shows the possible components considered in the optimisations. DC nominal voltage is 48 V. As c-Si PV panels used are of 12 V nominal voltage, 4 of them connected in series are needed in all possible combinations. Also, OPzV batteries are of 2 V nominal so that 24 in series will be connected. A minimum battery bank of 215 A h (10.32 kW h) is considered to cover for a few hours the most critical load in case of incidence or maintenance in the diesel. The expected lifetime is 25 years for PV panels, 10 years for inverter/chargers, 12,000 h for diesel and 1250 IEC full cycles to failure for OPzV batteries. Each start of the diesel is considered equivalent to 5 min at full load ($F_{START} = 0.0083$). The SOC at the beginning (1st of July, 0 h) is $SOC(t = 0) = 0.5$.

Diesel fuel has a density of 0.845 kg/l. The possibility of PV–battery system (without diesel) has not taken into account as it is considered that the diesel must be present as a back-up even if a PV-battery system could cover the whole load. A minimum of diesel fuel litres has been considered so that the diesel can cover at least 30% of the load (to ensure that, in case of a problem with the PV and/or batteries, a 30% of the total load of the whole period could be covered with the diesel) in all the combinations, even for

Table 1
Possible components.

Component	Types	Cost (€)	Weight (kg)	Number in parallel
PV panels (2 types)	c-Si (normal), 200 Wp, 12 V	350	21	0–55
	c-Si-F (flexible), 200 Wp, 12 V	640	5	
Diesel generators (3 types)	9 kVA, O&M cost 0.14 €/h	4300	250	1
	11 kVA, O&M cost 0.15 €/h	4400	260	
	12.5 kVA, O&M cost 0.15 €/h	4500	275	
Batteries (8 types)	OPzV 215 A h	175	18.5	1
	OPzV 320 A h1755	222	27.5	
	OPzV 465 A h	270	36.3	
	OPzV 705 A h	332	55	
	OPzV 1170 A h	548	91.3	
	OPzV 1580 A h	782	120.1	
	OPzV 2640 A h	1363	200.6	
	OPzV 3170 A h	1584	240.9	
Inverter/chargers (7 types)	AC rated 4.5 kVA	3000	63	1
	AC rated 6 kVA	3400	68	
	AC rated 9 kVA	6000	126	
	AC rated 12 kVA	6800	136	
	AC rated 13.5 kVA	9000	189	
	AC rated 18 kVA	10,200	206	
	AC rated 24 kVA	13,600	236	

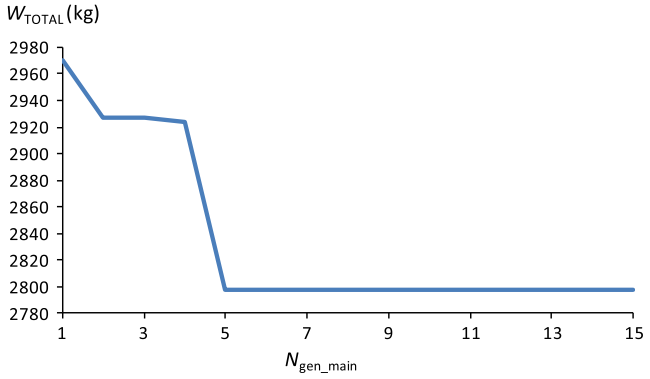

Fig. 5. Evolution of the main GA, minimisation of weight, case of N_{days} = 30 days.

the combinations with high-power PV generation. In order to perform a conservative study, high extra ageing factors for the PV generator and the inverter/charger are taken into account. The values used are: F_{ageing_PV} = 0.7, $F_{ageing\_I/C}$ = 0.5, F_{ageing_bat} = 0.3, $F_{ageing\_D\_gen}$ = 0.05. The transport cost is estimated in 0.12 €/(t km), and a distance of 200 km has been considered from the headquarters to the location of the hospital.

3.1. Mono-objective optimisation: minimisation of weight

The number of combinations of components is 2 types of PV panels × 56 possibilities in parallel × 3 types of diesel x 8 types of batteries × 7 types of inverter/chargers = 18,816. The number of combinations of control strategies is (using 10 steps for P_{min_gen}, $SOC_{min\_disconnect}$ and SOC_{stp_gen} and considering that SOC_{stp_gen} has meaning only for "Cycle charging strategy until setpoint" and

Table 2
Minimisation of weight. Optimal system found for each case of period of time.

Optimal system	N_{days} = 30 days	N_{days} = 60 days	N_{days} = 90 days	N_{days} = 180 days	N_{days} = 365 days
Configuration	No PV 24 × 215 A h (10.3 kW h) Inv/charger: 4.5 kVA Diesel: 9 kVA Load following, 1st diesel P_{min_gen} = 30% $SOC_{min\_disconnect}$ = 20%	No PV 24 × 215 A h (10.3 kW h) Inv/charger: 4.5 kVA Diesel: 9 kVA Load following, 1st diesel P_{min_gen} = 30% $SOC_{min\_disconnect}$ = 20%	4x24 c-Si-F (19.2 kWp) 24 × 215 A h (10.3 kW h) Inv/charger: 9 kVA Diesel: 9 kVA Load following, 1st diesel P_{min_gen} = 30% $SOC_{min\_disconnect}$ = 20%	4x34 c-Si-F (27.2 kWp) 24 × 215 A h (10.3 kW h) Inv/charger: 12 kVA Diesel: 9 kVA Load following, 1st diesel P_{min_gen} = 30% $SOC_{min\_disconnect}$ = 20%	4x39 c-Si-F (31.2 kWp) 24 × 465 A h (22.3 kW h) Inv/charger: 18 kVA Diesel: 9 kVA Cycle charging strategy, 1st battery, $SOC_{min\_disconnect}$ = 20%
Total load, L_{total} (kW h)	3694	7388	11,083	22,166	44,947
Renewable fraction (%)	0	0	41.6	48.6	62.7
Fuel consumption (l)	1516.3	3034.5	2761.4	4991	5775.6
Fuel minimum (l)	363	725	1087	2175	4410
Hours of diesel operation, h_{D_gen} (h)	720	1440	1598	3230	2457
Battery ageing (Deg_{bat}) (per unit)	0	0	0.018	0	0.29
Total weight, W_{total} (kg)	**2798.8**	**4081.6**	**5020.9**	**7240.7**	**9097.3**
Total cost, C_{total} (€)	2433.4	4830.7	5821.2	11,518	18834.2
Weight per kW h consumed, $W_{per\_kW\ h}$ (kg/kW h)	**0.758**	**0.552**	**0.453**	**0.327**	**0.202**
Cost per kW h consumed, $C_{per\_kW\ h}$ (€/kW h)	0.659	0.654	0.525	0.520	0.419

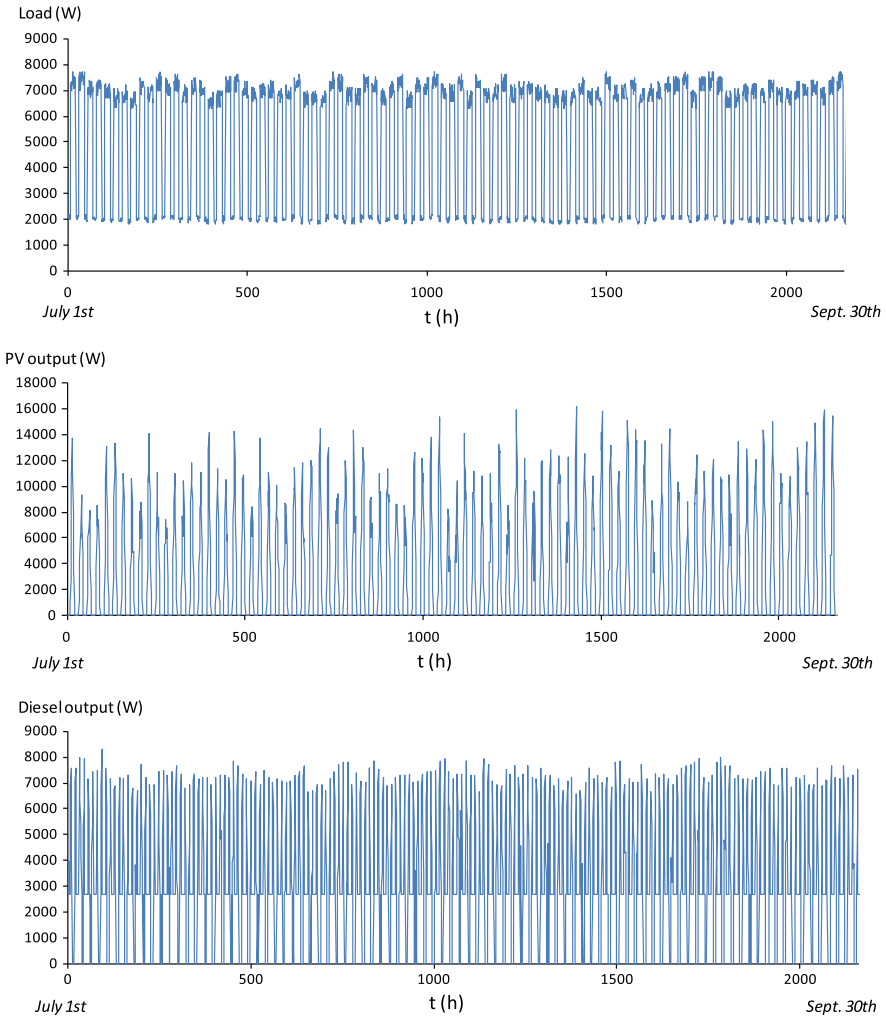

Fig. 6. Simulation of the optimal configuration, minimisation of weight, N_{days} = 90 days.

P_{min_gen} has only meaning on "Load following strategy") is $2 \cdot (2 \cdot 10^2 + 10) = 420$. The total number of combinations is $18{,}816 \times 420 = 7.92 \cdot 10^6$. Considering that around 50 cases can be simulated and evaluated per second in a 2.4 GHz, 4 GB RAM computer, around 2 days would be needed to evaluate all the combinations. By means of the genetic algorithms, using a population of 200 for the main GA and 10 for the secondary, with 15 generations for the main GA and 10 for the secondary, 90% crossing rate and 1% mutation rate [33], in around 1.6 h the optimal or a solution very near to optimal is obtained.

Five optimisations have been performed, for different cases of the number of days the temporary hospital is working in the place it will installed, N_{days} = 30; 60; 90, 180 and 365 days (starting all of them the 1st of July).

Fig. 5 shows the evolution of the weight of the best solution found in each generation (main GA), for the case of N_{days} = 30 days.

Table 2 shows the results of the optimal solution found for each optimisation (different cases of N_{days}). The most important results are shown in bold.

The optimal solution (system with minimum weight) for the cases of 30 and 60 days does not include PV generator (renewable penetration 0%), and the battery bank is the minimum allowed. However, for the cases of 90 days or more, the optimal system includes PV (with flexible c-Si panels), with renewable penetration increasing with the number of days the installation works. The system with the lowest weight for the cases of 90 or more days include PV, even considering that a minimum weight of diesel fuel is mandatory (to cover, in case of problems with PV or battery bank, the 30% of the total load of the whole period by diesel). Fig. 6 shows the hourly simulation of the optimal system found for the case of N_{days} = 90 days.

3.2. Mono-objective optimisation: minimisation of cost

Same parameters of the GA used in Section 3.1 have been used for the optimisation of total cost. Fig. 7 shows the evolution of the cost of the best solution found in each generation (main GA) for the case of N_{days} = 30 days. Table 3 shows the optimal solutions found for each case.

All the optimal solutions (systems with minimum cost) for the different periods include PV generator (with normal c-Si panels) with high renewable penetration (>88%) and relatively high battery capacity.

3.3. Multi-objective optimisation: minimisation of weight and cost

The MOEA used for the optimisation of both weight and cost uses the same parameters of the GA used in previous sections.

The Pareto Optimal Set includes the extreme solutions found in each of the mono-objective optimisations performed in the previous sections. For example, in the case of N_{days} = 30 days, the Pareto Optimal Set (Pareto of the 15th generation, the last one) is

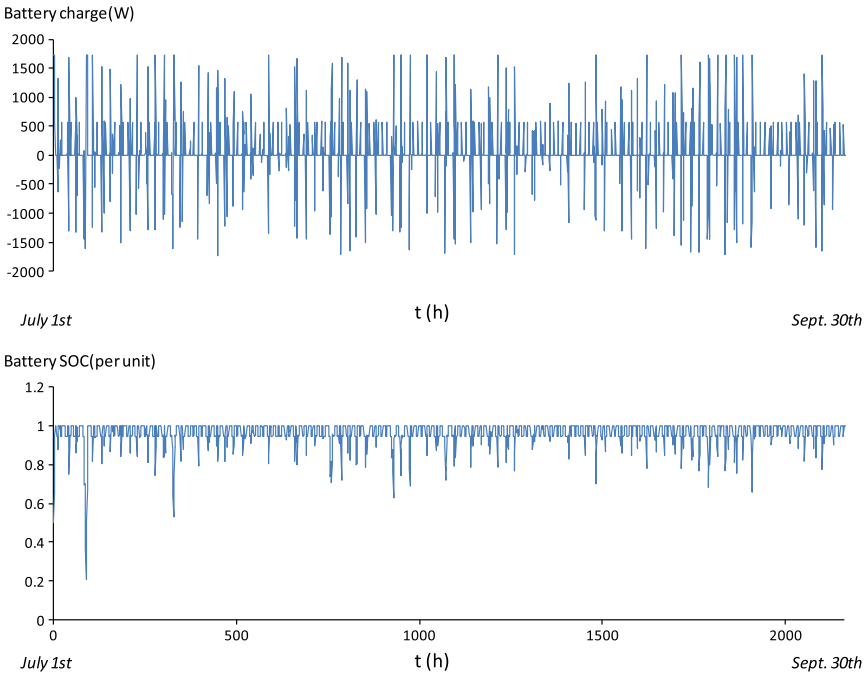

Fig. 6 (*continued*)

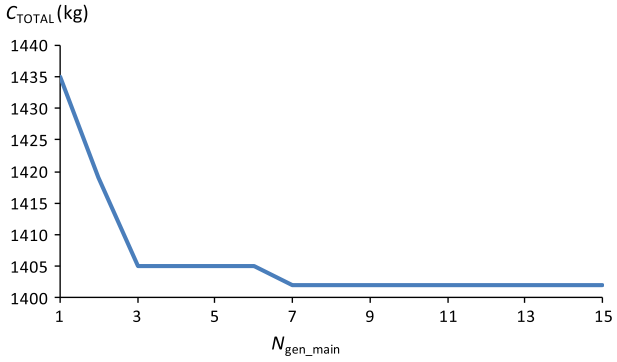

Fig. 7. Evolution of the main GA, minimisation of cost, case of N_{days} = 30 days.

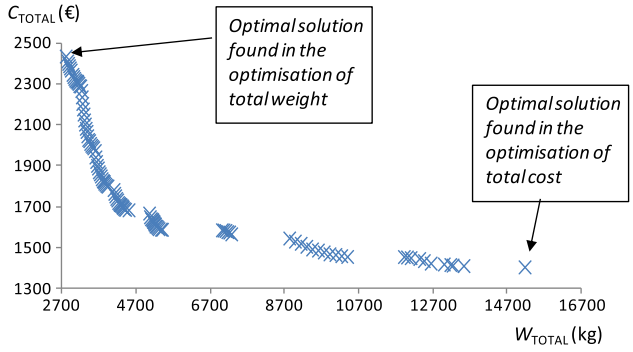

Fig. 8. Pareto set of the last generation (15th) of the MOEA, case of N_{days} = 30 days.

Table 3
Minimisation of cost.

Optimal system	N_{days} = 30 days	N_{days} = 60 days	N_{days} = 90 days	N_{days} = 180 days	N_{days} = 365 days
Optimal system found	4 × 47 c-Si (37.6 kWp) 24 × 1580 A h (75.8 kW h) Inv/charger: 18 kVA Diesel: 9 kVA Cycle charging strategy, 1st battery, $SOC_{min\_disconnect}$ = 20%	4 × 49 c-Si (38.4 kWp) 24 × 3170 A h (152.1 kW h) Inv/charger: 18 kVA Diesel: 9 kVA Cycle charging strategy, 1st battery, $SOC_{min\_disconnect}$ = 20%	4 × 49 c-Si (38.4 kWp) 24 × 3170 A h (152.1 kW h) Inv/charger: 18 kVA Diesel: 9 kVA Cycle charging strategy, 1st battery, $SOC_{min\_disconnect}$ = 20%	4 × 46 c-Si (36.8 kWp) 24 × 3170 A h (152.1 kW h) Inv/charger: 18 kVA Diesel: 9 kVA Cycle charging strategy, 1st battery, $SOC_{min\_disconnect}$ = 20%	4 × 44 c-Si (35.2 kWp) 24 × 3170 A h (152.1 kW h) Inv/charger: 18 kVA Diesel: 9 kVA Cycle charging strategy, 1st battery, $SOC_{min\_disconnect}$ = 20%
Total load, L_{total} (kW h)	3694	7388	11,083	22,166	44,947
Renewable fraction (%)	88.8	99	99.3	98.3	97.9
Fuel consumption (l)	136.1	25.5	25.5	127.6	317.7
Fuel minimum (l)	363	725	1087	2175	4410
Hours of diesel operation, h_{D_gen} (h)	52	10	10	49	121
Battery ageing (Deg_{bat}) (per unit)	0.017	0.019	0.029	0.056	0.11
Total weight, W_{total} (kg)	15138.3	21979.8	22591.6	23840.1	27120.6
Total cost, C_{total} (€)	**1402.3**	**2418.4**	**3348.6**	**6086.4**	**11620.4**
Weight per kW h consumed, $W_{per\_kW\ h}$ (kg/kW h)	4.098	2.975	2.038	1.076	0.603
Cost per kW h consumed, $C_{per\_kW\ h}$ (€/kW h)	**0.380**	**0.327**	**0.302**	**0.275**	**0.259**

composed by 108 individuals, shown in Fig. 8. With this optimisation, the designer has a set of solutions where no one is better than another one in both of the two objectives. So the designer can choose one of the extreme solutions (the one with minimal cost or the one with minimal weight) or any other intermediate solution.

4. Conclusions

This work shows a new method for the optimisation of hybrid renewable systems (PV + diesel + batteries) to supply the electrical load of temporary facilities which must be transported from a headquarters to a certain location and which works during a specified period of time; after that, they must be transported back to the headquarters and stored for the next need or emergency. Such needs include field hospitals or camps used by NGO or by military to help in humanitarian disasters or being placed in conflicted or war regions. In these situations, the transport of the components of the system must be done by difficult and/or dangerous accesses, so the total weight of the system can be the most important variable to be minimised. Also, the cost is usually an important variable. This kind of system is usually powered only by a diesel generator (generally with batteries to cover the load during maintenance or reparation of the diesel); however, it could be better to use hybrid systems. A new method for the optimisation of the electrical supply of this kind of system is shown, performing three types of optimisations: (a) minimisation of weight; (b) minimisation of cost; and (c) minimisation of both weight and cost. The two first optimisations are mono-objective and performed by genetic algorithms, while the third one is a multi-objective optimisation performed by multi-objective evolutionary algorithms.

A case of a hospital in Central African Republic has been studied with periods of time the facility must work of 30, 60, 90, 180 and 365 days, and considering relatively low transport cost (transport by truck, low cost compared to air cargo or helicopter transportation), for a distance of 200 km. If the period is of 90 or more days, the minimal weight is obtained with a hybrid system (including c-Si flexible PV panels and batteries, with renewable penetration of more than 40%). For the cases of 30 and 60 days, the optimal system which minimises the total weight does not include PV. However, taking into account only the total cost in the optimisation, in all the cases the optimal solution includes PV generator (with c-Si normal panels, obtaining a high renewable penetration of more than 88%, even considering a very high extra ageing factor for the PV) and a battery bank with high capacity.

The main conclusion is that, in many areas in the world, even considering only the minimisation of the total weight, if the facility must work more than a specific number of days, a hybrid system (PV + diesel + batteries) is the optimal solution, while, considering only the cost, in all the cases the optimal solution is a hybrid system.

References

[1] Bína L, Bínová H, Březina E, Kumpošt P, Padělek T. Comparative model of unit costs of road and rail freight transport for selected European countries. Eur J Bus Soc Sci 2014;3:127–36.

[2] European Commission E. EU transport in figures. Statistical Pocketbook 2014 2014. http://dx.doi.org/10.2832/63317.

[3] Research and Innovative Technology Administration. U.S. Department of Transportation. Bureau of Transportation Statistics. National Transportation Statistics; 2015.

[4] Teravaninthorn S, Raballand G. Transport prices and costs in Africa: a review of the main international corridors. Afr Infraestruct Country Diagn 2008.

[5] Rancourt M-È, Bellavance F, Goentzel J. Market analysis and transportation procurement for food aid in Ethiopia. Socioecon Plan Sci 2014;48:198–219. http://dx.doi.org/10.1016/j.seps.2014.07.001.

[6] Ahlborg H, Hammar L. Drivers and barriers to rural electrification in Tanzania and Mozambique – grid-extension, off-grid, and renewable energy technologies. Renew Energy 2014;61:117–24. http://dx.doi.org/10.1016/j.renene.2012.09.057.

[7] Borhanazad H, Mekhilef S, Saidur R, Boroumandjazi G. Potential application of renewable energy for rural electrification in Malaysia. Renew Energy 2013;59:210–9. http://dx.doi.org/10.1016/j.renene.2013.03.039.

[8] Adaramola MS, Agelin-Chaab M, Paul SS. Analysis of hybrid energy systems for application in southern Ghana. Energy Convers Manag 2014;88:284–95. http://dx.doi.org/10.1016/j.enconman.2014.08.029.

[9] Ismail MS, Moghavvemi M, Mahlia TMI. Design of an optimized photovoltaic and microturbine hybrid power system for a remote small community: case study of Palestine. Energy Convers Manag 2013;75:271–81. http://dx.doi.org/10.1016/j.enconman.2013.06.019.

[10] Ismail MS, Moghavvemi M, Mahlia TMI. Techno-economic analysis of an optimized photovoltaic and diesel generator hybrid power system for remote houses in a tropical climate. Energy Convers Manag 2013;69:163–73. http://dx.doi.org/10.1016/j.enconman.2013.02.005.

[11] Kumar U Suresh, Manoharan PS. Economic analysis of hybrid power systems (PV/diesel) in different climatic zones of Tamil Nadu. Energy Convers Manag 2014;80:469–76. http://dx.doi.org/10.1016/j.enconman.2014.01.046.

[12] Campana PE, Li H, Zhang J, Zhang R, Liu J, Yan J. Economic optimization of photovoltaic water pumping systems for irrigation. Energy Convers Manag 2015;95:32–41. http://dx.doi.org/10.1016/j.enconman.2015.01.066.

[13] Edwin M, Joseph Sekhar S. Techno-economic studies on hybrid energy based cooling system for milk preservation in isolated regions. Energy Convers Manag 2014;86:1023–30. http://dx.doi.org/10.1016/j.enconman.2014.06.075.

[14] Dufo-López R, Pérez-Cebollada E, Bernal-Agustín JL, Martínez-Ruiz I. Optimisation of energy supply at off-grid healthcare facilities using Monte Carlo simulation. Energy Convers Manag 2016;113:321–30. http://dx.doi.org/10.1016/j.enconman.2016.01.057.

[15] Akikur RK, Saidur R, Ping HW, Ullah KR. Comparative study of stand-alone and hybrid solar energy systems suitable for off-grid rural electrification: a review. Renew Sustain Energy Rev 2013;27:738–52. http://dx.doi.org/10.1016/j.rser.2013.06.043.

[16] Mohammed YS, Mustafa MW, Bashir N. Hybrid renewable energy systems for off-grid electric power: review of substantial issues. Renew Sustain Energy Rev 2014;35:527–39. http://dx.doi.org/10.1016/j.rser.2014.04.022.

[17] Bajpai P, Dash V. Hybrid renewable energy systems for power generation in stand-alone applications: a review. Renew Sustain Energy Rev 2012;16:2926–39. http://dx.doi.org/10.1016/j.rser.2012.02.009.

[18] Bernal-Agustín JL, Dufo-López R. Simulation and optimization of stand-alone hybrid renewable energy systems. Renew Sustain Energy Rev 2009;13:2111–8. http://dx.doi.org/10.1016/j.rser.2009.01.010.

[19] Sinha S, Chandel SS. Review of software tools for hybrid renewable energy systems. Renew Sustain Energy Rev 2014;32:192–205. http://dx.doi.org/10.1016/j.rser.2014.01.035.

[20] Goldberg DE. Genetic algorithms in search, optimization, and machine learning. 1989th ed. Addison-Wesley Publishing Company; 1989.

[21] Dufo-López R, Bernal-Agustín JL. Design and control strategies of PV–diesel systems using genetic algorithms. Sol Energy 2005;79:33–46. http://dx.doi.org/10.1016/j.solener.2004.10.004.

[22] Ismail MS, Moghavvemi M, Mahlia TMI. Genetic algorithm based optimization on modeling and design of hybrid renewable energy systems. Energy Convers Manag 2014;85:120–30. http://dx.doi.org/10.1016/j.enconman.2014.05.064.

[23] Coello CA, Veldhuizen DAV, Lamont GB. Evolutionary algorithms for solving multi-objective problems. New York: Kluwer Aca; 2002.

[24] Fadaee M, Radzi MAM. Multi-objective optimization of a stand-alone hybrid renewable energy system by using evolutionary algorithms: a review. Renew Sustain Energy Rev 2012;16:3364–9. http://dx.doi.org/10.1016/j.rser.2012.02.07.

[25] Higier A, Arbide A, Awaad A, Eiroa J, Miller J, Munroe N, et al. Design, development and deployment of a hybrid renewable energy powered mobile medical clinic with automated modular control system. Renew Energy 2013;50:847–57. http://dx.doi.org/10.1016/j.renene.2012.07.036.

[26] Skarstein O, Uhlen K. Design considerations with respect to long-term diesel saving in wind/diesel plants. Wind Eng 1989;13:72–87.

[27] Bleijs J, Nightingale C, Infield D. Wear implications of intermittent diesel operation in wind/diesel systems. Wind Energy 1993;17:206–18.

[28] International Electrotechnical Commission. IEC 60896-1:1987 Stationary lead–acid batteries. General requirements and methods of test. Vented types; 1987.

[29] Bernal-Agustín JL, Dufo-López R. Multi-objective design and control of hybrid systems minimizing costs and unmet load. Electr Power Syst Res 2009;79:170–80. http://dx.doi.org/10.1016/j.epsr.2008.05.011.

[30] Dufo-López R, Bernal-Agustín JL. Multi-objective design of PV–wind–diesel–hydrogen–battery systems. Renew Energy 2008;33:2559–72. http://dx.doi.org/10.1016/j.renene.2008.02.027.

[31] NASA surface meteorology and solar energy; n.d. https://eosweb.larc.nasa.gov/cgi-bin/sse/retscreen.cgi [accessed January 20, 2016].

[32] Graham VA, Hollands KGT. A method to generate synthetic hourly solar radiation globally. Sol Energy 1990;44:333–41. http://dx.doi.org/10.1016/0038-092X(90)90137-2.

[33] Bernal-Agustín JL, Dufo-López R. Efficient design of hybrid renewable energy systems using evolutionary algorithms. Energy Convers Manag 2009;50:479–89. http://dx.doi.org/10.1016/j.enconman.2008.11.007.

Renewable Energy 94 (2016) 280–293

Contents lists available at ScienceDirect

Renewable Energy

journal homepage: www.elsevier.com/locate/renene

Optimisation of PV-wind-diesel-battery stand-alone systems to minimise cost and maximise human development index and job creation

Rodolfo Dufo-López [a, *], Iván R. Cristóbal-Monreal [b], José M. Yusta [a]

[a] Electrical Engineering Department, University of Zaragoza, Calle María de Luna, 3, 50018 Zaragoza, Spain
[b] Centro Universitario de la Defensa, Academia General Militar, Ctra. de Huesca s/n, 50.090 Zaragoza, Spain

ARTICLE INFO

Article history:
Received 10 February 2016
Received in revised form
16 March 2016
Accepted 21 March 2016

Keywords:
Renewable stand-alone systems
Net present cost
Human development index
Job creation
Multi-objective evolutionary algorithms

ABSTRACT

In this paper we show a multi-objective evolutionary algorithm (MOEA) for the optimisation of stand-alone (off-grid) hybrid systems (photovoltaic-wind-diesel-battery) to minimise total net present cost (NPC) and maximise human development index (HDI) and job creation (JC). Optimisation of this kind of system is usually performed considering only the minimisation of cost (NPC or the levelised cost of energy), as well as the emissions and the unmet load in some cases. In this paper, for the first time, we consider the maximisation of HDI and JC as part of optimisation. HDI depends on the consumption of electricity, so the extra energy that can supply the hybrid system can improve the HDI index. JC is different for each technology, obtaining different values for each combination of components in the system. The three objectives are often opposed, so a Pareto-optimisation MOEA is a good option to obtain a set of possible solutions in which no solution is better than another one for all three objectives (optimal Pareto set). We provide an example in the optimisation of a hybrid system to supply electricity to a small community in the Sahrawi refugee camps of Tindouf.

1. Introduction

In off-grid stand-alone systems (far from the electrical grid), the electrical supply is usually provided by diesel generator (with or without battery storage), photovoltaic generator (PV) with battery storage, wind turbines with batteries or hybrid systems. Previous studies show drivers and barriers to rural electrification by off-grid renewable energy systems [1–4]. Other works show the optimisation of stand-alone hybrid systems by minimising the NPC of the system or the levelised cost of energy (LCE) [5–11]. In some previous works, the authors apply heuristic techniques as genetic algorithms (GA) [12,13] in order to reduce the computation time of the optimisation. Most of these studies only optimise the cost (NPC or LCE), but some previous works also consider other objectives, such as the minimisation of CO_2 emissions and/or unmet load by applying Pareto-optimisation MOEA [14–20].

In this paper we present, for the first time, a methodology for the optimisation of a hybrid system (Fig. 1) to supply the electrical load of a rural off-grid area without electricity access while minimising NPC and also maximising HDI and JC. As each component (PV generator, wind turbines, diesel generator, battery bank and inverter/charger) can present different sizes or technologies, the number of possible combinations of components and control strategies could be too high, and the evaluation of all of them could imply inadmissible computation time, so heuristic techniques are applied to perform the optimisations within an acceptable computation time. In this paper we use an MOEA combined with a GA.

In the literature review, we found no previous work which has considered the three objectives (NPC, HDI and JC) using an optimisation methodology. Rojas-Zerpa and Yusta [21,22] proposed a combined application of two multi-criteria decision-making methods (Analytical Hierarchy Process and Compromise Ranking method) to facilitate the selection of the best solution for electrical supply of remote rural locations, considering technical, economic, environmental and social criteria (including HDI and JC). Their work uses weights for each criterion, which are selected based on the opinions of experts, and uses multi-criteria methods, not multi-objective optimisation methodologies.

The system with all possible components is shown in Fig. 1. It is

* Corresponding author.
E-mail addresses: rdufo@unizar.es (R. Dufo-López), icristob@unizar.es (I.R. Cristóbal-Monreal), jmyusta@unizar.es (J.M. Yusta).

http://dx.doi.org/10.1016/j.renene.2016.03.065
0960-1481/

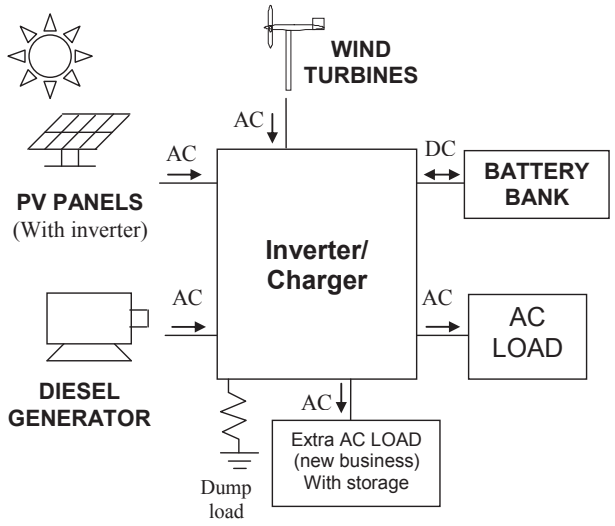

Fig. 1. AC coupled PV-wind-diesel-battery system.

an AC coupled system; different possible configurations are shown by Salas et al. [23]. In Fig. 1, the AC load is the load that must be covered by the hybrid system; that is, the expected load that is mandatory to cover. The excess energy produced by the PV and the wind turbines (when the AC load is fully covered and the battery bank is at full charge) can be used by new extra business or services (extra AC load, with their own battery storage), incrementing the total load consumed by the community and then increasing the HDI. A dump load is used to consume electricity produced by the wind turbines when the AC load and the extra AC load are covered and the batteries are full.

HDI is a country development indicator that takes into account life expectancy at birth, expected years of schooling and gross national income per capita [24]. In 2014, 17.8% of the world's population did not have access to electricity; i.e. 1285 million people [24,25].

Access to electricity can improve all of these indicators and then increase HDI. For example, life expectancy can be increased by the supply of potable water (which can be easily extracted by electrical pumps) and food conservation can be improved by means of electrical refrigerators, among other factors. Education can be improved with electricity, as it enables the use of computers and electric lighting. Gross national income per capita is also improved with electricity access, as new services and business can be developed.

The United Nations [24] classifies countries as having a low, medium, high or very high human development index. HDI depends on the electricity use per capita in a logarithmic dependency introduced by Pasternak [26] with data for 60 countries from the United Nations Human Development Report 1999 [27] (Eq. (1)).

$$\mathrm{HDI} = 0.091\ \ln\left(E_{\mathrm{load\_annual\_per\_capita}}\right) + 0.0724 \quad (1)$$

where $E_{\mathrm{load\_annual\_per\_capita}}$ (kWh/yr/person) is the annual electricity consumption per capita.

Later Rojas-Zerpa [28] showed also a logarithmic dependence (with different fit parameters) with data for 128 countries [29] (Eq. (2)).

$$HDI = 0.0978\ \ln\left(E_{\mathrm{load\_annual\_per\_capita}}\right) - 0.0319 \quad (2)$$

The JC of various electricity generation technologies has been studied by different researchers [30–36]. Ramanathan and Gadesh [30] studied the number of employees per GWh/yr (energy supplied during one year) by the different technologies in India. The unit jobs/(GWh/yr) are adequate for fossil fuel technologies like diesel generators, as the lifetime of a generator (and also the operation and maintenance cost) depends on the number of hours of operation (and therefore on the energy supplied). Fuel consumption also depends on the amount of energy supplied, so the jobs related to this kind of technology are correctly measured in jobs/(GWh/yr) of energy supplied. These researchers [30] reported 0.17 jobs/(GWh/yr) for electricity generated by diesel in India in 1984–85. This value has fallen since then due to technological advances and improved labour productivity; Rojas-Zerpa [28] proposes a value of 0.14 jobs/(GWh/yr) for diesel or gasoline electricity generation.

For other technologies, such as PV generators or wind turbines, different units are used for job creation. Many studies use units for jobs in manufacturing and installation (non-continuous activities) of PV and wind power plants in terms of job·years per MW (where MW means peak power for PV and maximum output power for wind turbines), denoted in many cases as job-years/MW or person-years/MW. One job·year means a full-time job for one person for a duration of 1 year. However, operation and maintenance (O&M) jobs (continuous activities whose duration is the whole lifetime of the system) are usually measured in jobs/MW. For example, in a power plant of 20 MW that requires 50 persons for 1 year for the manufacturing of its components and 25 persons for 6 months for the installation, the number of job·year/MW is calculated as (50 job·1 year + 25 job·0.5 year)/20 MW = 3.125 job·year/MW. If the power plant's expected lifetime is 25 years, we could normalize to the average jobs during its lifetime, so we can consider that it has created an equivalent number of full-time permanent jobs (i.e. jobs during its lifetime) of 3.125 job·year/MW/25 years = 0.125 jobs/MW. In the same example, if for O&M the power plant of 20 MW needs 5 persons, then 5 job/20 MW = 0.25 jobs/MW in O&M during its lifetime. So, during its lifetime, the equivalent total number of permanent full-time jobs is 0.125 + 0.25 = 0.375 jobs/MW.

Wei et al. [31] compare three previous studies of PV generators obtaining a great range between 0.41 and 2.48 jobs/MW (including manufacturing, installation and O&M), and compares five studies of wind turbines obtaining a range between 0.39 and 0.8 jobs/MW. Many other studies obtain different values using different units, including or excluding indirect jobs. Cameron and Van der Zwaan [36] compare different studies, including all the phases (manufacturing, installation and O&M) and considering both direct and indirect jobs, normalized to the units of jobs/MW, obtaining the results shown in Table 1.

2. Methodology

In this section the mathematical models of the components used in the simulation and evaluation of each combination of components and control strategy are shown. After that, we describe the multi-objective optimisation techniques using MOEA and GA. Finally, in this section we show the calculation of the variables to be optimised (NPC, HDI and JC).

Table 1
Total job creation including all phases, direct and indirect jobs [36].

	Total job creation (jobs/MW)		
	Minimum	Mean	Maximum
PV	0.5	2.7	7.6
Wind	0.2	1.1	2.9

2.1. Mathematical model for the hourly simulation of the system

The evaluation of each combination of components and control strategy implies that the performance of that combination must be simulated. The simulation is performed in hourly steps, during a number of years n_y (not known a priori) until the battery bank's remaining capacity drops to 80% (in that moment the battery bank is considered to have reached the end of its lifetime, and a new battery bank will replace the old one). We suppose the load, irradiation and wind speed have the same values for the different years; i.e. their hourly values in one year are repeated in the next year. However, the performance of the battery bank will not be the same for the different years, as the remaining capacity of the battery bank is continuously being reduced. When the hourly performance of the first n_y years is known, we suppose the next n_y years the system will have the same performance, and so on until the lifetime of the system (usually 20 or 25 years) ends.

After the simulation we will know whether that combination of components and control strategy can supply the whole AC load, and we will also know the battery charging/discharging energy over the years, the battery lifetime in years, the number of hours the diesel generator runs in the year (and therefore the diesel generator lifetime in years), the annual fuel consumption, the annual energy supplied by the diesel generator, the excess energy generated by the renewable sources, the annual O&M cost, the replacement costs of the components during the system lifetime, etc. With these results we will be able to calculate the NPC, HDI and JC.

The simulation of the system is performed in hourly time steps, from the first hour ($t = 0$) until the last hour ($t = 8760\ n_y$). The mathematical models of the PV generator, wind turbines, diesel generator and battery bank are described below.

During each hour the power balance must be satisfied:

- If the renewable output power is higher than the AC load demand, the difference will be used to charge the battery bank. If there is still any excess energy, it can be used or stored by the extra AC load (new businesses or services with their own battery storage, Fig. 1).
- If the renewable output power is not enough to supply the AC load demand, the battery bank and/or the diesel must supply the rest. It depends on the state of charge (SOC) of the battery bank and control strategy).

2.1.1. PV generator

We consider that the PV inverter includes a maximum power point tracking (MPPT) system, so the output power $P_{PV}(t)$ (W) of the PV generator during hour t of the year ($t = 0 \ldots 8760$) is calculated as shown in the next equation, and it is considered to repeat for all years:

$$P_{PV}(t) = P_{STC} \cdot \frac{G_h(t)}{1\text{kWh/m}^2} \cdot \left[1 + \frac{\alpha}{100}(T_c(t) - 25)\right] \cdot F_{dirt} \quad (3)$$

where P_{STC} (Wp) is the output power in standard test conditions; $G_h(t)$ (kWh/m^2) is the irradiation over the tilted surface of the PV panels during hour t; F_{dirt} is a factor to consider the losses due to dirt, wires, module mismatch or power tolerance and other losses (around 0.9); α is the power temperature coefficient (%/ºC); and $T_c(t)$ (ºC) is the PV cell temperature, which can be calculated as follows:

$$T_c(t) = T_a(t) + \left(\frac{NOCT - 20}{0.8}\right) \cdot \frac{G_{h\_yearY}(t)}{1\text{kWh/m}^2} \quad (4)$$

where $T_a(t)$ is the ambient temperature (ºC) and $NOCT$ is the nominal operation cell temperature (ºC).

2.1.2. Wind turbines

The power curve supplied by the manufacturer shows the output power vs. the wind speed in standard conditions at sea level (standard pressure $P_0 = 101{,}325$ Pa, standard temperature $T_0 = 288.15$ K, standard air density $\rho_0 = 1.225$ kg/m^3). For example, in Fig. 2, a solid line, the output curve of a commercial wind turbine of 43 kW maximum power is shown. During each hour, the power curve must be converted to the power curve at the height of the location and temperature $T(t)$ (K) of that hour, with an air density $\rho(t)$ (kg/m^3) different than the one at standard conditions, by multiplying the output power by the relation $\rho(t)/\rho_0$ (for example, in Fig. 2, dotted line, at 400 m height and temperature 298 K). This relation is based on the ideal gas law:

$$\frac{\rho(t)}{\rho_0} = \left(1 - \frac{L \cdot H}{T_o}\right)^{\frac{gM}{RL}} \cdot \frac{T_0}{T(t)} \quad (5)$$

where L is the variation rate of temperature vs. height (0.0065 K/m), $g = 9.80665$ m/s^2, R is the ideal gas constant (8,31432 J/mol·K) and M is the molecular weight of dry air ($28.9644 \cdot 10^{-3}$ kg/mol).

If the hub height z_{hub} (m) of the wind turbine is different from the anemometer height where the wind speed data were measured z_{anem} (m), the wind speed at the hub height W_{HUB_h} (t) can be obtained from the wind speed measured by the anemometer W_h (t), as follows:

$$W_{HUB\_h}(t) = W_h(t) \cdot \frac{\ln \frac{z_{hub}}{z_0}}{\ln \frac{z_{anem}}{z_0}} \quad (6)$$

where z_0 is the surface roughness length (m).

2.1.3. Diesel generator

The diesel generator output power $P_{GEN}(t)$ depends on the output power of the renewable generators, the AC load, the control strategy and the SOC of the batteries. The diesel fuel consumption (l/kWh) during hour t is calculated as follows:

- If the diesel generator was running during the previous hour:

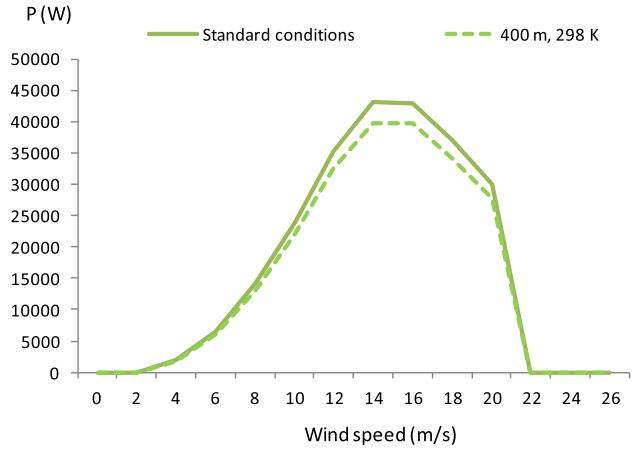

Fig. 2. Output curve of a wind turbine.

$$Cons_{fuel}(t) = B \cdot P_{GEN,rated} + A \cdot P_{GEN}(t) \quad (7)$$

- Otherwise:

$$Cons_{fuel}(t) = B \cdot P_{GEN,\ rated} + A \cdot P_{GEN}(t) + F_{START}(B + A) \cdot P_{GEN,\ rated} \quad (8)$$

where $A = 0.246$ l/kWh and $B = 0{,}08415$ l/kWh are the fuel curve coefficients [37] and F_{START} is a factor to consider the extra fuel due to the start of the generator, which is usually lower than 0.0083, equivalent to 5 min at rated power [38].

2.1.4. Battery bank

The battery output current depends on the output power of the renewable generators, the AC load, the control strategy and its SOC.

One of the most important issues in the simulation of the battery performance is the correct prediction of its ageing during the years, as its lifetime depends on that. Classical models that are used to evaluate battery ageing (equivalent cycles to failure model or cycle counting model) have been widely used in the optimisation of hybrid systems. However, these classical models assume that operating conditions are the same as the conditions of the standard tests used by the manufacturers, often predicting battery bank lifetimes too optimistically (in some cases they can predict a battery bank lifetime that is several times the real lifetime) [39].

In this paper we use a weighted Ah-throughput model introduced by Schiffer et al. [40], which considers the real operating conditions. This model is much more accurate than classical models, obtaining a much more realistic battery lifetime prediction [39].

2.1.5. Inverter/charger

The inverter/charger is modelled as a PWM controller with the charge in three stages. The charger efficiency $\mu_{I/C\text{-charger}}$ is usually considered a fixed value. However, the inverter efficiency $\mu_{I/C\text{-inverter}}$ depends on the output power, as shown in Fig. 3.

2.2. Multi-objective optimisation algorithm

If the number of possible combinations of components and control strategies is too high, evaluating all of them would imply an inadmissible computation time. Heuristic techniques have been applied by combining two algorithms:

- The main algorithm is an MOEA used for the optimisation of the components (considering the three objectives: minimisation of NPC, maximisation of HDI and maximisation of JC)
- The secondary algorithm is a GA used for the optimisation of the control strategy (for each combination of components considered in the main algorithm), considering only the minimisation of NPC.

For each combination of components, the secondary algorithm (GA) looks for the best control strategy that minimises the NPC of that combination of components. The main algorithm (MOEA) considers the three objectives and obtains the Pareto-set of the non-dominated combinations of components (with the best control strategy found for each one by the secondary GA).

2.2.1. Main algorithm (MOEA)

A multi-objective optimisation problem can be defined as follows [15]:

Minimise or maximise the objective functions included in the vector:

$$F(x) = [f_1(x),\ f_2(x), \ldots,\ f_k(x)] \quad (9)$$

Satisfying the m restrictions of inequality and the p restrictions of equality:

$$g(x) \geq 0 \quad i = 1, 2, \ldots,\ m \quad (10)$$

$$h_i(x) = 0 \quad i = 1, 2, \ldots, p \quad (11)$$

When there are two objectives to be minimised, Fig. 4 shows the Pareto front [17]: solutions "a" to "f" are non-dominated individuals (there is no other individual better in both objectives), and they compose the Pareto front. At the end of the optimisation process, the non-dominated solutions constitute the Pareto optimal set. The solutions "1"–"3" are dominated solutions, as there is at least one non-dominated solution which is better in the two objectives.

If there are three objectives to be minimised, the Pareto front can be shown graphically in a 3D graph.

The MOEA (main algorithm) implemented in this paper uses an integer vector with the PV panel type code (a), the number of PV panels in parallel (b), the wind turbine type code (c), the number of wind turbines in parallel (d), the battery type code (e), the number of batteries in parallel (f), the diesel generator type code (g) and the inverter/charger type code (h):

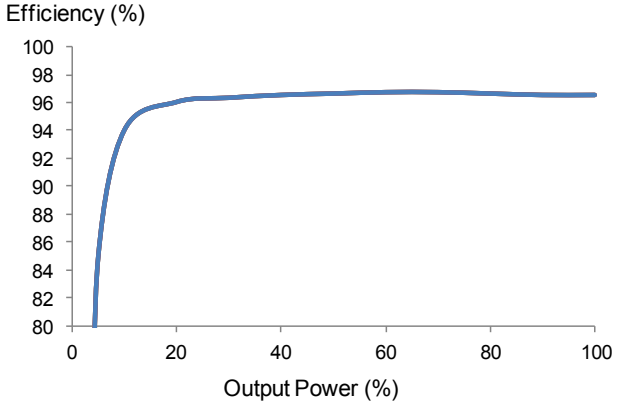

Fig. 3. Inverter efficiency.

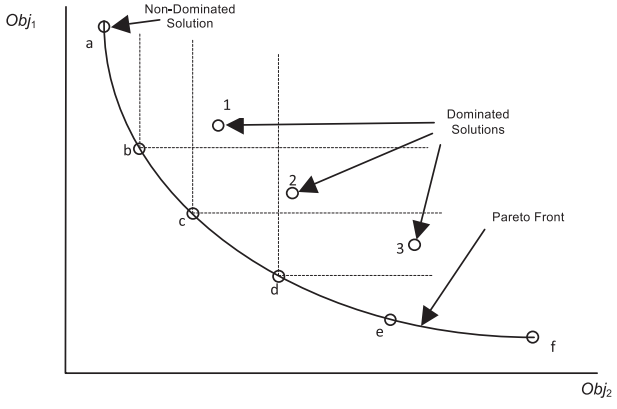

Fig. 4. Pareto front of the MOEA.

|a|b|c|d|e|f|g|h|

The flowchart of the MOEA is shown in Fig. 5 (left part).

First a random generation of a population of N_{MAIN} vectors (also called individuals or solutions, i.e. combinations of components) ($i = 1 \ldots N_{MAIN}$) is obtained, constituting the first generation ($N_{gen\_main} = 1$). For each combination of components i, the secondary algorithm (GA) is used to obtain the optimal control strategy k so that the NPC of that combination of components is minimised. Once the best control strategy is found for each combination of components, they are sorted according to the number of solutions they are dominated by, considering the three objectives (minimisation of NPC, maximisation of HDI and maximisation of JC). The fitness function of the combination i of the MOEA is assigned according to its rank in the population. The solutions that are dominated by the same number of solutions must have the same fitness, which will be the average fitness of these solutions:

$$fitness_{MAIN_i} = \frac{\sum_n \left[\frac{(N_{MAIN}+1)-i}{\sum_m [(N_{MAIN}+1)-m]} \right]}{(b-a+1)} \quad (12)$$

where i is the rank of the solution evaluated, m are all the solutions of the MOEA ($m = 1 \ldots N_{MAIN}$) and n are all the solutions dominated by the same number of solutions as the solution evaluated ($n = a \ldots b$).

If there is a high number of non-dominated solutions (N_{non_dom}) near the total number of solutions N_{MAIN}, that means that there are solutions too near each other in the Pareto set, which is not providing variety. Then, in order to improve the evolution of the MOEA, some of them must be eliminated, reducing the number of non-dominated solutions. Relatively complex techniques for eliminating the inefficient Pareto optimal solutions are shown in Ref. [41]. In this work a simple truncation technique has been used: if N_{non_dom} is higher than a maximum allowed value ($N_{non\_dom\_max}$), the solution which has the minimum distance to another solution in the non-dominated Pareto set is selected.

The distance between two non-dominated solutions i and j is:

$$D_{i-j} = \sqrt{\left(\frac{NPC_i - NPC_j}{NPC_{max}}\right)^2 + \left(\frac{HDI_i - HDI_j}{HDI_{max}}\right)^2 + \left(\frac{JC_i - JC_j}{JC_{max}}\right)^2} \quad (13)$$

where NPC_i, HDI_i, and JC_i are the total net present cost, the human development index and the job creation of solution i. NPC_{max}, HDI_{max}, and JC_{max} are the maximum values of the non-dominated solutions. After knowing the minimum value of D_{i-j}, the solution (i or j) selected to be eliminated is the one that has the shortest

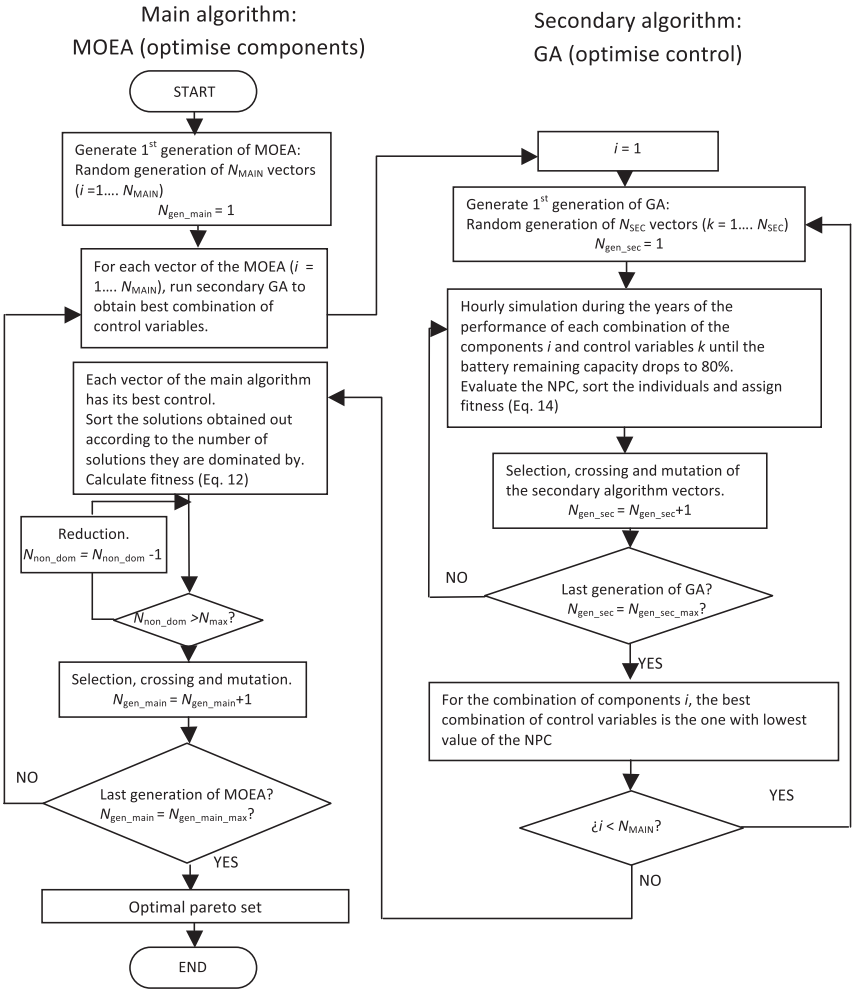

Fig. 5. Multi-objective optimisation flowchart.

distance to another solution in the set. Solutions at the extremes of the Pareto front will never be eliminated.

Selection, crossing and mutation are performed to obtain a new generation of individuals.

The best vectors have a greater probability of reproducing themselves, crossing with other vectors. The individuals are selected by the roulette wheel selection method. In each cross of two vectors, a single point crossover is applied and two new vectors are obtained. Also the mutation operator (uniform mutation) is applied.

The process continues until a determined number of generations $N_{gen\_main\_max}$ has been evaluated.

Comparison with advanced multi-objective algorithms as NSGA-III [42–44] will be done in a future work.

2.2.2. Secondary algorithm (GA)

The secondary GA also uses an integer vector with five variables related to the control strategy:

$$|P_{min\_gen}|P_{limit\_disch}|P_{critical\_gen}|SOC_{stp\_gen}|SOC_{minimum}|$$

These variables were defined in Ref. [45] as follows:

P_{min_gen}: Minimum output power of the diesel generator. The specific fuel consumption of the diesel generator (l/kWh) for low output power is higher than for high power [37], so the optimal P_{min_gen} could be higher than the manufacturer recommendation.

P_{limit_disch}: When the AC load cannot be covered by the renewable sources, it must be supplied by the battery bank or by the diesel generator. Generally, at low power the cost of supplying energy by the batteries is lower than supplying energy by the diesel generator. If the power is lower than P_{limit_disch}, it will be supplied with the battery bank; otherwise the diesel generator will be used. The optimal value of P_{limit_disch} depends on real operating conditions, which are not known a priori, so this variable is part of the control strategy to be optimised.

$P_{critical\_gen}$ and SOC_{stp_gen}: Due to the aforementioned high specific consumption of the diesel generator at low power, when the amount of power the diesel must supply is lower than a critical power limit, $P_{critical\_gen}$, it may be optimal to run at rated power, using the extra power to charge the batteries up to an SOC denoted as SOC_{stp_gen}.

$SOC_{minimum}$: minimum SOC of the battery. When the battery is discharging and reaches this value, the load is disconnected from the battery, preventing over-discharge. The manufacturer recommends a value (usually 20–40%); however, the optimal value can be higher.

The flowchart of the secondary algorithm optimisation is shown in Fig. 5 (right part). For each combination of components evaluated by the MOEA, the secondary GA looks for the best control strategy (combination of control variables).

A first generation of vectors or individuals (combinations of control variables, i.e. control strategies) is randomly obtained. Each vector of the secondary GA is evaluated by means of an hourly simulation of the system during a number of years n_y until the battery bank's remaining capacity drops to 80% (end of battery lifetime). Then the performance of the first n_{years} years is expected to be repeated during the next n_{years} and so on until the lifetime of the system is finished. At the end of the simulation of each individual (combination of components and control strategy), if the unmet load is higher than a specific value (for example, 0 or 0.1%), this individual is discarded. Otherwise the NPC of that solution is calculated. Then the vectors (combinations of control variables) are sorted by their NPC. The first (rank 1) is the best individual, whereas the last (rank N) is the worst. The fitness function of the individual with rank k is assigned as follows:

$$fitness_k = \frac{(N_{SEC}+1)-k}{\sum_j[(N_{SEC}+1)-j]} \quad j = 1\ldots N_{SEC} \tag{14}$$

Then selection (roulette wheel), crossing (single point crossover) and mutation (uniform) are performed to obtain a new generation of individuals, and the process continues until a determined number of generations $N_{gen\_sec\_max}$ has been evaluated.

2.3. Evaluation of the objectives

The evaluation of the different objectives (NPC, HDI and JC) is shown below.

2.3.1. Minimisation of net present cost (NPC)

The NPC (€) of a combination of components i and control strategy k ($NPC_{i,k}$) is calculated considering the acquisition cost of all the components, the installation cost and also the replacement cost of the components, the O&M cost and the fuel cost during the system lifetime, $Life_{system}$ (years). All the cash flows are converted to the initial moment of the system (hour 0, year 1) considering the inflation and the interest rate.

$$NPC_{i,k} = \sum_j \left(Cost_j + NPCrep_j + \sum_{l=1}^{Life_{system}} \left(Cost_{O\&M\_j} \cdot \frac{\left(1+Inf_{general}\right)^l}{(1+I)^l} \right) \right) + \sum_{l=1}^{Life_{system}} \left(Cost_{fuel} \cdot \frac{\left(1+Inf_{fuel}\right)^l}{(1+I)^l} \right) + Cost_{INST} \tag{15}$$

where j are the different components (PV generator, wind turbines, battery bank, diesel generator and inverter/charger), $Cost_j$ is the acquisition cost of component j, $NPCrep_j$ is the sum of the replacement costs of component j during the system lifetime minus the residual cost of component j at the end of the system lifetime (all of them converted to the initial moment of the system), $Cost_{O\&M\_j}$ is the annual O&M cost of component j, $Inf_{general}$ is the general annual expected inflation, I is the annual interest rate, $Cost_{fuel}$ is the annual cost of the fuel used by the diesel generator, Inf_{fuel} is the annual diesel fuel expected inflation and $Cost_{INST}$ is the installation cost.

The cost of the fuel is calculated as follows:

$$Cost_{fuel} = \sum_{t=0}^{8760} Cons_{fuel}(t) \cdot Pr_{fuel} \tag{16}$$

where Pr_{fuel} is the diesel fuel cost per litre.

The replacement total cost of component j is calculated as:

$$NPCrep_j = \sum_{m=1}^{Nrep_j} \left(Cost_j \cdot \frac{\left(1+Inf_j\right)^{m \cdot Life_j}}{(1+I)^{m \cdot Life_j}} \right) - Cost_j \cdot \frac{\left(Life_j - \left(Life_{system} - Nrep_j \cdot Life_j\right)\right)}{Life_j} \cdot \frac{\left(1+Inf_j\right)^{Life_{system}}}{(1+I)^{Life_{system}}} \tag{17}$$

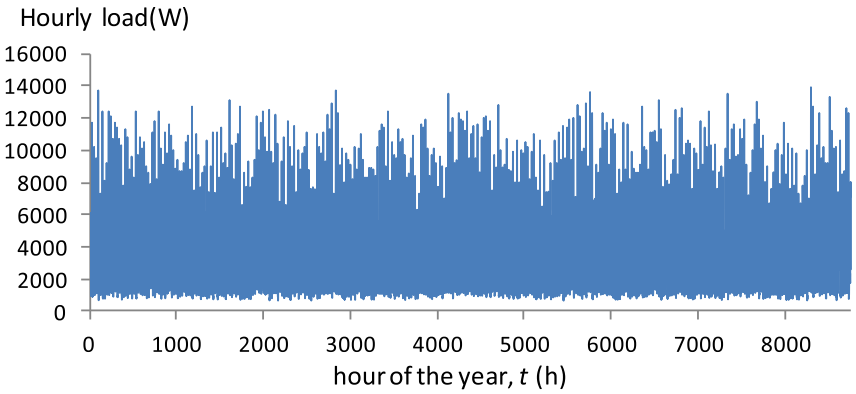

Fig. 6. Hourly load.

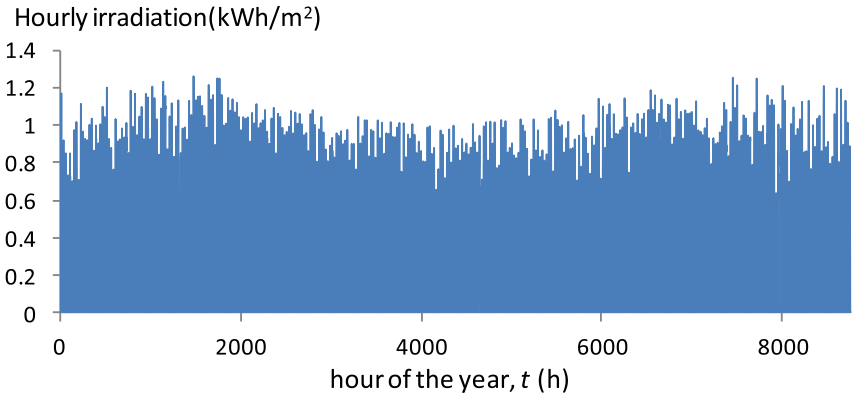

Fig. 7. Hourly irradiation.

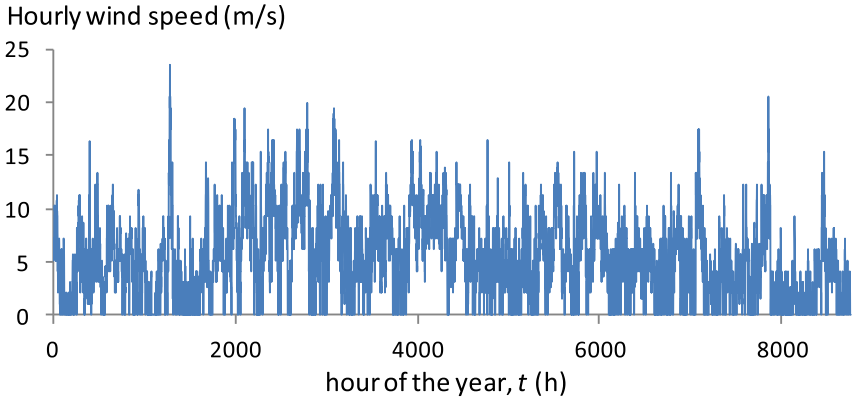

Fig. 8. Hourly wind speed.

where $Life_j$ (years) is the lifetime of component j, Inf_j is the annual expected inflation of the acquisition cost of component j and $Nrep_j$ is the number of times component j is replaced during the system lifetime, calculated as:

$$Nrep_j = \text{Integer}\left(\frac{Life_{system}}{Life_j}\right) \tag{18}$$

The LCE (€/kWh) is calculated as follows:

$$LCE_{i,j} = \frac{NPC_{i,j}}{E_{load} \cdot Life_{system}} \tag{19}$$

where E_{load} (kWh/yr) is the annual expected AC load of the system.

2.3.2. Maximisation of human development index (HDI)

The HDI of a combination of components i and control strategy k ($HDI_{i,k}$) is calculated based on the equation introduced by Rojas-Zerpa (2012). We consider that a fraction of the annual excess energy can be used by new businesses, services or small workshops, which can improve the standard of living and therefore the HDI.

Table 2
Possible components.

Component	Types	Acq. cost (€)	Number in parallel
PV panels[a] (1 type)	c-Si, 200 Wp, 12 V	350	0–30
Wind turbines[b] (5 types)	0 kW	0	1–2
	14.7 kW max power at 14 m/s	14,000	
	26.9 kW max power at 14 m/s	22,000	
	43.1 kW max power at 14 m/s	34,000	
	72.5 kW max power at 14 m/s	59,000	
Diesel generators[c] (3 types)	9 kVA, O&M cost 0.14 €/h	4300	1
	11 kVA, O&M cost 0.15 €/h	4400	
	12.5 kVA, O&M cost 0.15 €/h	4500	
Batteries[d] (3 types)	OPzS 1580 Ah	782	0–2
	OPzS 2640 Ah	1363	
	OPzS 3170 Ah	1584	
Inverter/chargers[e] (5 types)	AC rated 9 kVA	6000	1
	AC rated 12 kVA	6800	
	AC rated 13.5 kVA	9000	
	AC rated 18 kVA	10,200	
	AC rated 24 kVA	13,600	

[a] Includes their own MPPT inverter.
[b] Includes their own controller and dump load.
[c] Minimum output power 30%.
[d] 2 V nominal. SOC min. 20%, self-discharge 3%/month, roundtrip efficiency 85% (same value is considered for charge and discharge: $\eta_{ch} = \eta_d = \sqrt{0.85} = 0.922$), float life at 20 °C 18 years.
[e] SOC control. $\mu_{I/C\text{-charger}} = 0.9$, $\mu_{I/C\text{-inverter}}$ variable with output power (Fig. 3).

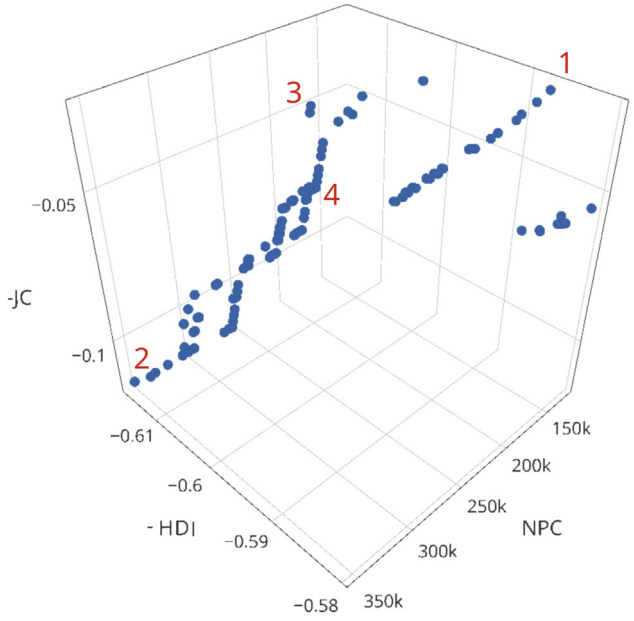

Fig. 9. Pareto optimal set (Pareto set of the last generation of the MOEA).

Excess energy is the energy generated by the renewable sources that cannot be used; i.e. it is the energy generated during each hour by the PV generator and the wind turbines that cannot be consumed by the expected AC load because the AC load is lower and it is already covered. Such excess energy cannot be stored in the battery bank of the system because it is fully charged. Part of the excess energy can be used by AC extra loads (new business or services with their own storage systems) which were not considered when the load was defined. These new business or services can use the excess energy directly (in the hours the excess energy is available) or store it on their own batteries to use it later when there is no excess energy. Then the equation introduced by Rojas-Zerpa (Eq. (2)) is converted to the next equation:

$$HDI_{i,k} = 0.0978 \ln[(E_{load} + \min(F_{max\_E\_excess} \cdot E_{excess}, F_{max\_E\_load} \cdot E_{load}))/ N_{persons}] - 0.0319 \quad (20)$$

where E_{excess} (kWh/yr) is the annual excess energy of the system, $F_{max\_E\_excess}$ is the factor to obtain the maximum excess energy that can be used by new AC extra loads, $F_{max\_E\_load}$ is the factor to multiply the annual AC load so that the maximum excess energy used by the new AC extra loads cannot be higher than that product and $N_{persons}$ is the number of persons living in the community supplied by the system. For example, if we consider that 20% of the excess energy can be used by new AC extra loads but we consider that these AC extra loads cannot be higher than 50% of the expected AC load, then $F_{max\_E\_excess} = 0.2$ and $F_{max\_E\_load} = 0.5$.

2.3.3. Maximisation of job creation (JC)

The JC of a combination of components i and control strategy k ($JC_{i,k}$) is calculated considering the job creation by the different technologies.

$$JC_{i,k} = JC_{PV} \cdot P_{PV} + JC_{Wind} \cdot P_{Wind} + JC_{Diesel} \cdot E_{Diesel} + JC_{BAT} \cdot E_{BAT} \quad (21)$$

where JC_{PV} (job/MW) is the number of jobs per MW_p of the PV generator, P_{PV} (MW_p) is the peak power of the PV generator, JC_{Wind} (job/MW) is the number of jobs per MW of the wind turbines, P_{Wind} (MW) is the maximum power of the group of wind turbines, JC_{Diesel} (job/GWh/yr) is the number of jobs created by diesel and E_{diesel} (GWh/yr) is the annual energy supplied by the diesel. For the jobs created by the battery bank, we consider the parameter JC_{BAT} (job/MWh), which is the number of jobs created per MWh of nominal capacity of storage of the battery bank. E_{BAT} (MWh) is the nominal capacity of the battery bank.

3. Results and discussion

Following the methodology shown in Section 2, we describe the optimisation of a PV-wind-diesel-battery system to supply the load of a small community in the Sahrawi refugee camps of Tindouf (latitude

Table 3
Some of the solutions of the optimal Pareto set.

Solution#	1	2	3	4
Configuration	PV[a]: 4 × 9 × 200 Wp (7.2 kWp) Wind[b]: 1 × 14.7 (14.7 kW) Diesel: 11 kVA Bat: 24 × 1 × 2 V × 1580 Ah (75.84 kWh) Inv/Charger: 13.5 kVA P_{min_gen} = 9075 W P_{limit_disch} = 9776 W $P_{critical\_gen}$ = 3658 SOC_{stp_gen} = 20% $SOC_{minimum}$ = 20%	PV[a]: 4 × 30 × 200 Wp (24 kWp) Wind[b]: 2 × 72.5 (145 kW) Diesel: 11 kVA Bat: 24 × 1 × 2 V × 3170 Ah (152.16 kWh) Inv/Charger: 18 kVA P_{min_gen} = 9075 W P_{limit_disch} = 0 $P_{critical\_gen}$ = 7316 W SOC_{stp_gen} = 100% $SOC_{minimum}$ = 100%	PV[a]: 4 × 17 × 200 Wp (13.6 kWp) Wind[b]: 1 × 43.1 (43.1 kW) Diesel: 9 kVA Bat: 24 × 1 × 2 V × 1580 Ah (75.84 kWh) Inv/Charger: 13.5 kVA P_{min_gen} = 2700 W P_{limit_disch} = 8765 W $P_{critical\_gen}$ = 0 SOC_{stp_gen} = 40% $SOC_{minimum}$ = 40%	PV[a]: 4 × 30 × 200 Wp (24 kWp) Wind[b]: 1 × 26.9 (26.9 kW) Diesel: 12.5 kVA No battery bank Inv/Charger: 18 kVA P_{min_gen} = 3750 W $P_{critical\_gen}$ = 3658 W
Total load, E_{load} (kWh/year)	29,983	29,983	29,983	29,983
Energy generated by PV (kWh/year)	14,164	47,213	26,754	47,213
Energy generated by wind T. (kWh/year)	32,710	297,829	83,952	60,565
Energy supplied by diesel, E_{diesel} (kWh/yr)[c]	4674	11,846	1434	11,125
Energy discharged by battery bank (kWh/year)[c]	9593	0[d]	7217	0
Excess energy, E_{excess} (kWh/year)[c]	18,476	316,521	73,385	87,469
Renewable fraction (%)[c]	84.35	60.41	95.13	62.86
Annual cost of diesel fuel (€/year)[c]	1601	4079	512	5124
Annual hours of diesel operation (h/year)[c]	545	1408	236	2540
Battery lifetime (years)	4.5	9.5[e]	3.6	–
NPC (€)	**125,465**	338,383	161,733	166,729
LCE (€/kWh)	**0.21**	0.56	0.27	0.28
HDI	0.5871	**0.6155**	0.6154	**0.6155**
JC (number of jobs)	0.0277	**0.1185**	0.0531	0.08

[a] Include their own MPPT inverter.
[b] Include their own controller and dump load.
[c] For each year of the simulation the results are slightly different, as battery bank remaining capacity is continuously being reduced. Values shown are average of all the years.
[d] The strategy forces the battery to remain at 100% SOC, i.e., diesel must supply the load first (battery bank is used as back-up).
[e] Battery bank at float-charge conditions.

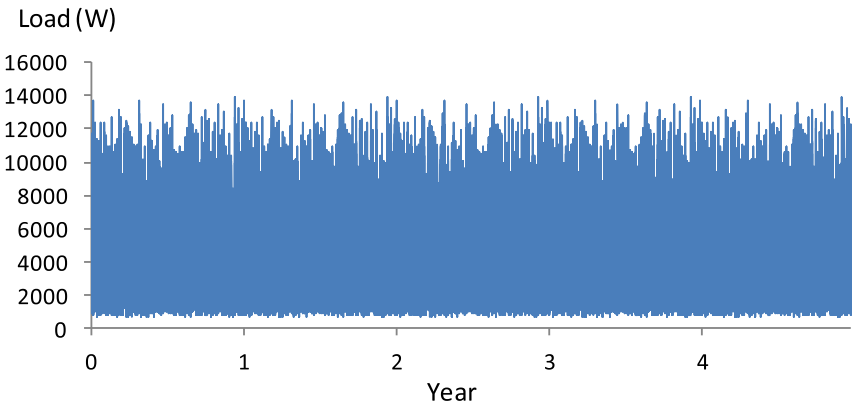

Fig. 10. Hourly load.

27.67° N, longitude 8.14° W, 400 m above sea level). Nowadays the electrical supply of these camps is provided by diesel generators for the public administrative buildings, and many houses are supplied a minimum amount of electricity by means of small PV panels.

We consider a community of $N_{persons}$ = 60 persons and an average daily load of 82.14 kWh/day (different for each day, Fig. 6), with a total annual AC load of E_{load} = 29,983 kWh/yr, which corresponds to an HDI = 0.5756. This will be the minimum HDI as the whole AC load must be covered by the system, corresponding to the HDI of medium development countries [24]. We consider $F_{max\_E\_excess}$ = 0.2 and $F_{max\_E\_load}$ = 0.5, so considering the maximum extra AC load (new businesses or services with their own storage, which could use part of the excess energy), the maximum HDI could be HDI_{max} = 0.6155. The parameters of job creation are JC_{PV} = 2.7 job/MW, JC_{Wind} = 1.1 job/MW (mean values of Table 1, [31]) and JC_{Diesel} = 0.14 job/(GWh/yr) [28], while for the battery bank we have estimated a very conservative value of JC_{BAT} = 0.01 job/MWh.

Hourly solar irradiation data are not usually available from measured values, but they can be synthetically generated from monthly average data, obtained from the web of PVGIS [46], using the model of Graham and Hollands [47], which includes the randomness of cloudiness. To optimise the irradiation of the worst month, which is December, a 55° of slope would be optimal;

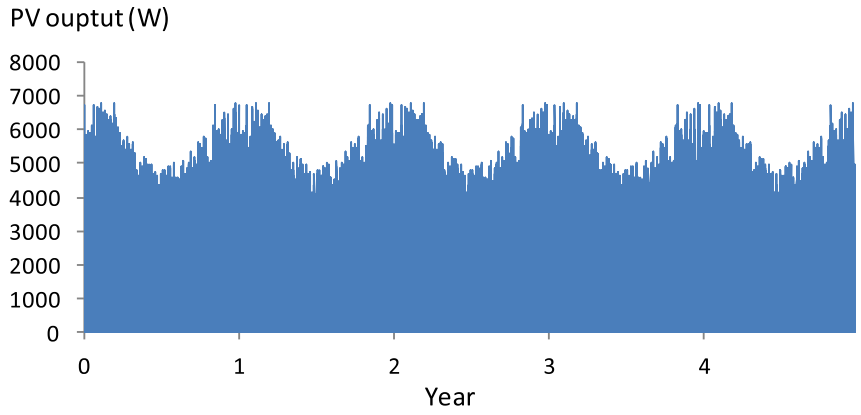

Fig. 11. Hourly PV output.

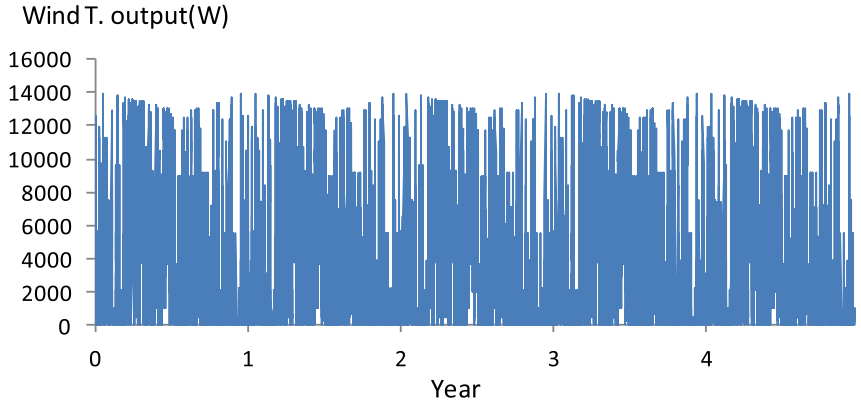

Fig. 12. Hourly wind turbine output.

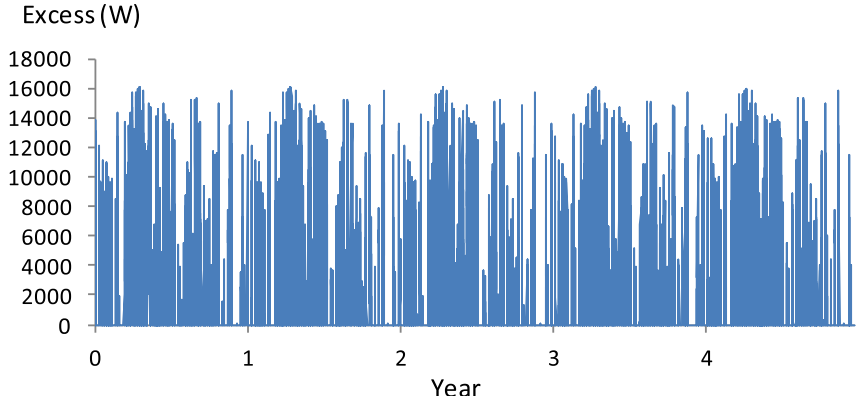

Fig. 13. Hourly excess energy.

however, this would imply that in July the irradiation over the PV panels would be much lower. A slope of 35° is optimal to maximise the minimum irradiation during the year (hourly irradiation over the PV panels with a slope of 35° is shown in Fig. 7). The hourly wind speed was obtained from data for the Tindouf international airport for the year 2007 (this year was selected because it has the lowest average wind speed of the years available, 5.34 m/s, to perform a conservative study), shown in Fig. 8. The average temperature for each month is obtained from NASA webpage [48], and the average value for the whole year was 25.6 °C.

Table 2 shows the possible components considered in the optimisations. There is the possibility of not including the PV generator or not including wind turbines. The DC bus nominal voltage is 48 V. As the c-Si PV panels used are of 12 V nominal voltage, 4 of them in a series are connected in all possible combinations and the number in parallel can vary from 0 (no PV generator) to 30. Tubular OPzS batteries are of 2 V nominal, so 24 must be connected in a series, varying the possible number of parallel rows between 0 (i.e., no battery bank) and 2. A diesel generator must be in the system at least to be used as backup emergency supply. The expected lifetime is 20 years for the crystalline Silicon (c-Si) PV panels and for the wind turbines (we also use this value for the

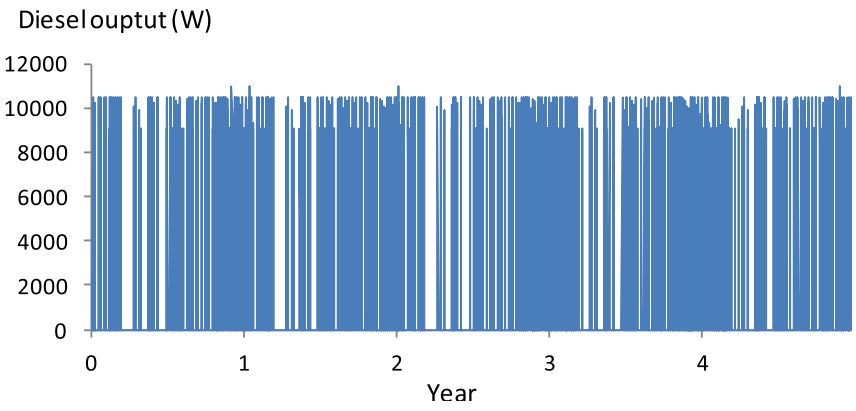

Fig. 14. Hourly diesel output.

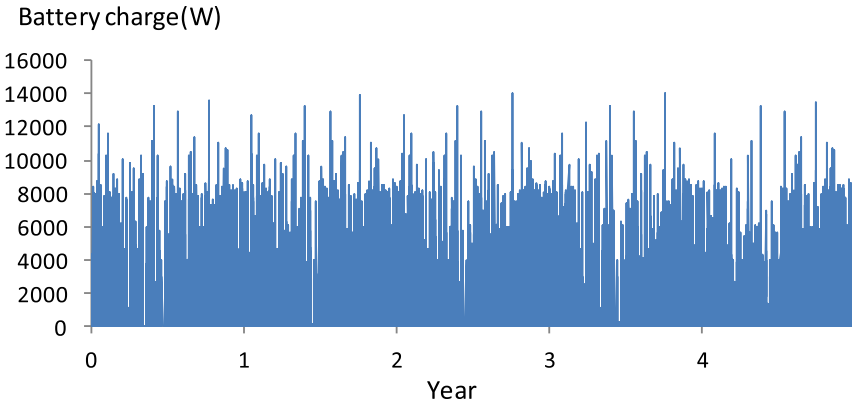

Fig. 15. Hourly battery charge.

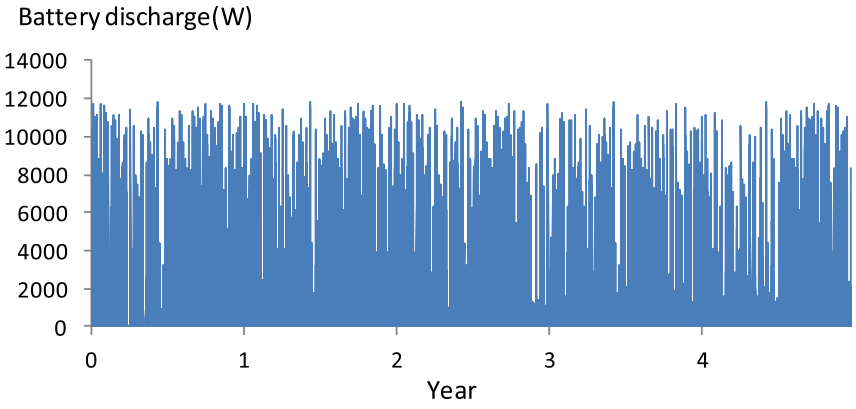

Fig. 16. Hourly battery discharge.

system lifetime), 10 years for inverter/chargers, 12,000 h for diesel and 1250 IEC full cycles to failure for OPzS batteries. Each start of the diesel generator is considered equivalent to 5 min at full load ($F_{START} = 0.0083$). The diesel fuel price in Algeria was around 0.16 €/l in 2015, but in Tindouf only a few litres per vehicle are available at that price. Diesel fuel is usually obtained at much higher prices [49], so we consider a price of 0.5 €/l, with an annual expected inflation of 4%. The annual expected inflation of the acquisition cost of the components is −2% annual for the batteries (i.e. a reduction in cost is expected) and 2% for the diesel generator (as it is a very mature technology). A general annual inflation of 2% and an interest rate of 4% are considered. Also, an installation cost of 1000 € plus a 5% acquisition cost of the components has been taken into account.

There are 41,850 possible combinations of components ($1 \cdot 31 \cdot 5 \cdot 2 \cdot 3 \cdot 1 \cdot 3 \cdot 3 \cdot 5 \cdot 1$). For the control variables, we have considered that considered that each one can take 5 values, so the total number of possible combinations of control strategies is $5^5 = 3125$. The total number of combinations of components and control strategies is $1.3 \cdot 10^8$. Around 7 combinations per second can be simulated and evaluated in a 2.4 GHz, 4 GB RAM computer; therefore, it would take about 216 days to evaluate all of them. By

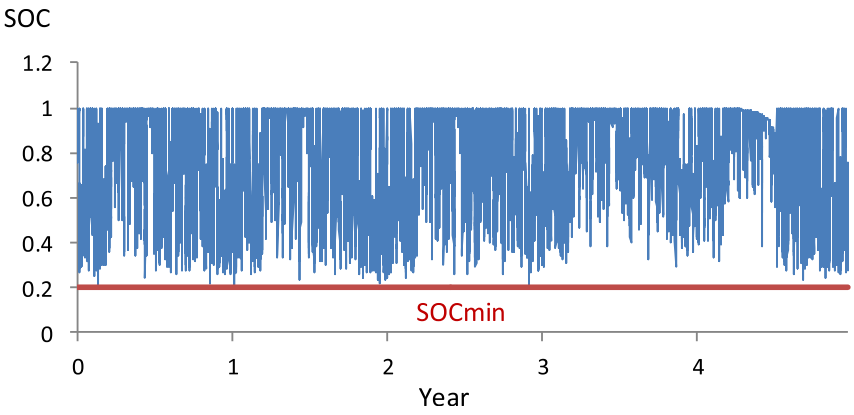

Fig. 17. Hourly SOC.

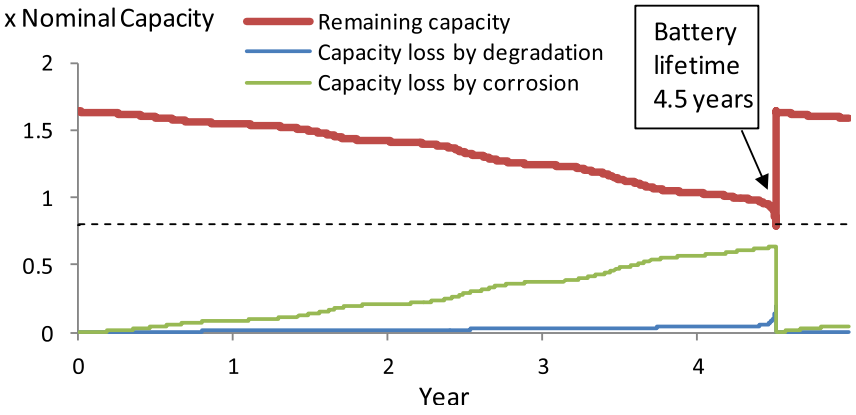

Fig. 18. Hourly capacity loss by degradation and corrosion and remaining capacity.

using evolutionary algorithms, the optimisation can be performed in a reasonable computation time. The MOEA uses a population of 200 (0.48% of possible combinations of components) with 15 generations, while the GA uses a population of 20 (0.64% of possible combinations of control variables) and 15 generations, these values were selected considering the results of [50] and some tests in similar optimisations. There is a 90% crossing rate and 1% mutation rate for both algorithms [50]. In around 1.5 days the evolutionary algorithms performed the optimisation, obtaining the Pareto optimal set shown in Fig. 9. HDI and JC are maximised in the optimisation; however, the Pareto is clearly shown in a graph if the variables are minimised, not maximised. Then, in the 3D graph shown in Fig. 9, instead of HDI and JC, they are represented as their opposite values (−HDI and −JC). Table 3 shows the details of some of the solutions of the optimal Pareto set, identified in Fig. 9 by the numbers in red. In Table 3 the minimum NPC and maximum HDC and JC are marked in bold. In this case, as wind speed is relatively high, most of the solutions of the optimal Pareto set are PV-wind-diesel-battery hybrid systems, whereas in other locations with lower wind speed, most of the solutions of the optimal Pareto set do not include wind turbines.

Once the optimal Pareto set is known, the designer can see the differences in the objectives of the different solutions and can choose the one that best fits for him/her. The designer can see the hourly performance of each solution; for example, Figs. 10–18 shows the hourly simulation of solution #1 during the first $n_y = 5$ years, as battery lifetime is 4.5 years. The hourly values of AC load, PV output and wind turbine output during one year are repeated for all the years.

Solution #1 is the most cost-effective solution (lowest NPC, 125,465 €, i.e. LCE of 0.21 €/kWh). Solution #2 has the maximum HDI and also the maximum JC, as it has the maximum allowed size of PV generator, wind turbines and battery bank, and it forces the battery bank to be always in a float state so the energy supplied by the diesel is high, obtaining a high JC but also a very high NPC (2.7 times the NPC of solution #1). This solution, like many others, would be discarded for economic reasons. Also, solution #2 has a low renewable fraction (60.41%), which is another reason to discard this solution. Solution #3 does not have any extreme value of NPC, HDI or JC but could be an interesting solution, as the NPC is not much higher than the one of solution #1 but its HDI and JC are higher and the renewable fraction is high (95.13%). Solution #4 is also an interesting solution, as its NPC is slightly higher than the NPC of solution #3 but its JC is higher; however, this solution has no battery bank, so the diesel must supply a high amount of energy (as in solution #2), presenting a low relative fraction.

Solution #3, or another solution with not too high NPC but high HDI, relatively high JC (compared to solution #1), a high renewable fraction could be a good solution to select.

4. Conclusions

This work presents a new methodology for the multi-objective optimisation of stand-alone (off-grid) hybrid renewable systems (PV-wind-diesel-battery) to minimise net present cost and maximise human development index (HDI) and job creation (JC). The optimisation performed uses an MOEA in order to obtain the

optimal Pareto set of the combinations of components considering the three objectives. The best control strategy for each combination of components used by the MOEA is obtained by means of a GA, which optimises the NPC.

HDI and JC had not been considered previously in the optimisation of this kind of system. HDI depends in a logarithmic function on the annual electrical consumption per capita; thus we consider a minimum load to be covered (corresponding to a specific value of HDI) and consider that the excess energy generated by the renewable sources could be used by new extra loads (new businesses or services, with or without their own electricity storage systems), which would increase HDI.

Each generation technology has a specific job creation factor, which includes direct and indirect jobs in manufacturing, installation and O&M. A review of the state of the art of JC has been conducted to obtain a high variation in the job creation factors for PV and wind. The number of jobs created by a hybrid system depends on the combination of components (mix of technologies).

We present an example of application of the multi-objective optimisation (minimisation of NPC, maximisation of HDI and maximisation of JC) to obtain an optimal Pareto set in which none of the solutions is better for all three objectives than any other one.

References

[1] H. Ahlborg, L. Hammar, Drivers and barriers to rural electrification in Tanzania and Mozambique - grid-extension, off-grid, and renewable energy technologies, Renew. Energy 61 (2014) 117–124, http://dx.doi.org/10.1016/j.renene.2012.09.057.

[2] H. Borhanazad, S. Mekhilef, R. Saidur, G. Boroumandjazi, Potential application of renewable energy for rural electrification in Malaysia, Renew. Energy 59 (2013) 210–219, http://dx.doi.org/10.1016/j.renene.2013.03.039.

[3] M.S. Adaramola, M. Agelin-Chaab, S.S. Paul, Analysis of hybrid energy systems for application in southern Ghana, Energy Convers. Manag. 88 (2014) 284–295, http://dx.doi.org/10.1016/j.enconman.2014.08.029.

[4] U. Suresh Kumar, P.S. Manoharan, Economic analysis of hybrid power systems (PV/diesel) in different climatic zones of Tamil Nadu, Energy Convers. Manag. 80 (2014) 469–476, http://dx.doi.org/10.1016/j.enconman.2014.01.046.

[5] P. Bajpai, V. Dash, Hybrid renewable energy systems for power generation in stand-alone applications: a review, Renew. Sustain. Energy Rev. 16 (2012) 2926–2939, http://dx.doi.org/10.1016/j.rser.2012.02.009.

[6] S. Sinha, S.S. Chandel, Review of software tools for hybrid renewable energy systems, Renew. Sustain. Energy Rev. 32 (2014) 192–205, http://dx.doi.org/10.1016/j.rser.2014.01.035.

[7] Y.S. Mohammed, M.W. Mustafa, N. Bashir, Hybrid renewable energy systems for off-grid electric power: review of substantial issues, Renew. Sustain. Energy Rev. 35 (2014) 527–539, http://dx.doi.org/10.1016/j.rser.2014.04.022.

[8] M. Sharafi, T.Y. ElMekkawy, Stochastic optimization of hybrid renewable energy systems using sampling average method, Renew. Sustain. Energy Rev. 52 (2015) 1668–1679, http://dx.doi.org/10.1016/j.rser.2015.08.010.

[9] J.L. Bernal-Agustín, R. Dufo-López, Simulation and optimization of stand-alone hybrid renewable energy systems, Renew. Sustain. Energy Rev. 13 (2009) 2111–2118, http://dx.doi.org/10.1016/j.rser.2009.01.010.

[10] R.K. Akikur, R. Saidur, H.W. Ping, K.R. Ullah, Comparative study of stand-alone and hybrid solar energy systems suitable for off-grid rural electrification: a review, Renew. Sustain. Energy Rev. 27 (2013) 738–752, http://dx.doi.org/10.1016/j.rser.2013.06.043.

[11] P. Nema, R.K. Nema, S. Rangnekar, A current and future state of art development of hybrid energy system using wind and PV-solar: a review, Renew. Sustain. Energy Rev. 13 (2009) 2096–2103, http://dx.doi.org/10.1016/j.rser.2008.10.006.

[12] D.E. Goldberg, Genetic Algorithms in Search, Optimization, and Machine Learning, 1989th ed., Addison-Wesley Publishing Company, 1989.

[13] S. Sinha, S.S. Chandel, Review of recent trends in optimization techniques for solar photovoltaic–wind based hybrid energy systems, Renew. Sustain. Energy Rev. 50 (2015) 755–769, http://dx.doi.org/10.1016/j.rser.2015.05.040.

[14] P. Hajela, C.Y. Lin, Genetic search strategies in multi-criterion optimal design, Struct. Optim. 4 (1992) 99–107.

[15] C.A. Coello, D.A.V. Veldhuizen, G.B. Lamont, Evolutionary Algorithms for Solving Multi-objective Problems, Kluwer Aca, New York, 2002.

[16] M. Fadaee, M. a M. Radzi, Multi-objective optimization of a stand-alone hybrid renewable energy system by using evolutionary algorithms: a review, Renew. Sustain. Energy Rev. 16 (2012) 3364–3369, http://dx.doi.org/10.1016/j.rser.2012.02.071.

[17] J.L. Bernal-Agustín, R. Dufo-López, Multi-objective design and control of hybrid systems minimizing costs and unmet load, Electr. Power Syst. Res. 79 (2009) 170–180, http://dx.doi.org/10.1016/j.epsr.2008.05.011.

[18] R. Dufo-López, J.L. Bernal-Agustín, Multi-objective design of PV-wind-diesel-hydrogen-battery systems, Renew. Energy 33 (2008) 2559–2572, http://dx.doi.org/10.1016/j.renene.2008.02.027.

[19] R. Dufo-López, J.L. Bernal-Agustín, J.M. Yusta-Loyo, J. a Domínguez-Navarro, I.J. Ramírez-Rosado, J. Lujano, et al., Multi-objective optimization minimizing cost and life cycle emissions of stand-alone PV-wind-diesel systems with batteries storage, Appl. Energy 88 (2011) 4033–4041, http://dx.doi.org/10.1016/j.apenergy.2011.04.019.

[20] J.L. Bernal-Agustín, R. Dufo-López, D.M. Rivas-Ascaso, Design of isolated hybrid systems minimizing costs and pollutant emissions, Renew. Energy 44 (2012) 215–224, http://dx.doi.org/10.1016/j.renene.2012.01.011.

[21] J.C. Rojas-Zerpa, J.M. Yusta, Methodologies, technologies and applications for electric supply planning in rural remote areas, Energy Sustain. Dev. 20 (2014) 66–76, http://dx.doi.org/10.1016/j.esd.2014.03.003.

[22] J.C. Rojas-Zerpa, J.M. Yusta, Application of multicriteria decision methods for electric supply planning in rural and remote areas, Renew. Sustain. Energy Rev. 52 (2015) 557–571, http://dx.doi.org/10.1016/j.rser.2015.07.139.

[23] V. Salas, W. Suponthana, R. a Salas, Overview of the off-grid photovoltaic diesel batteries systems with AC loads, Appl. Energy 157 (2015) 195–216, http://dx.doi.org/10.1016/j.apenergy.2015.07.073.

[24] United Nations Development Programme, Human Development Report 2014. Sustaining Human Progress: Reducing Vulnerabilities and Building Resilience, 2014, 978-92-1-126340-4.

[25] International Energy Agency, World Energy Outlook 2014, 2014, p. 207. http://www.iea.org/publications/freepublications/publication/WEO_2014_ES_English_WEB.pdf.

[26] A.D. Pasternak, Global Energy Futures and Human Development: a Framework for Analysis, U.S. Department of Energy, 2000. UCRL-ID-140773, http://www.geni.org/globalenergy/issues/global/qualityoflife/HDI-and-electricity-consumption.pdf.

[27] United Nations Development Program, Human Development Report 1999, 1999. http://hdr.undp.org/sites/default/files/reports/260/hdr_1999_en_nostats.pdf.

[28] Tesis doctoral J.C. Rojas-Zerpa, Planificación del suministro eléctrico en áreas rurales de los países en vías de desarrollo: un marco de referencia para la toma de decisiones, Univ. Zaragoza, 2012.

[29] United Nations Development Program, Human Development Report - 2009 Overcoming Barriers: Human Mobility and Development, 2009, http://dx.doi.org/10.1016/S0883-153X(98)80004-0.

[30] R. Ramanathan, L.S. Ganesh, Energy resource allocation incorporating qualitative and quantitative criteria: an integrated model using goal programming and AHP, Socioecon. Plann. Sci. 29 (1995) 197–218, http://dx.doi.org/10.1016/0038-0121(95)00013-C.

[31] M. Wei, S. Patadia, D.M. Kammen, Putting renewables and energy efficiency to work: how many jobs can the clean energy industry generate in the US? Energy Policy 38 (2010) 919–931, http://dx.doi.org/10.1016/j.enpol.2009.10.044.

[32] M. Ortega, P. Ruiz, C. Thiel, Employment effects of renewable electricity deployment. A novel methodology,, Energy 91 (2015) 940–951.

[33] T.M. Sooriyaarachchi, I. Tsai, S. El Khatib, A.M. Farid, Job creation potentials and skill requirements in, PV, CSP, wind, water-to-energy and energy efficiency value chains, Renew. Sustain. Energy Rev. 52 (2015) 653–668.

[34] IRENA, Renewable Energy Jobs & Access, 2012. www.irena.org/DocumentDownloads/Publications/RenewableEnergyJobs.pdf.

[35] M. Simas, S. Pacca, Assessing employment in renewable energy technologies: a case study for wind power in Brazil, Renew. Sustain. Energy Rev. 31 (2014) 83–90, http://dx.doi.org/10.1016/j.rser.2013.11.046.

[36] L. Cameron, B. van der Zwaan, Employment factors for wind and solar energy technologies: a literature review, Renew. Sustain. Energy Rev. 45 (2015) 160–172, http://dx.doi.org/10.1016/j.rser.2015.01.001.

[37] O. Skarstein, K. Uhlen, Design considerations with respect to long-term diesel saving in wind/diesel plants, Wind Eng. 13 (1989) 72–87.

[38] J. Bleijs, C. Nightingale, D. Infield, Wear implications of intermittent diesel operation in wind/diesel systems, Wind Energy 17 (1993) 206–218.

[39] R. Dufo-López, J.M. Lujano-Rojas, J.L. Bernal-Agustín, Comparison of different lead–acid battery lifetime prediction models for use in simulation of stand-alone photovoltaic systems, Appl. Energy 115 (2014) 242–253, http://dx.doi.org/10.1016/j.apenergy.2013.11.021.

[40] J. Schiffer, D.U. Sauer, H. Bindner, T. Cronin, P. Lundsager, R. Kaiser, Model prediction for ranking lead-acid batteries according to expected lifetime in renewable energy systems and autonomous power-supply systems, J. Power Sources 168 (2007) 66–78, http://dx.doi.org/10.1016/j.jpowsour.2006.11.092.

[41] M. Tavana, Z. Li, M. Mobin, M. Komaki, E. Teymourian, Multi-objective control chart design optimization using NSGA-III and MOPSO enhanced with DEA and TOPSIS, Expert Syst. Appl. 50 (2016) 17–39, http://dx.doi.org/10.1016/j.eswa.2015.11.007.

[42] K. Deb, H. Jain, An evolutionary many-objective optimization algorithm using reference-point based non-dominated sorting approach, part I: solving problems with box constraints, IEEE Trans. Evol. Comput. 18 (2014) 577–601, http://dx.doi.org/10.1109/TEVC.2013.2281534.

[43] K. Deb, H. Jain, An evolutionary many-objective optimization algorithm using reference-point based non-dominated sorting approach, part II: handling constraints and extending to an adaptive approach, IEEE Trans. Evol. Comput. 18 (2014) 602–622, http://dx.doi.org/10.1109/TEVC.2013.2281534.

[44] H. Seada, K. Deb, A unified evolutionary optimization procedure for single,

multiple, and many objectives, IEEE Trans. Evol. Comput. (2015) 1–13, http://dx.doi.org/10.1109/TEVC.2015.2459718.
[45] R. Dufo-López, J.L. Bernal-Agustín, J. Contreras, Optimization of control strategies for stand-alone renewable energy systems with hydrogen storage, Renew. Energy 32 (2007) 1102–1126, http://dx.doi.org/10.1016/j.renene.2006.04.013.
[46] PVGIS, interactive Maps, JCR European Commission, 2016 (n.d.), http://re.jrc.ec.europa.eu/pvgis/apps4/pvest.php# (accessed 01.20.16).
[47] V.A. Graham, K.G.T. Hollands, A method to generate synthetic hourly solar radiation globally, Sol. Energy 44 (1990) 333–341, http://dx.doi.org/10.1016/0038-092X(90)90137-2.
[48] NASA Surface Meteorology and Solar Energy, 2016 (n.d.), https://eosweb.larc.nasa.gov/cgi-bin/sse/retscreen.cgi (accessed 01.20.16).
[49] V. Trasasmontes, Los Campamentos de refugiados saharauis en Tinduf: Una aproximación desde la economía, Rev. Econ. Mund. 29 (2011) 287–317. http://www.redalyc.org/articulo.oa?id=86622169010.
[50] J.L. Bernal-Agustín, R. Dufo-López, Efficient design of hybrid renewable energy systems using evolutionary algorithms, Energy Convers. Manag. 50 (2009) 479–489, http://dx.doi.org/10.1016/j.enconman.2008.11.007.

Renewable Energy 99 (2016) 919–935

Contents lists available at ScienceDirect

Renewable Energy

journal homepage: www.elsevier.com/locate/renene

Stochastic-heuristic methodology for the optimisation of components and control variables of PV-wind-diesel-battery stand-alone systems

Rodolfo Dufo-López [a, *], Iván R. Cristóbal-Monreal [b], José M. Yusta [a]

[a] Electrical Engineering Department, University of Zaragoza, Calle María de Luna, 3, 50018, Zaragoza, Spain
[b] Centro Universitario de la Defensa, Academia General Militar, Ctra. de Huesca s/n, 50.090, Zaragoza, Spain

ARTICLE INFO

Article history:
Received 18 January 2016
Received in revised form
19 July 2016
Accepted 27 July 2016

Keywords:
Renewable stand-alone systems
Battery
Control variables
Monte Carlo simulation
Correlated Gaussian random variables
Genetic algorithms

ABSTRACT

In this paper a new stochastic-heuristic methodology for the optimisation of the electrical supply of stand-alone (off-grid) hybrid systems (photovoltaic-wind-diesel with battery storage) is shown. The objective is to minimise the net present cost of the system. The stochastic optimisation is developed by means of Monte Carlo simulation, which takes into account the uncertainties of irradiation, temperature, wind speed and load (correlated Gaussian random variables), using their probability density functions and the variance-covariance matrix. Also the uncertainty of diesel fuel price inflation rate was considered. The heuristic approach uses genetic algorithms to obtain the optimal system (or a solution near the optimal) in a reasonable computation time. This methodology includes an accurate weighted Ah-throughput battery model with several control variables, which can be set in the modern battery controllers or inverter/chargers with State of Charge control. A case study is analysed as an example of the application of this methodology, obtaining the stochastic optimisation an optimal system similar to the one obtained by the deterministic optimisation. It is recommended to perform first the deterministic optimisation (with low computation time), then the search space should be reduced and finally the stochastic optimisation can be obtained in a reasonable computation time.

1. Introduction

A very important factor for the sustainable development of human society is the access to electricity. However, nowadays electricity is still not accessible for 1,200 million people [1] due to the lack of electricity grids in remote areas of developing countries. In developed countries, there is also a need of electricity in remote locations (telecom stations, farms, mountain refuges, etc.) far from the electrical grid. In many remote locations, stand-alone systems (off-grid systems) are more cost-effective than extending a power line to the electricity grid. In some cases hybrid stand-alone systems (using more than one source of energy) are more cost-effective than systems that use a unique energy source. The most widely energy source used in stand-alone systems is photovoltaic (PV), combined with battery storage. In areas where solar irradiation is much lower in winter than in summer, hybrid PV-diesel-battery systems can be cost-effective. In areas with high wind speed, the optimal system is usually a hybrid PV-wind-battery or a PV-wind-diesel-battery system.

The optimisation of the stand-alone systems, i.e., the minimisation of the net present cost of the system (NPC, which includes all the costs throughout the lifetime of the system, which are converted to the initial moment of the investment using the effective interest rate, according to standard economical procedures) is very important as the user usually want to choose the lowest cost system.

The optimisation of this kind of systems is usually carried out using a deterministic approach, i.e., considering that the electrical load and the meteorological data (irradiation, temperature and wind speed) do not vary during the years, i.e., the performance of one year can be extrapolated to the rest of the years of the system lifetime (which is usually considered to be 25 years or more). The cost of the diesel fuel is usually considered as a fixed cost during the system lifetime, or, in the best case, a fixed annual inflation for the diesel fuel price is taken into account.

However, the performance of the real system is different from one year to another one, as load and meteorological variables are different. Also, the cost of the diesel fuel consumed each year

* Corresponding author.
E-mail addresses: rdufo@unizar.es (R. Dufo-López), icristob@unizar.es (I.R. Cristóbal-Monreal), jmyusta@unizar.es (J.M. Yusta).

http://dx.doi.org/10.1016/j.renene.2016.07.069
0960-1481/

depends on the actual price of the fuel of each year. These are the motivations to perform in this paper a probabilistic optimisation of stand-alone systems. The stochastic approach will allow to consider the different performance of the system during the years of its lifetime, considering the uncertainties of meteorological variables and load, and its correlations, and it will also allow to consider the uncertainty of the diesel price fuel. The designer will obtain probability functions for the variables of the results (expected cost, lifetime of the battery bank,…), knowing the mean, standard deviation, minimum and maximum expected for each of the results and therefore having much more information than using the deterministic approach.

Also, the optimisation of this kind of systems is usually done using simple battery models, which can imply an estimation of the battery storage lifetime much higher than the real battery lifetime. In this work an accurate model for the estimation of the battery lifetime is used.

This paper is structured as follows. Section 2 shows the literature review and research gap. Section 3 shows the methodology of the optimisation, including the variables involved in the optimisation and the mathematical models of the components of the system. Section 4 shows an example of application and section 5 shows the main conclusions.

2. Literature review and research gap

Many previous studies have examined the performance and the optimisation of the electrical supply of stand-alone systems, usually PV panels and/or wind turbines and/or diesel generators with battery storage. Reviews of relevant works related to stand-alone hybrid systems can be found in Refs. [2–4]. A comparative study of stand-alone hybrid solar energy systems is shown in Ref. [5]. Reviews of the software tools used for the optimisation of hybrid systems are shown in Refs. [6,7]. The optimisation of PV-wind systems is discussed in Ref. [8] while a review of relevant papers of optimisation of stand-alone systems is shown in Ref. [9]. A novel optimisation method for stand-alone PV systems was recently shown in Ref. [10]. In Ref. [11] the energetic and economic optimisation of a PV system (with battery storage) is shown. A methodology based on levelized cost of supplied and lost energy for the design of stand-alone systems is shown in Ref. [12]. Previous relevant works of the authors of this work related to the optimisation of hybrid stand-alone systems can be found in Refs. [13–15].

In some cases the stand-alone system does not include battery storage [16], but storage is needed (and cost-effective) in most of the off-grid applications. In most of the previous works, the optimisation tries to obtain the combination of components (and/or, in some cases, of control strategies), which minimises the NPC, the levelised cost of energy (LCE, calculated as NPC divided by the total energy consumed by the load during the lifetime of the system) or the operation cost of a short interval. Some of these works use heuristic techniques, like genetic algorithms (GA) [17,18] in the optimisation. A recent application of GA in the optimisation of hybrid stand-alone systems is shown in Ref. [19]. In Ref. [20] a meta-heuristic algorithm (Cuckoo Search) is applied in the optimisation of hybrid stand-alone systems. Other works consider several variables to be minimised, usually LCE, CO_2 emissions and unmet load or loss of power probability, most of them using Pareto-optimisation techniques as multi-objective evolutionary algorithms (MOEA's) [21–23].

The optimisation in previous studies was usually carried out using a deterministic approach, although some previous studies used a stochastic approach, taking into account the uncertainties in renewable sources.

In Refs. [24], Paliwal et al. show a probabilistic model for battery-storage systems to facilitate the reliability assessment of stand-alone renewable systems. They compare with Monte Carlo simulation (MCS), obtaining better results with their probabilistic model. However, in this work the battery lifetime estimation is not obtained and no optimisation is performed.

Arun et al. [25] optimised a PV-battery system using MCS, including the uncertainty of solar irradiation. Kamjoo et al. [26] showed a method based on chance-constrained programming (CCP) for the optimisation of a PV-wind-battery system, including the uncertainties in wind speed and irradiation. In Refs. [27], Kamjoo et al. use GA in the multi-objective optimisation of PV-wind-batteries systems, considering uncertainties by means of CCP and comparing the results with MCS. Maheri [28] evaluates the reliability of different PV-wind-diesel-battery systems obtained by deterministic design, and later [29], uses two algorithms (with MCS) in the optimisation of the margin of safety.

Recently, Alharbi and Raahemifar [30] presented a stochastic model for the coordination of distributed energy resources in an islanded microgrid, considering the uncertainties of load, wind and irradiation. Chang and Lin [31] also considered the uncertainties of load, wind and irradiation and proposed the optimal design of hybrid renewable energy systems using MCS with simulation optimisation techniques (stochastic trust-region response-surface method). The effect of the uncertainties in the economics of renewable grid-connected generators have been studied in Refs. [32], where Falconett and Nagasaka show a probabilistic model to evaluate the effects of different support mechanisms (governmental grant, feed in tariff and renewable energy certificate) on the net present value of grid-connected small-scale hydroelectric, wind energy and solar PV systems. Tina and Gagliano [33] studied the impact of the tracking system on the probability density function (PDF) of the power produced by the PV system while Pereira et al. [34] used MCS in risk analysis in small renewable systems.

All the previous works use a different stochastic approach and probabilistic models. However, some of them do not calculate costs (they do not perform the optimisation), most of them do not consider correlation between the input variables, others do not consider storage and others use simple classical Ah-battery models and simple models for the estimation of the batteries' lifetime.

The use of simple models for the batteries can imply a too optimistic estimation of the batteries' lifetime (several times the real lifetime [35]) and therefore, erroneous results for the NPC and the LCE, as the battery bank total cost (acquisition cost plus maintenance plus replacement at the end of its lifetime) is usually the system's highest cost [36]. The battery lifetime in the previous optimisation works has always been estimated in fixed values or by means of classical models (the number of equivalent full cycles or the cycle counting method). These classical models assume that operating conditions are the same as the conditions of the standard tests that battery manufacturers use to obtain the lifetime number of IEC (International Electrotechnical Commission) cycles (shown in the battery datasheet). Therefore, they can predict an overly optimistic battery lifetime, as Dufo-López et al. showed in Ref. [35], in which different ageing models for lead-acid batteries were compared and the Schiffer et al. weighted Ah-throughput model [37] was shown to obtain the most accurate results in terms of battery lifetime.

Also, none of the previous studies include the model of the PWM (pulse-width modulation) battery charge controller (or inverter/charger), and therefore, none consider the optimisation of the control variables, which can be set in the battery controller.

In the present paper, it is shown a new methodology for the stochastic-heuristic optimisation of stand-alone hybrid renewable systems (Fig. 1) considering the uncertainties of the input variables

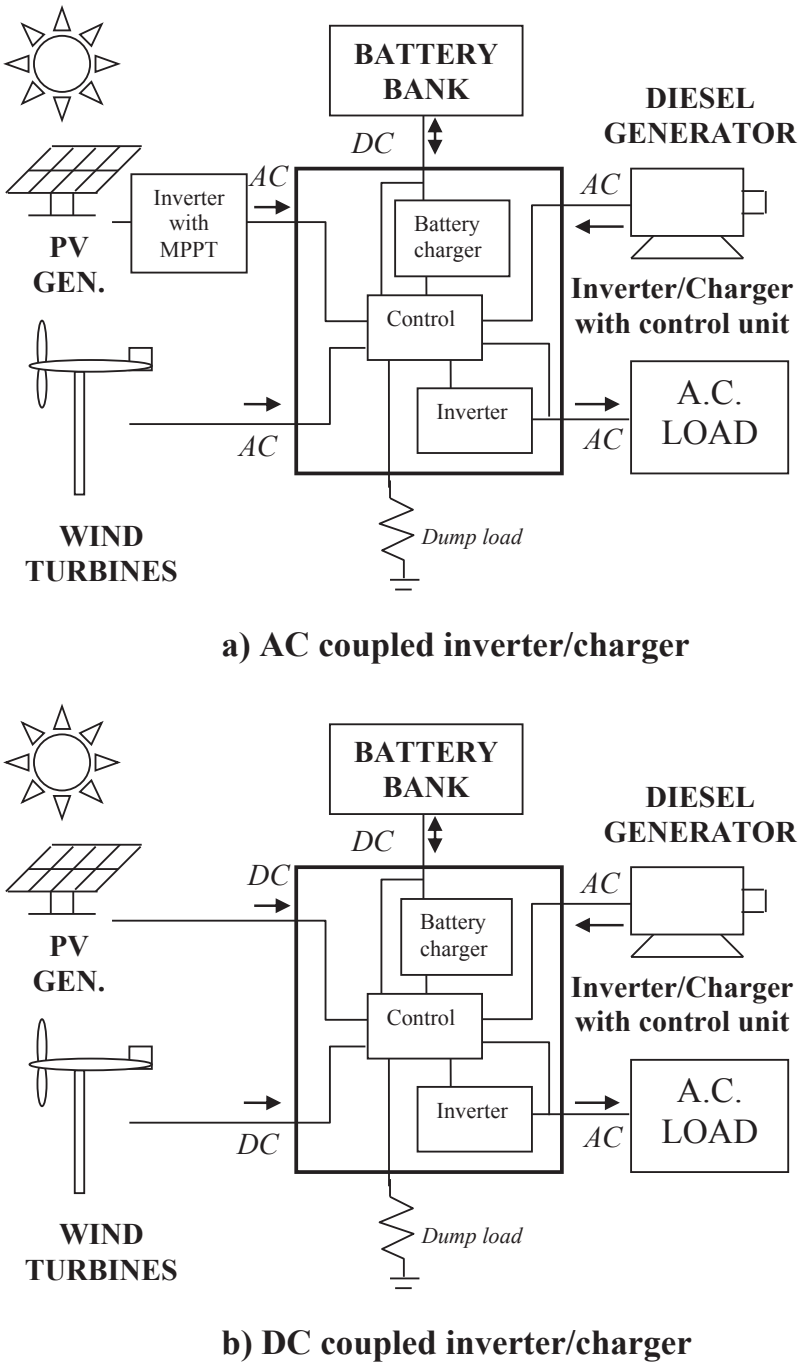

Fig. 1. PV-wind-diesel-battery system. AC coupled or DC inverter/charger.

(load, irradiation, temperature and wind speed), taking into account their correlations. Also the uncertainty of annual fuel price inflation is considered (none of the previous works consider this variable, which has a great influence in the NPC).

In the optimisation model, the Ah-throughput model for the lead-acid batteries ([37]) (including accurate lifetime estimation) is applied, which is much more realistic than the approach used in the previous studies. Here, a PWM charge controller (charging in three stages: bulk, boost and float) with state of charge (SOC) control is modelled. Furthermore, a complex control strategy has been implemented, with up to eight variables. Also, the stochastic approach is used combined with GA (heuristic approach) to obtain the optimal solution or a solution near the optimal in a reasonable time.

3. Methodology

This study uses a methodology that combines MCS and GA for the optimisation of the combination of components and control variables of hybrid renewable systems. This methodology can be applied to optimise stand-alone systems of any size, including micro-grids. Usually, the number of possible combinations of components and control strategies is so high, it would imply inadmissible computation time, which means that heuristic models

must be used for the optimisation (in our case, GA). The model has been programmed in C++ language.

3.1. Variables involved in the optimisation

Two GA are applied, one for the optimisation of components (main algorithm) and another for the optimisation of the control strategy (secondary algorithm).

The main GA works with an integer vector with the number of PV panels in parallel (a), the PV panel type code (b), the number of wind turbines in parallel (c), the wind turbine type code (d), the battery type code (e), the number of batteries in parallel (f), the diesel generator type code (g), and the inverter/charger type code (h):

$$(a,\ b,\ c,\ d,\ e,\ f,\ g,\ h) \tag{1}$$

The secondary GA also uses an integer vector—in this case, with eight control variables.

$$\left(P_{\text{min\_gen}},\ P_{\text{limit\_discharge}},\ P_{\text{critical\_gen}},\ SOC_{\text{stp\_gen}},\ SOC_{\text{min\_disconnect}},\ SOC_{\text{min\_reconnect}},\ SOC_{\text{boost}},\ SOC_{\text{equal}}\right) \tag{2}$$

The first four variables were used in Ref. [15]. The meaning of the control variables is explained as follows:

$P_{\text{min\_gen}}$: Minimum output power of the diesel generator. It is generally set to the minimum value recommended by the manufacturer, below which it should not work. As the specific consumption (litres/kWh) for low output power is always higher than for high power, the optimal $P_{\text{min\_gen}}$ could be higher than the manufacturer recommendation.

$P_{\text{limit\_discharge}}$: when the load cannot be covered by the renewable sources (PV generator and/or wind turbines), it must be supplied by the batteries or by the diesel. The cost of supplying a specific power by means of the batteries, for 1 h, can be modelled as proportional to the power (Fig. 2), if it is only considered the replacement cost (supposing that ageing depends only on the energy cycled and that the operating conditions are the same as the standard conditions considered by the manufacturer, neglecting the effects of the SOC dependency versus time, the current, the gassing and the acid stratification, and the capacity loss due to corrosion, which depends on voltage and temperature) and the operationt and maintenance (O&M) cost is negligible. This cost can be modelled as $C{\cdot}P$, where C (€/kWh) is the cost of supplying power by means of the batteries and P is the power supplied (kW). The cost of supplying a specific power by means of the diesel is also modelled in Fig. 2, $A{\cdot}P + B{\cdot}P_{GEN,\ rated}$, where A and B (€/kWh) are the fuel curve coefficients and $P_{GEN,\ rated}$ is the rated power of the diesel generator (kW). The intersecting point between the two curves is the discharge limit power $P_{\text{limit\_discharge}}$. Then, if the power is lower than $P_{\text{limit\_discharge}}$, the optimal solution would be to supply it with batteries or otherwise use diesel. The value of $P_{\text{limit\_discharge}}$ can be calculated, however, as the real battery operating conditions are usually different from those recommended by the manufacturer; the real intersection point can be different from the $P_{\text{limit\_discharge}}$ calculated, so this value can be optimised.

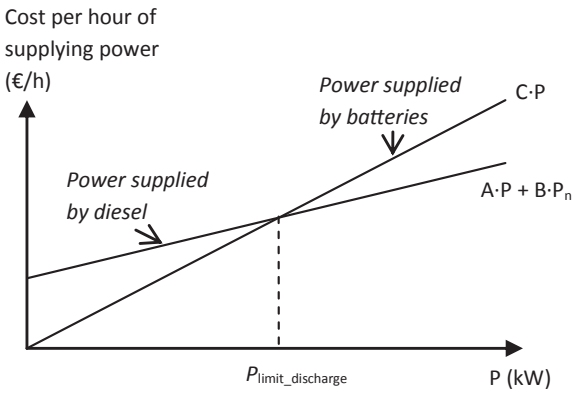

Fig. 2. Graphical calculation of $P_{\text{limit\_discharge}}$.

$P_{\text{critical\_gen}}$ and $SOC_{\text{stp\_gen}}$: Due to the high specific consumption of the diesel generator at low power, when the power demanded by the diesel is low (lower than the critical power limit, $P_{\text{critical\_gen}}$), it may be optimal to run at rated power. That extra power is used to charge the batteries up to the $SOC_{\text{stp\_gen}}$. If $P_{\text{critical\_gen}} = 0$, the classical control strategy "Load following" is used (the diesel just runs to meet the load). On the other hand, if $P_{\text{critical\_gen}} \rightarrow \infty$, the classical control strategy "Cycle charging" is used (the diesel will run when the batteries cannot meet the load at the rated power, not just to meet the demand but also to charge the batteries until $SOC_{\text{stp\_gen}}$ is reached).

The last four control variables are set in the modern PWM battery controllers (or the inverter/charger) with SOC control [35].

In this work, the charging stages used by the most of the PWM chargers are included in the simulations. Charge is conducted in three stages: bulk, boost and float (also an equalisation stage is performed under certain conditions). During bulk stage, the battery is charged at the maximum current. Later, when the battery reaches the boost voltage (BV) setpoint, the current tapers to maintain voltage at that value. Then, when the battery current drops to a certain level or a specific time has passed in boost stage (BTime), the setpoint is dropped to a lower float voltage (FV) setpoint. This kind of controllers overcharges the battery at regular intervals (equalisation), applying an equalisation voltage (EV) setpoint during a specified time (ETime).

The control of the discharge process is usually done by voltage setpoints: when a voltage to disconnect (VD) setpoint is reached, the load is disconnected from the battery (preventing overdischarge); then, when the battery is recharged and reaches a voltage to reconnect (VR) setpoint, the load is reconnected.

Some modern PWM controllers include algorithms to calculate the real SOC of the battery so that the battery can be optimally protected. They do this using SOC setpoints, which can be optimised (depending on the operating conditions, the optimal values of these setpoints can be different from the default values set in the controller):

$SOC_{\text{min\_ disconnect}}$: minimum SOC of the battery. When the battery is discharging and reaches this value, the load is disconnected from the battery, preventing overdischarge.

$SOC_{\text{min\_ reconnect}}$: after disconnecting the load from the battery, if the battery is recharged, the load is reconnected when the battery has reached this SOC.

SOC_{boost}: If the battery has fallen since the last full charge of the SOC, denoted as SOC_{boost}, the next charge will include a boost-

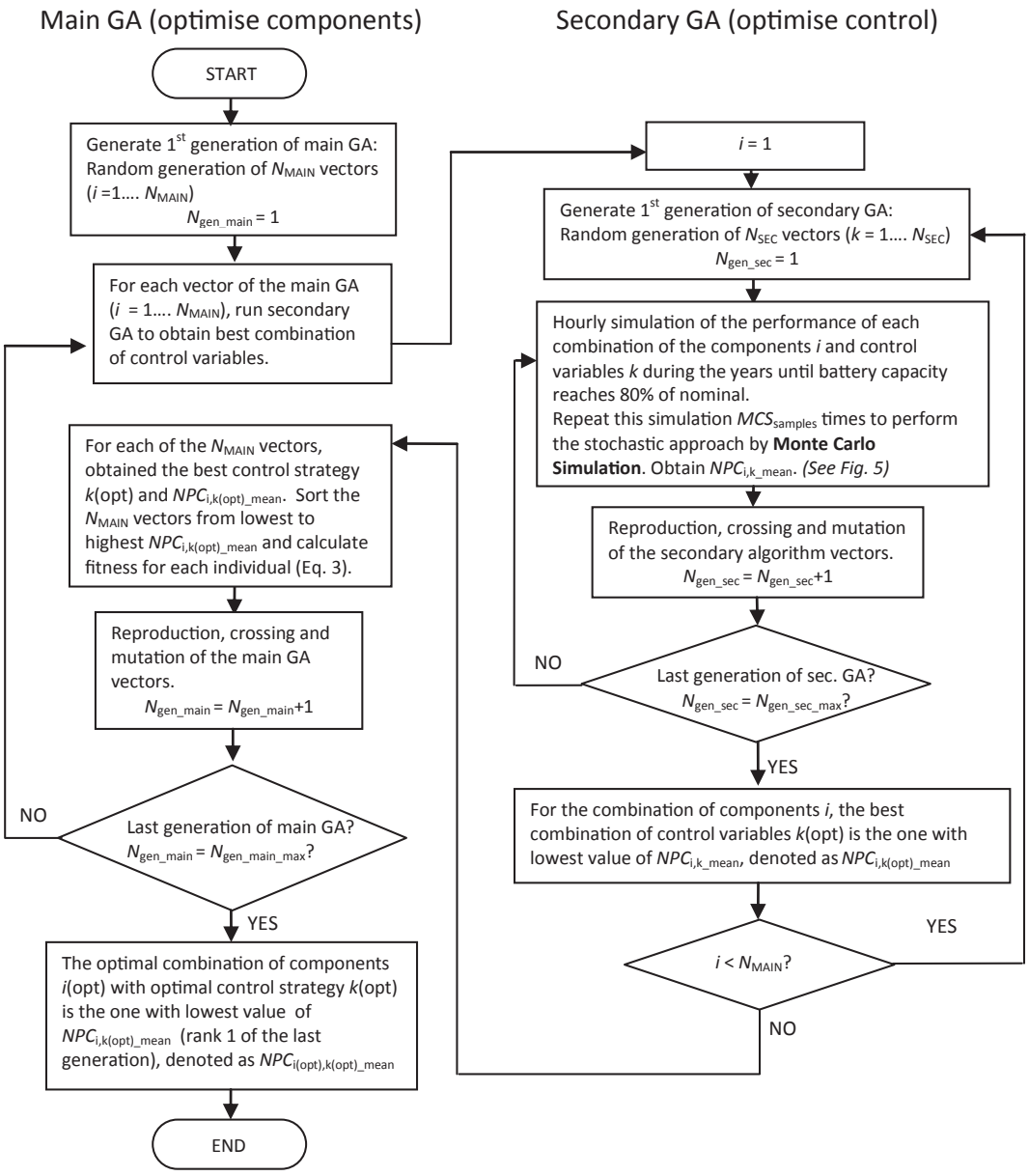

Fig. 3. Mono-objective optimisation by means of two GA (main and secondary) including MCS.

charge stage; otherwise, this stage will not be used.

SOC_{equal}: If the battery has fallen since the last full charge of the SOC, denoted as SOC_{equal}, equalisation will be done as programmed; otherwise, this stage will not be used.

3.2. Optimisation using GA and including MCS

Two GA (based on [13]) are applied in the stochastic-heuristic optimisation of the hybrid system (Fig. 3).

In this study, MCS is performed for the stochastic approach, so each combination of components i and control strategy k is evaluated $MCS_{samples}$ times (number of samples of the MCS or until a stopping rule is reached) so a probability density function (PDF) for each of the result variables (energy supplied by PV, by wind turbines, by diesel, unmet load, energy cycled by batteries, batteries lifetime, fuel consumption, O&M costs, replacement costs, NPC, LCE, etc.) is obtained. The mean of the PDF distribution of NPC is denoted as $NPC_{i\_k\_mean}$.

For each combination of components i that is evaluated by the main GA, a sub-algorithm (called the secondary GA) is used to obtain the optimal control strategy k, denoted as $k(opt)$ (optimal combination of control variables), and to minimise the mean of the NPC distribution, denoted as $NPC_{i,k(opt)\_mean}$.

The main GA is used to obtain the optimal combination of components i, denoted as $i(opt)$ (with the optimal combination of control variables obtained by the secondary algorithm), which minimises the $NPC_{i,k(opt)\_mean}$, denoted as $NPC_{i(opt),k(opt)\_mean}$.

For each GA, a population of N vectors (or individuals) is initially obtained randomly (first generation). Each vector is evaluated by means of an hourly simulation of the system during the years of the battery lifetime (since it is previously unknown, the system is simulated until the battery's remaining capacity is 80% of nominal, when it is considered the end of its lifetime [35]), repeated $MCS_{samples}$ times, to obtain the probabilistic approach. Then, the probability density function (PDF) of the result variables is known. The individuals with a mean of unmet load higher than a specific

value (for example, 0.01%) are discarded. The main result is the mean of the NPC distribution, which is the variable used to sort the set of vectors. The first (rank 1) is the best individual, i.e., the one with the lowest NPC mean, whereas the last (rank N) is the worst, i.e., the one with the highest NPC mean. Once the N individuals are sorted, the fitness function of the individual with rank i is assigned as follows:

$$fitness_i = \frac{(N+1)-i}{\sum_j[(N+1)-j]} \qquad j = 1...N \tag{3}$$

The best individuals (fittest) have a higher probability of reproducing, which crosses with other vectors. In each cross, two new vectors are obtained. Some individuals randomly change some of their components, i.e., a component of the integer vector is randomly selected and its value is randomly changed by another one (mutation) in order to avoid a local minimum (to maintain diversity within the population and inhibit premature convergence). The individuals obtained from reproduction and mutation are evaluated, and the best individuals replace the worst in the previous generation, thereby obtaining the next generation. The process continues until a determined number of generations N_{gen_max} has been evaluated. The best solution obtained is that which has the lowest value of the mean of the NPC distribution.

GA are heuristic techniques, which do not evaluate all the possible combinations, so it is impossible to say that it will always obtain the optimal solution. In some cases it can obtain a solution near the optimal.

An hourly time step is used as it is the usual time step in the optimisation of this kind of systems in a deterministic approach. Lower time steps would imply inadmissible computation time. In the probabilistic approach, which can imply x 50 or x 100 (or even more) the computation time of the deterministic approach, the hourly step must be used.

3.3. Monte Carlo simulation

As explained in section 3.2 and in Fig. 3, the secondary GA, which is used to optimise the control variables, includes MCS.

Usually, the series of several years (for example, 10 or 20 years) of the average daily irradiation during a whole year vary from year to year so that its PDF approximately follows a normal or Gaussian curve distribution (Fig. 4), with a mean (X_{mean}) and a standard deviation (X_{SD}, square root of the variance). The same thing occurs with the load, the temperature, the wind speed and the diesel fuel-price interest rate.

The procedure of the MCS applied for each combination of components i and control strategy k is shown in Fig. 5.

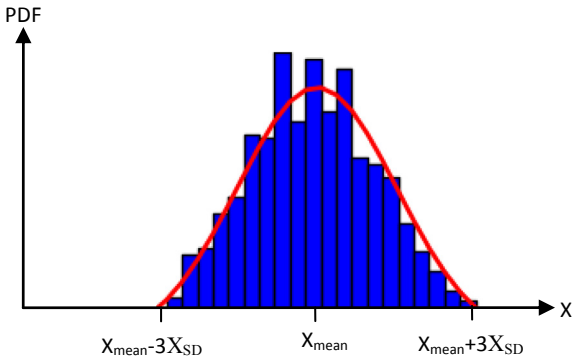

Fig. 4. Variable X approximately following a normal PDF.

The PDF of the average daily load of a whole year E (kWh), the PDF of the average daily irradiation of a whole year over the surface of the PV panels G (kWh/m^2), the PDF of the average temperature of a whole year T (°C), the PDF of the average wind speed of a whole year W (m/s) and the PDF of the annual diesel fuel price interest rate Int (%) are known as data.

E, G, T and W are usually correlated variables and their variance-covariance matrix is known.

Also, the hourly time series for a whole year (8760 h) of E, G, T and W with mean values E_{mean}, G_{mean}, T_{mean} and W_{mean} are known and denoted as $E_h(t)$, $G_h(t)$, $T_h(t)$ and $W_h(t)$, $t = 1 \ldots 8760$ h.

For each combination of components i and control strategy k, each year a vector of correlated Gaussian random variables $\boldsymbol{Z}$ is obtained:

$$\boldsymbol{Z} = \begin{bmatrix} E_{year} \\ G_{year} \\ T_{year} \\ W_{year} \end{bmatrix} \tag{4}$$

which is distributed according to:

$$\boldsymbol{Z} \sim \boldsymbol{N}(\boldsymbol{\mu}, \boldsymbol{\Sigma}) \tag{5}$$

where $\boldsymbol{\mu}$ is the vector of means, and $\boldsymbol{\Sigma}$ is the variance-covariance matrix (symmetrical) [38,39].

$$\boldsymbol{\mu} = \begin{bmatrix} E_{mean} \\ G_{mean} \\ T_{mean} \\ W_{mean} \end{bmatrix}; \ \boldsymbol{\Sigma} = \begin{bmatrix} \mathrm{var}(E) & \mathrm{cov}(E,G) & \mathrm{cov}(E,T) & \mathrm{cov}(E,W) \\ \mathrm{cov}(G,E) & \mathrm{var}(G) & \mathrm{cov}(G,T) & \mathrm{cov}(G,W) \\ \mathrm{cov}(T,E) & \mathrm{cov}(T,G) & \mathrm{var}(T) & \mathrm{cov}(T,W) \\ \mathrm{cov}(W,E) & \mathrm{cov}(W,G) & \mathrm{cov}(W,T) & \mathrm{var}(W) \end{bmatrix} \tag{6}$$

The procedure is shown in Ref. [40]. First it is generated a vector $\boldsymbol{X}$ which is distributed as

$$\boldsymbol{X} \sim \mathrm{N}(0, \mathbf{I}) \tag{7}$$

where $\mathbf{I}$ is an appropriately-sized identity matrix.

The vector of correlated Gaussian random variables is obtained using the following expression:

$$\boldsymbol{Z} = \boldsymbol{C}\boldsymbol{X} + \boldsymbol{\mu} \tag{8}$$

where $\boldsymbol{C}$ is a lower triangular matrix called the Cholesky factor of the variance-covariance matrix ($\boldsymbol{C}\boldsymbol{C}' = \boldsymbol{\Sigma}$).

For the first year, these values obtained in $\boldsymbol{Z}$ are E_{year1}, G_{year1}, T_{year1} and W_{year1}, which will be the average values of the hourly time series for the first year.

Then the hourly time series of E, G, T and W for the first year $E_{h\_year1}(t)$, $G_{h\_year1}(t)$, $T_{h\_year1}(t)$ and $W_{h\_year1}(t)$ are obtained proportional to the original series $E_h(t)$, $G_h(t)$, $T_h(t)$ and $W_h(t)$ as follows:

$$E_{h\_year1}(t) = E_h(t) \cdot \frac{E_{year1}}{E_{mean}} \qquad 0 < t \le 8760\ h \tag{9}$$

$$G_{h\_year1}(t) = G_h(t) \cdot \frac{G_{year1}}{G_{mean}} \qquad 0 < t \le 8760\ h \tag{10}$$

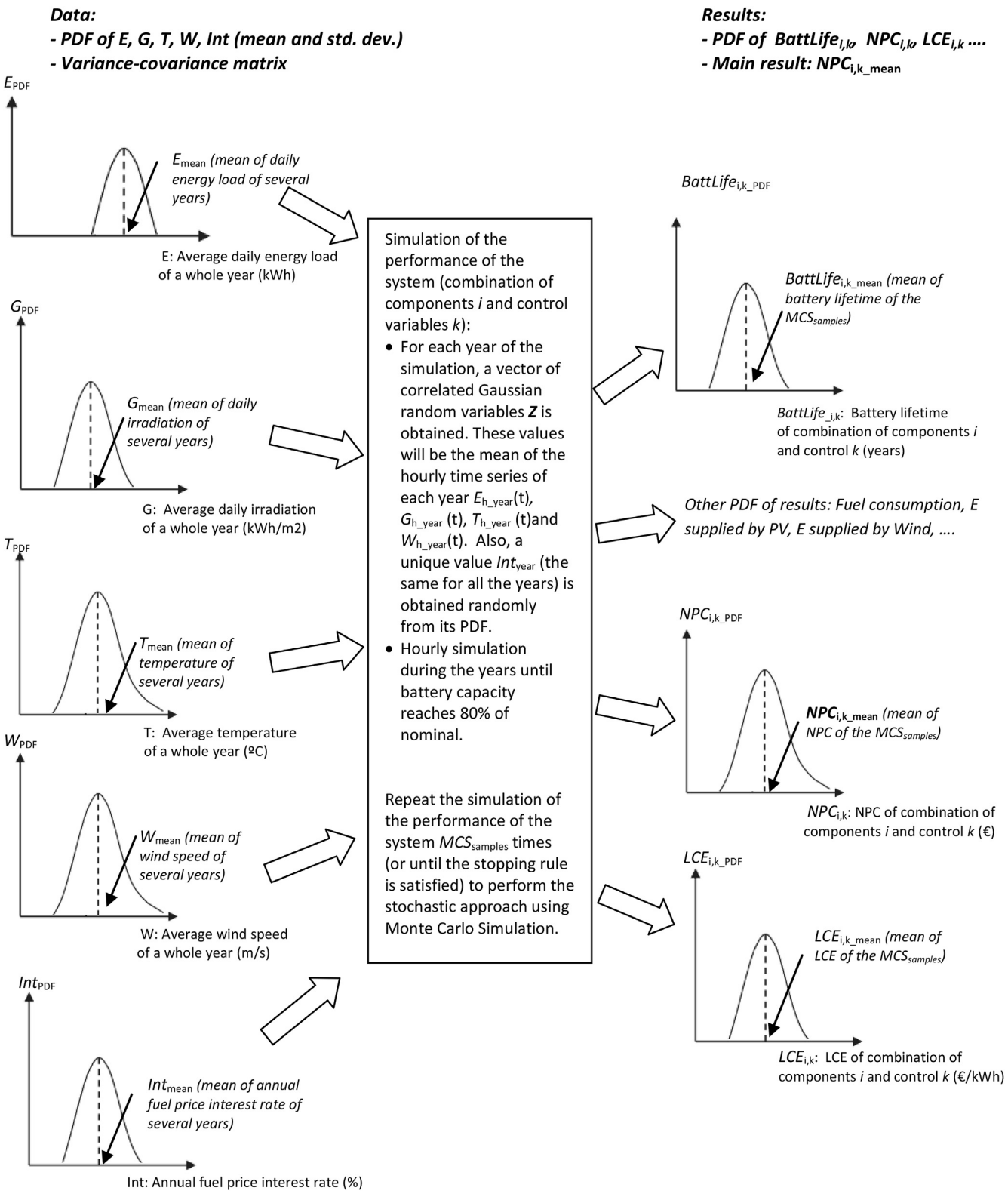

Fig. 5. Stochastic approach by MCS for each combination of components *i* and control strategy *k*.

$$T_{h\_year1}(t) = T_h(t) \cdot \frac{T_{year1}}{T_{mean}} \qquad 0 < t \leq 8760\ h \qquad (11)$$

$$W_{h\_year1}(t) = W_h(t) \cdot \frac{W_{year1}}{W_{mean}} \qquad 0 < t \leq 8760\ h \qquad (12)$$

Also, a value Int_{year} (which will be the same for all the years) is

obtained from its PDF.

The hourly simulation of the performance of the system is done during the first year. At the end of the first year, if the battery bank's remaining capacity is still higher than 80% of its nominal value, this means that the battery still has not reached the end of its lifetime, so the simulation must continue during year 2 (obtaining the correlated Gaussian random variables values of E_{year2}, G_{year2}, T_{year2} and W_{year2} and calculating the hourly time series as done for year 1). The process continues until the year when the battery bank's remaining capacity reaches 80% of its nominal value. Then it is known the battery lifetime for that combination of components i and control strategy k ($BattLife_{i,k}$) and the performance of the system during that time (assuming that this performance will be repeated until the end of the system lifetime). All the other results are then calculated, including $NPC_{i,k}$ and $LCE_{i,k}$.

The whole process explained before is repeated $MCS_{samples}$ times ($MCS_{samples}$ is the number of samples or trials or sample size of the MCS) or until the stopping rule of the MCS is reached. Then, the results are displayed as PDF distribution curves. The mean of the PDF of the $NPC_{i,k}$, which is called $NPC_{i,\ k\_mean}$, will be the value used to evaluate the fitness of the combination of components i and control strategy k.

There are many stopping rules for MCS [41,42]. A simple stopping rule is to let the simulation run until the relative standard error [39] of the NPC (standard error of the mean divided by the mean) reaches a specified value RSE (for example 0.1%):

$$100\frac{\frac{NPC_{i,k\_SD}}{\sqrt{n}}}{NPC_{i,k\_mean}} < RSE \tag{13}$$

where $NPC_{i,\ k\_mean}$ and NPC_{i,k_SD} are the mean and standard deviation of the NPC obtained in the n samples evaluated.

Another widely used method [43] is to run the MCS until a specified precision (a maximum error ε in the obtained mean over the true mean, for example, 1%) under a specified confidence level CL (for example, 95%):

$$100\frac{\frac{NPC_{i,k\_SD}}{\sqrt{n}}\cdot Z_{CL}}{NPC_{i,k\_mean}} < \varepsilon \tag{14}$$

where Z_{CL} is the confidence coefficient for the confidence level under a normal distribution. For example, for $CL = 95\%$, $Z_{CL} = 1.96$. In the application example (section 4) this stopping rule has been used.

3.4. Mathematical model for the hourly simulation of the system

In this section the mathematical models of the components used in the hourly simulation of the system are shown.

3.4.1. PV generator

A maximum power point tracking (MPPT) system is considered in the system, so the power of the PV generator coming into the inverter/charger is calculated as follows:

$$P_{PV}(t) = P_{STC}\cdot\frac{G_{h\_yearY}(t)}{1kWh/m^2}\cdot f_{mm}f_{dirt}\cdot\mu_{DC/DC}\cdot\mu_{DC/AC\_PV}\cdot\mu_{wire\_PV}\cdot f_{temp} \tag{15}$$

where P_{STC} is the output power in standard test conditions (Wp), $G_{h\_yearY}(t)$ (kWh/m^2) is the irradiation over the surface of the PV panels during hour t of year Y, f_{mm} is module mismatch or power tolerance, f_{dirt} is dirt derating factor, $\mu_{DC/DC}$ is the efficiency of the DC/DC system for the MPPT, μ_{DC/AC_PV} is the efficiency of the inverter (if AC coupled system) and μ_{wire_PV} is wire efficiency (from the PV generator to the inverter/charger) and f_{temp} is temperature derating factor, which is calculated as follows:

$$f_{temp} = 1 + \frac{\alpha}{100}(T_c(t) - 25) \tag{16}$$

where α is the power temperature coefficient (%/°C) and $T_c(t)$ (°C) is the PV cell temperature, which can be calculated as:

$$T_c(t) = T_a(t) + \left(\frac{NOCT - 20}{0.8}\right)\cdot\frac{G_{h\_yearY}(t)}{1kWh/m^2} \tag{17}$$

where $T_a(t)$ is the ambient temperature (°C) and $NOCT$ is the nominal operation cell temperature (°C).

3.4.2. Wind turbine

The power curve supplied by the manufacturer (in standard conditions, at sea level; examples shown in Fig. 6 with red curves) must be converted to the power curve at the height of the location and temperature of each hour.

Atmospheric pressure P (Pa) at the altitude above sea level H (m) can be approximated as follows:

$$P = P_o\left(1 - \frac{L\cdot H}{T_o}\right)^{\frac{gM}{RL}} \tag{18}$$

where P_o is the standard pressure at sea level (101325 Pa), T_0 is the temperature at the height of sea level (288.15 K), L is the variation rate of temperature vs. height (0.0065 K/m), $g = 9.80665$ m/s^2, R is the ideal gas constant (8,31432 J/mol·K) and M is the molecular weight of dry air ($28.9644\cdot10^{-3}$ kg/mol).

Considering the ideal gas law:

$$\frac{\rho}{\rho_0} = \left(1 - \frac{L\cdot H}{T_o}\right)^{\frac{gM}{RL}}\cdot\frac{T_0}{T} \tag{19}$$

where ρ (kg/m^3) is the air density at the altitude above sea level H and temperature T (K) and ρ_0 is the air density at sea level (1.225 kg/m^3).

The output power of a wind turbine at the height above sea level H and temperature T can be calculated as the output power at sea level (given by the power curve supplied by the manufacturer)

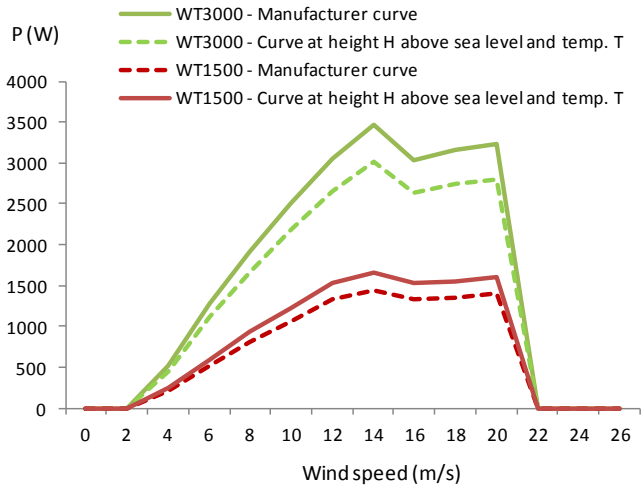

Fig. 6. Example of power curves of two wind turbines.

multiplied by the ratio ρ/ρ_0. In the example of Fig. 6, the dotted curves are at height $H = 1024$ m and $T = 293$ K.

If the hub height z_{hub} (m) of the wind turbine is different from the anemometer height where the wind speed data were measured z_{anem} (m), the wind speed at the hub height can be obtained from the wind speed $W_{h\_yearY}(t)$, as follows:

$$W_{HUB\_h\_yearY}(t) = W_{h\_yearY}(t)\cdot\frac{\ln\frac{z_{hub}}{z_0}}{\ln\frac{z_{anem}}{z_0}} \quad (20)$$

where z_0 is the surface roughness length (m).

$$SOC(t+\Delta t) = SOC(t) + \left(I_{bat}(t) - I_{gas}(t)\right)\Delta t/C_N \quad (23)$$

where $I_{bat}(t)$ (A) is the battery input current, $I_{gas}(t)$ (A) is the gassing current (during discharge it is 0), C_N (Ah) is the nominal capacity and Δt is the time step of the simulation (in this case 1 h).

The battery input current is calculated as:

$$I_{bat}(t) = P_{bat}(t)/U_{bat}(t) \quad (24)$$

where $U_{bat}(t)$ (V) is the battery voltage, calculated by the modified Shepherd equations [37].

$$\begin{aligned} U_{bat}(t) &= U_0 - \left(\frac{10}{13}\right)gDOD(t) + \rho_C(t)\left(\frac{I_{bat}(t)}{2C_{10}}\right) + \rho_C(t)M_C\left(\frac{I_{bat}(t)}{2C_{10}}\right)\left(\frac{SOC(t)}{C_C - SOC(t)}\right) \quad \forall\ I_{bat}(t) > 0 \\ U_{bat}(t) &= U_0 - \left(\frac{10}{13}\right)gDOD(t) + \rho_D(t)\left(\frac{I_{bat}(t)}{2C_{10}}\right) + \rho_D(t)M_D\left(\frac{I_{bat}(t)}{2C_{10}}\right)\left(\frac{DOD(t)}{C_D(t) - DOD(t)}\right) \quad \forall\ I_{bat}(t) < 0 \end{aligned} \quad (25)$$

This value of $W_{HUB\_h\_yearY}(t)$ is used as an input in the power curve at the height of the location H and the temperature $T(t)$ to obtain the power generated by the wind turbine P_{WT} (t) during hour t of year Y. If the wind turbine output is in DC and the inverter/charger is AC coupled, the efficiency of the inverter μ_{DC/AC_WT} must be considered. The power of the wind turbine coming into the inverter/charger is also affected by the wire efficiency from the wind turbine to the inverter/charger, μ_{wire_WT}.

3.4.3. Diesel generator

The diesel generator output power $P_{GEN}(t)$ (kW) depends on the output power of the renewable sources, the load, the control strategy and the SOC of the battery bank. The diesel fuel consumption (l/kWh) during hour t is considered as follows:

- If the diesel was running during previous hour:

$$Cons_{fuel}(t) = B\cdot P_{GEN,\ rated} + A\cdot P_{GEN}(t) \quad (21)$$

- Else:

$$Cons_{fuel}(t) = B\cdot P_{GEN,\ rated} + A\cdot P_{GEN}(t) + F_{START}\cdot\left(B\cdot P_{GEN,\ rated} + A\cdot P_{GEN,\ rated}\right) \quad (22)$$

where $A = 0.246$ l/kWh and $B = 0.08415$ l/kWh are the fuel curve coefficients [44], $P_{GEN,\ rated}$ (kW) is the rated power and F_{START} is a factor to consider the extra fuel due to the start of the generator, it is usually lower than 0.0083, equivalent to 5 min at rated power [45].

3.4.4. Battery bank

The battery bank input power P_{bat} (t) (>0 battery charging, <0 battery discharging) depends on the output power of the renewable sources, the load, the control strategy, the output power of the diesel and the SOC of the battery bank. The weighted Ah-throughput lead-acid battery model shown by Schiffer et al. [37], which includes an accurate ageing model, has been used in this work.

The *SOC* (per unit of the nominal capacity) is calculated adding the effective charge that comes into the battery to the *SOC* of the previous hour:

where: U_0 (V) is the open-circuit equilibrium cell voltage at the fully-charged state, g (V) is an electrolyte proportionality constant, $DOD = 1-SOC$ is the depth-of-discharge; ρ_C and ρ_D (ΩAh) are the aggregated internal resistance during charge or discharge, C_{10} is the rated capacity of the battery at 10 h discharge, C_C and C_D are the normalized capacity of the battery during charge or discharge.

Battery efficiency is implicitly considered in Eq. (21), as the gassing current affects the SOC during charge. It is also implicitly considered in the battery voltage (Eq. (23)): during charge U_{bat} increases its value, so the power required to charge the battery bank ($U_{bat}\cdot I_{bat}$) (from Eq. (22)) must be higher, i.e., not all the power is converted in energy stored. During discharge, U_{bat} decreases its value, so the power supplied by the battery bank ($U_{bat}\cdot I_{bat}$) is lower, i.e., not all the power that is extracted from the battery is converted in energy supplied to the load.

This model calculates the capacity loss by corrosion, $C_{corr}(t)$ and the capacity loss by degradation (cycling), $C_{deg}(t)$. During each hour the remaining battery capacity, $C_{remaining}(t)$, can be calculated as the normalised initial battery capacity ($C_{normalised}$) minus the capacity loss by corrosion and degradation:

$$C_{remaining}(t) = C_{normalised} - C_{corr}(t) - C_{deg}(t) \quad (26)$$

When the remaining capacity is 0.8 (i.e., 80% of the nominal capacity) the battery is considered that has finished its lifetime.

The capacity loss by degradation is calculated as:

$$C_{deg}(t) = C_{deg,limit}\cdot\exp\left[-c_z\left(1 - \frac{Z_W(t)}{1.6\cdot Z_{IEC}}\right)\right] \quad (27)$$

where $C_{deg,\ limit}$ is the degradation limit (reached when the remaining battery capacity is 80% of the nominal capacity taking into account only cycling, not corrosion), c_Z is a constant equal to 5, Z_W is the weighted number of cycles (with the impact of the *SOC*, the discharge current and the acid stratification) and Z_{IEC} is the lifetime number of IEC cycles [46].

$$Z_W(t+\Delta t) = Z_W(t)\cdot\frac{\left|I_{disch\_bat}(t)\right|\cdot f_{SOC}(t)\cdot f_{acid}(t)\cdot\Delta t}{C_N} \quad (28)$$

where I_{disch_bat} is the discharge current of the battery (A), f_{SOC} is a factor which takes into account the influence of the *SOC* and

includes the impact of the current and f_{acid} takes into account the impact of the acid stratification.

The influence of the *SOC* is calculated as follows:

$$f_{SOC}(t) = 1 + \left(c_{SOC,0} + c_{SOC,\min} \cdot \left(1 - SOC_{\min}(t)\big|_{to}^{t}\right) \cdot f_I(I,n) \cdot (t - t_0)\right) \tag{29}$$

where t_0 is the time of the last full charge, $SOC_{min}(t)$ is the minimum *SOC* since the last full charge, $c_{SoC,0}$ is a constant which represent the increase in f_{SoC} with time at $SOC = 0$, $c_{SoC,min}$ is a constant to consider the impact of $SOC_{min}(t)$ and $f_I(I, n)$ is the current factor, which depends mainly on the current at the beginning of the discharge after a full charge (I), so the current factor is also affected by the number of bad charges (n), which takes into account the charges which end between 0.9 and 0.9998 SOC.

The current factor can be calculated by the following expression:

$$f_I(I,n) = \sqrt{I_{10}/I_{bat}(t)} \cdot \sqrt[3]{\exp(n(t)/3.6)} \tag{30}$$

where I_{10} (A) is the 10 h current ($I_{10} = C_{10}/10$).

The number of bad charges is reset to zero when the *SOC* reaches 0.9999. When the maximum *SOC* reached during a charge (SOC_{max}) is between 0.9 and 1, n is increased as follows:

$$n(t+\Delta t) = n(t) + \Delta n = n(t) + \frac{0.0025 - (0.95 - SOC_{\max})^2}{0.0025} \tag{31}$$

The influence of acid stratification on active mass degradation is taken into account by the factor f_{acid}:

$$f_{acid}(t) = 1 + f_{stratification}(t) \cdot \sqrt{\frac{I_{10}}{|I_{bat}(t)|}} \tag{32}$$

where $f_{stratification}$ is the stratification factor, increased or decreased by the factors f_{plus} and f_{minus} (the reader is referred to [37] for further details).

$$f_{stratification}(t+\Delta t) = f_{stratification}(t) + \left(f_{plus}(t) - f_{\mathrm{minus}}(t)\right)\Delta t \tag{33}$$

The capacity loss by corrosion is modelled using the concept of a corrosion layer, which grows during the lifetime of the battery. The effective corrosion layer thickness $\Delta W(t)$ is calculated during each hour depending on the corrosion voltage of the positive electrode and on temperature (see Ref. [37] for further details). The capacity loss by corrosion, $C_{corr}(t)$, is proportional to the effective layer thickness at time t, based on:

$$C_{corr}(t) = C_{corr,limit} \cdot \frac{\Delta W(t)}{\Delta W_{limit}} \tag{34}$$

where $C_{corr,\ limit}$ is the limit of the loss of capacity by corrosion and ΔW_{limit} is the corrosion layer thickness when the battery has reached the end of its float lifetime (given in the battery datasheet).

3.4.5. Inverter/charger

The inverter/charger (also called bi-directional converter) is modelled as a PWM controller with the charge in three stages and SOC control, with the cut limits and setpoints shown in section 3.1. The inverter/charger includes the output inverter (DC/AC) to supply the AC load from the DC bus and the rectifier (AC/DC, also called battery charger) so that the AC sources can charge the battery bank.

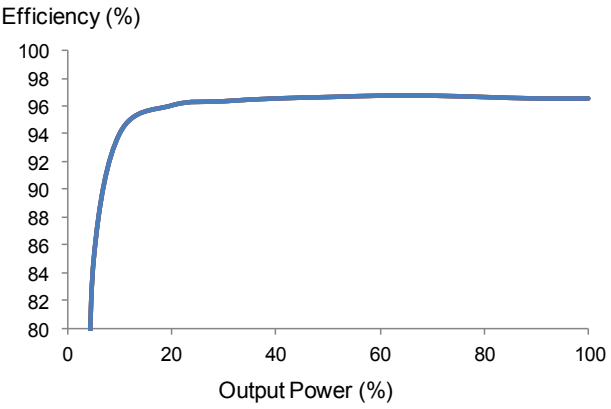

Fig. 7. Inverter efficiency.

The control unit in usually included in the inverter/charger. The inverter/charger performs a complete off-grid management. It controls the charge/discharge of the battery bank, calculating the SOC of the battery bank. When the SOC is lower than a specified limit, the inverter/charger turns on the diesel generator. The output power of the diesel can be controlled by the inverter charger and the SOC limit to stop it. Many inverter/chargers also include MPPT (to obtain the maximum power from the PV).

PV panels produce electricity in DC so the PV bus is in DC, using in this case a DC coupled inverter/charger (Fig. 1) b). To use an AC coupled inverter/charger (Fig. 1) a), the PV generator must include an inverter so its output bus will be an AC bus. It is applied also for the wind turbines (wind turbines output power is usually DC for low power devices; AC for high power devices).

There are different commercial inverter/chargers which allow different bus voltage type (DC or AC coupled) for the PV and the wind turbines (Fig. 1).

The input power to the battery bank (from the AC sources) is affected by the battery charger efficiency. The inverter efficiency depends on the output power (example shown in Fig. 7).

4. Example of application

Following the methodology shown in section 3, a PV-wind-diesel-batteries system supplying the load of an off-grid telecom station located in Navarra, Spain (42.73° N, 1.71° W, height 1,024 m) has been optimized.

Table 1 shows the PDF data while their correlations are the following (variance-covariance matrix and its Cholesky factor matrix):

$$\boldsymbol{\Sigma} = \begin{bmatrix} 0.171 & 0.024 & 0.029 & -0.057 \\ 0.024 & 0.035 & 0.020 & -0.051 \\ 0.029 & 0.020 & 0.345 & -0.052 \\ -0.057 & -0.051 & -0.052 & 0.470 \end{bmatrix}$$
$$\boldsymbol{C} = \begin{bmatrix} 0.413 & 0 & 0 & 0 \\ 0.057 & 0.177 & 0 & 0 \\ 0.069 & 0.093 & 0.576 & 0 \\ -0.138 & -0.242 & -0.035 & 0.626 \end{bmatrix} \tag{35}$$

Fig. 8 represents the hourly time series for a whole year (8760 h) of E, G, T and W with average values E_{mean}, G_{mean}, T_{mean} and W_{mean}, i.e., $E_h(t)$, $G_h(t)$, $T_h(t)$ and $W_h(t)$. Table 2 shows the possible components considered in the optimisations (DC coupled system). The DC nominal voltage is 48 V. As the PV panels used are of 12 V nominal voltage, 4 of them connected in series are needed. The

Table 1
Data of PDF (set of several years) of load, irradiation, temperature, wind speed and fuel price interest rate.

	Mean	Standard deviation	Number of years
E: Average daily AC load of a whole year (obtained from a similar telecom station)	14.28 kWh	0.413 kWh	8
G: Average daily irradiation of a whole year over the surface of the PV panels (60° slope, optimal) [48]	4.51 kWh/m^2	0.186 kWh/m^2	22
T: Average temperature of a whole year [48]	9.08 °C	0.587 °C	16
W: Average wind speed of a whole year, 10 m height [48]	8.30 m/s	0.685 m/s	22
Int: Annual fuel price interest rate* [49] [47]	5.72%	1.33%	20

*Data of the average price (*Pr*) of diesel fuel of each year during 20 years is known (from 1995 to 2015). Annual interest rate has been calculated as the average annual interest rate from a year to 10 years later. For example, the annual interest rate from 1995 to 2005 is as follows.

$$Int = \left(\left(\frac{Pr_{2005}}{Pr_{1995}}\right)^{1/10} - 1\right)\cdot 100 \quad (36).$$

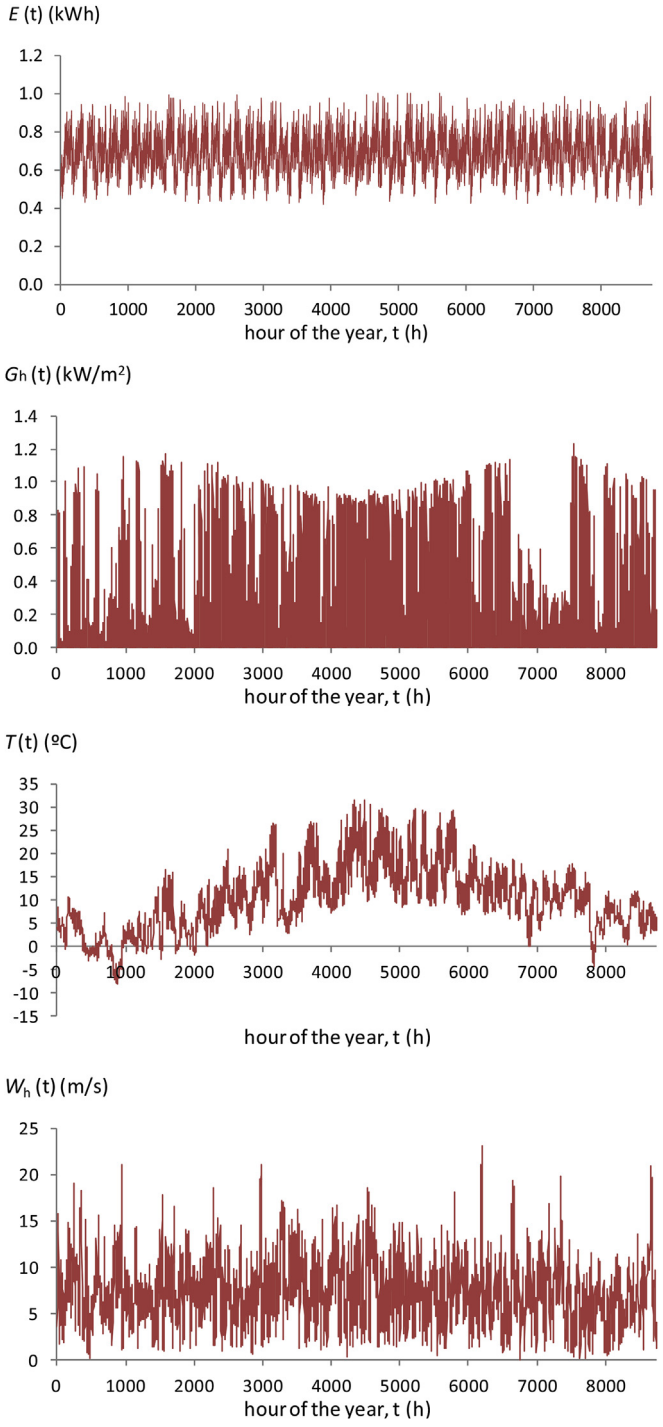

Fig. 8. Hourly time series for a whole year $E_h(t)$, $G_h(t)$, $T_h(t)$ and $W_h(t)$.

batteries are of 2 V nominal, which means 24 in series are needed. The diesel fuel price at the beginning of the installation was 1.1 €/l (present price in Spain [47]). The lifetime considered for the system is 25 years (the same as PV panels [13]). The installation cost is 1,000 € + 2% of the acquisition cost of all the components (estimated). To calculate NPC, the annual interest rate is considered (4%) and the annual general inflation (2%) (except for the fuel price, which is shown in Table 1). A minimum of 2 days of autonomy is required (if there is a diesel generator in the system, this requisite is not considered).

4.1. Deterministic-heuristic optimisation

First, it is performed the optimisation of the system without considering the uncertainties, i.e., a deterministic optimisation using the mean values of the data of Table 1, not considering the PDF of the data and not using MCS.

The number of possible combinations of components is obtained by the multiplication of the number of types of each component (with the range in parallel): 1x27x4x1x4x1x5x2x1x1 = 4,320 possible combinations.

It has been assumed that each control variable can take 4 values: P_{min_gen} between the minimum recommended by the manufacturer and the diesel rated power; P_{limit_disch} and $P_{critical\_gen}$ between 0 and the maximum hourly power demanded by the load; and SOC_{stp_gen}, $SOC_{min\_disconnect}$, $SOC_{min\_reconnect}$, SOC_{boost} and SOC_{equal} between the minimum SOC recommended by the manufacturer (20%) and 80% SOC. This means that a total number of $4^8 = 65{,}536$ combinations of control strategies can be considered.

Then a total of 4,320 × 65,536 = $2.83\cdot10^8$ combinations are possible in this case. At a rate of around 10 combinations per second (2.4 Ghz, 4 GB RAM computer), it would take 327 days to evaluate all of them. Obviously, this is inadmissible, so GA are used, as shown in section 3.2. (without MCS), with the parameters shown in Table 3, evaluating around 34,000 combinations of components and control variables and obtaining a computation time of around 12 h.

After obtaining the optimal system, the search space of the main GA was reduced and incremented the number of values the control variables could take to 6, evaluating around 30,000 combinations of components and control variables with a similar computation time, thereby obtaining the results shown in Tables 4 and 5 (left column). The optimal configuration is a PV-wind-diesel-battery system, with a very high penetration of the renewable sources (the diesel generator runs only 113 h in one year, supplying 146 kWh/yr (Annex 1, Fig. A.3), i.e., 2.7% of the annual load). In most of the locations in Spain, wind turbines are usually not part of the optimal system, as PV prices have dramatically fallen in recent years, however in this case (high wind speed) a wind turbine is part of the optimal system. Due to the high diesel fuel price (and its inflation) in Spain, diesel is practically used as a back-up system, supplying energy only when the battery bank reaches the minimum SOC.

Table 2
Possible components.

Component	Types	Number in parallel
PV panels (1 type)	1. P_{STC} = 100Wp, I_{SC} = 6.79A, NOCT = 49 °C, α = −0.2%/°C, acquisition cost (including support structure) 130 €, 12 V nominal (4 in serial). $f_{mm} \cdot f_{dirt} \cdot \mu_{DC\text{-}DC} \cdot \mu_{wire\_PV} = 0.85$	0–26
Wind turbines[a] (4 types)	1. No wind turbine 2. WT500 (max. power 580 W), hub height 10 m, cost 1,450 €, lifespan 15 yr, O&M cost 100 €/yr 3. WT1500 (max. power 1660 W), hub height 13 m, cost 4,875 €, lifespan 15 yr, O&M cost 100 €/yr 4. WT3000 (max. power 3520 W), hub height 15 m, cost 7,555 €, lifespan 15 yr, O&M cost 150 €/yr	1
Diesel[b] generators (4 types)	1. No diesel generator 2. Rated power 2 kVA, min. power 30%, acq. cost 800 €, lifespan 12,000 h, O&M cost 0.12 €/h 3. Rated power 3 kVA, min. power 30%, acq. cost 1,050 €, lifespan 12,000 h, O&M cost 0.13 €/h 4. Rated power 4 kVA, min. power 30%, acq. cost 1,200 €, lifespan 12,000 h, O&M cost 0.14 €/h	1
Batteries[c] (5 types)	1. OPZS 180 Ah, acq. cost 127 €, O&M cost 1.3 €/yr, 2 V nominal (24 in serial) 2. OPZS 270 Ah, acq. cost 178 €, O&M cost 1.8 €/yr, 2 V nominal (24 in serial) 3. OPZS 550 Ah, acq. cost 202 €, O&M cost 2 €/yr, 2 V nominal (24 in serial) 4. OPZS 816 Ah, acq. cost 298 €, O&M cost 3 €/yr, 2 V nominal (24 in serial) 5. OPZS 1340 Ah, acq. cost 412 €, O&M cost 4.1 €/yr, 2 V nominal (24 in serial)	2
Inverter/ chargers (1 type)	1. DC coupled. Continuous output power 4 kVA, MPPT, SOC control, charger efficiency 90%, inverter efficiency variable with output power (Fig. 7), acq. cost 4,200 €, lifespan 10 yr. BV = 2.4 V, FV = 2.3 V, EV = 2.45 V, BTime = 2 h, ETime = 2 h, VD = 1.85 V, VR = 2 V, $SOC_{min\_disconnect}$ = 30% (default), $SOC_{min\_reconnect}$ = 50% (default), SOC_{boost} = 70% (default), SOC_{equal} = 40% (default).	1

[a] For all the wind turbines $\mu_{wire\_WT} = 0.9$.
[b] For all the diesel generators, $F_{START} = 0.0083$.
[c] For all the batteries: SOC min. 20%, self-discharge 3%/month, float life at 20 °C 18 years, IEC full cycles to failure 1,260. Also for the whole battery bank a fixed O&M cost of 50 €/yr has been considered.

Table 3
Parameters of the GA used in the deterministic optimisation.

	Main GA	Secondary GA
Population ≥0.003% of all possible solutions [14]	$N_{MAIN} = 40$	$N_{SEC} = 40$
Generations ≥ 15 [14]	$N_{gen\_main\_max} = 15$	$N_{gen\_sec\_max} = 15$
Crossing rate = 90% [14]	90%	90%
Mutation rate = 1% [14]	1%	1%

Table 4
Configuration of the optimal system found in the optimisations.

	Optimal system, section 4.1 (**deterministic**)	Optimal system, section 4.2 (**stochastic**)
PV generator	100 Wp x 4 serial x 4 parallel. Total 1.6 kWp	100 Wp x 4 serial x 4 parallel. Total 1.6 kWp
Wind turbine	WT1500 (max. power 1660 W)	WT1500 (max. power 1660 W)
Diesel generator	2 kVA	2 kVA
Battery bank	OPZS 160 Ah, 2 V x 24 serial x 1 parallel. Total 8.64 kWh	OPZS 160 Ah, 2 V x 24 serial x 1 parallel. Total 8.64 kWh
P_{min_gen}	0.8 kVA	0.8 kVA
P_{limit_disch}	Max. load	Max. load
$P_{critical\_gen}$	Max. load	Max. load
SOC_{stp_gen}	50%	55%
$SOC_{min\_disconnect}$	30%	35%
$SOC_{min\_reconnect}$	40%	50%
SOC_{boost}	60%	60%
SOC_{equal}	50%	50%

Fig. 9 show the hourly simulation of the capacity loss and the remaining capacity of the battery bank of the optimal system during the first 9 years, as the battery lifetime is 8.7 years; the next years until 25 this performance is assumed to be repeated. The simulation of the power of the components is shown in Annex 1.

Figs. 10 and 11 show the hourly simulation during a week at the end of the first year. The surplus energy (from PV, wind turbines and also from diesel generator in the case its minimum output power is higher than the net load) is consumed by the dump load (Fig. 1).

4.2. Stochastic-heuristic optimisation

In this case, it has been considered the PDF of the data of Table 1 and the variance-covariance matrix shown in Fig. 8, using the methodology shown in section 3 with MCS.

A stopping rule of the MCS with a maximum error ε = 0.5% under a confidence level of CL = 95% has been considered. In the tests done previously, it was observed that the stopping rule in general is reached with around 200 MCS samples. This means that, using the stochastic approach, evaluating all the possible

Table 5
Main results of the optimal system found in the optimisations.

	Optimal system, section 4.1 (**deterministic**)	Optimal system, section 4.2 (**stochastic**)			
		Mean	**Std. Dev.**	Min.	Max.
Annual load (kWh/yr)	5,215	5,218	149	4,840	5,610
Anual unmet load (kWh/yr)	0	0	0	0	0
Annual energy generated by PV generator (kWh/yr)	2,124	2,134	84	1,886	2,383
Annual energy generated by wind turbines (kWh/yr)	6,463	6,465	752	3,869	8,150
Annual energy supplied by diesel generator (kWh/yr)	146	171	29.8	105.3	318.1
Annual diesel fuel consumption (l/yr)	52.3	62.1	15.5	35.5	107.5
Annual hours running the diesel generator (kWh/yr)	113	130.6	21.7	83	243
Annual energy charged by the battery bank (kWh/yr)	737	760.1	39.8	659.7	918.5
Annual energy supplied by the battery bank (kWh/yr)	679	694.4	38.7	597.7	856.8
Battery lifetime (yr)	8.70	8.69	0.098	8.41	9.04
NPC (€)	36,489	36,847	535	35,910	38,902
LCE (€/kWh)	0.280	0.282	0.0042	0.2725	0.2945

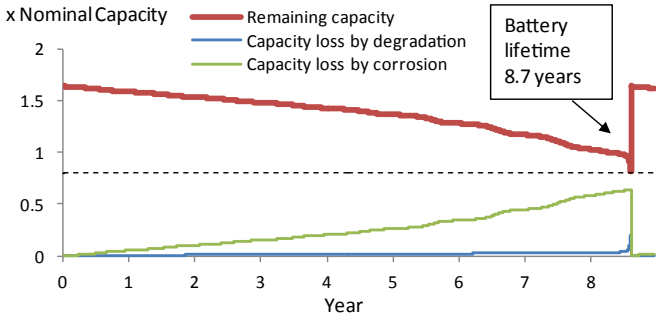

Fig. 9. Capacity loss and remaining capacity of the battery bank.

combinations would take around 200 times more than in section 4.1, which was already inadmissible. Using the GA high computation time is needed in this case, so it was decided to optimise only 3 control variables: SOC_{stp_gen}, $SOC_{min\_disconnect}$ and $SOC_{min\_reconnect}$. The rest will have fixed values, the ones obtained in the optimisation of section 4.1. The following parameters are used for the GA: $N_{MAIN} = 15$, $N_{gen\_main\_max} = 10$, $N_{SEC} = 10$, $N_{gen\_sec\_max} = 10$, crossing rate 90% and mutation rate 1%, thereby evaluating around 13,000 combinations of components and control variables, obtaining a computation time of around 78 h. The actual number of MCS samples needed to obtain $\varepsilon = 0.5\%$ under CL = 95% is different for each combination of components and control variables, typical values obtained are between 150 and 300. The optimal system found is the same (except for a little difference in the optimal control variables) as the one obtained in the deterministic

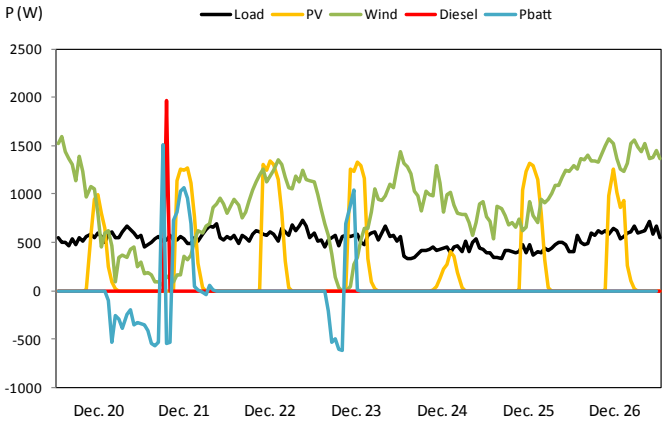

Fig. 10. Simulation during a week at the end of the first year.

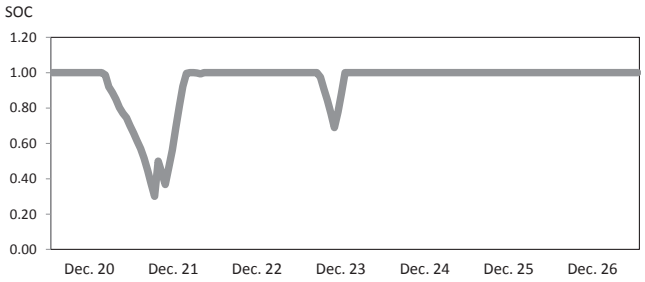

Fig. 11. SOC simulation during a week at the end of the first year.

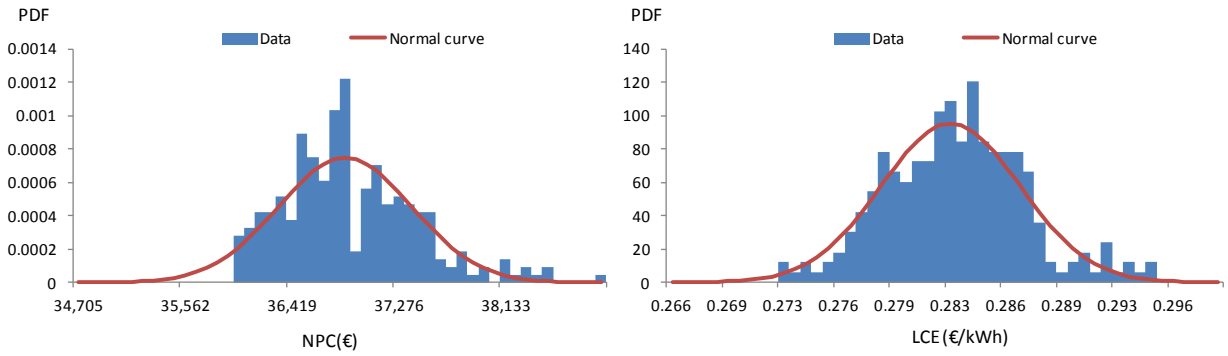

Fig. 12. PDF of the results of the optimal system (cont.).

optimisation (Table 4). The optimal configuration needed 243 MCS samples to reach the specified error under the confidence level, obtaining the mean, standard deviation, and minimum and maximum values of the results (shown in Table 4). Using the stochastic methodology, the designer can obtain results that include much more information and the ability to know the minimum, maximum and most probable values of the different results, including their variability. Fig. 12 shows the PDF of the 243 samples of the results of NPC and LCE and the normal curves, which best fit the PDF. In Annex 2 the rest of the PDF of the results are shown. In general the PDF curves follow Gaussian curves, however it can be observed that the PDF curves of the annual diesel consumption and the NPC are slightly different from a Gaussian curve because the distribution disappears on the left side of the Gaussian curve which fits better, while at the extreme right of said Gaussian curve there are many cases.

The stochastic optimisation has been repeated for different input data and locations, obtaining in most of the cases the same or a very similar optimal system to the one obtained using the deterministic optimisation for each case.

5. Conclusions

In this paper, a stochastic-heuristic methodology (combining MCS and GA) for the optimisation of components and control variables of stand-alone (off-grid) hybrid PV-wind-diesel-battery systems is shown. It has been applied a weighted Ah-throughput battery model that is much more accurate than classical battery models which only consider the energy cycled by the battery. It is also included the optimisation of several control variables that can be set in the modern battery controllers or inverter/chargers with State of Charge control.

The stochastic optimisation uses, as inputs, the PDF of several variables (load, irradiation, wind speed and diesel fuel price interest rate, taking into account their correlations) and obtains the PDF of the results. The designer of the system can, therefore, know the variability of the results and gain more information about the expected performance and costs of the system compared to using the deterministic optimisation.

However, the stochastic optimisation implies much higher computation times depending on the maximum error allowed. Under the confidence level desired, it can be hundreds of times higher, which, in many cases, is inadmissible even when using GA.

As an example, the deterministic optimisation of a system (12 h computation time) has been compared with the stochastic optimisation (78 h computation time even with reduced search space for the control variables), using GA for both. The hybrid system to supply a telecom station located in Navarra, Spain, in a windy hill, has been optimised. The optimal configuration is a PV-wind-diesel-battery system, with a very high penetration of the renewable sources. In this case (high wind speed) a wind turbine is part of the optimal system. Due to the high diesel fuel price (and its inflation) in Spain, diesel is practically used as a back-up system, supplying energy only when the battery bank reaches the minimum SOC. The optimal system found by the stochastic approach is very similar to the one obtained by the deterministic approach. However, the stochastic optimisation gives as results the PDF of the different result variables, with much more information about the expected performance of the system. The deterministic optimisation should be done first, with a low computation time. The search space can then be reduced around the optimal system found and the stochastic optimisation can be performed in a reasonable computation time, thereby obtaining the PDF of the results.

Annex 1. Simulation of the optimal system found in the deterministic optimisation.

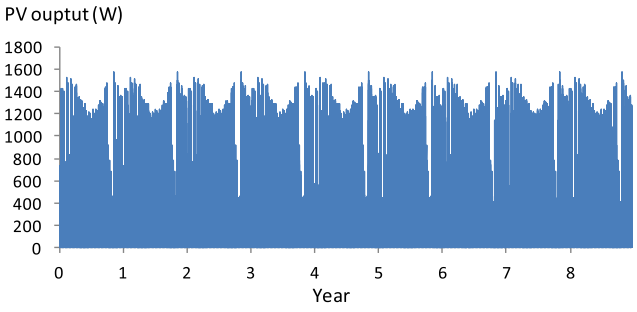

Fig. A1. PV generator output power.

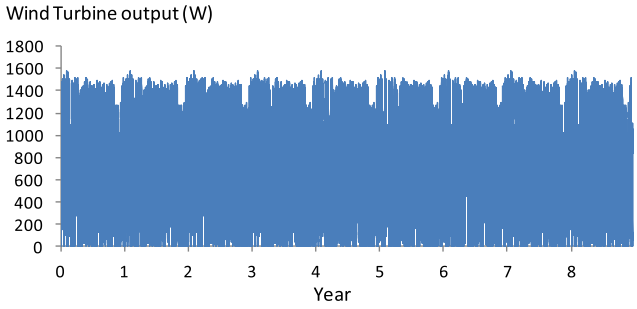

Fig. A2. Wind turbine output power.

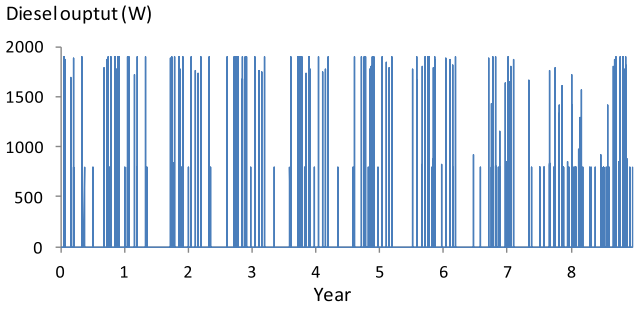

Fig. A3. Diesel generator output power.

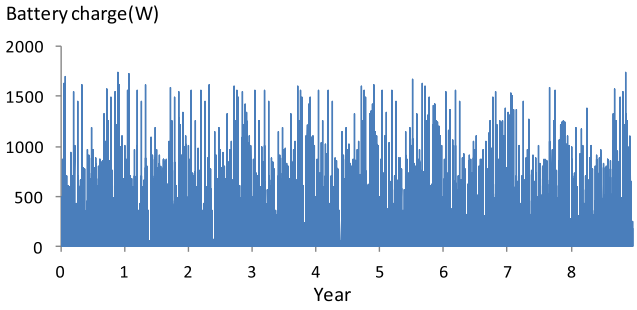

Fig. A4. Battery bank charge power.

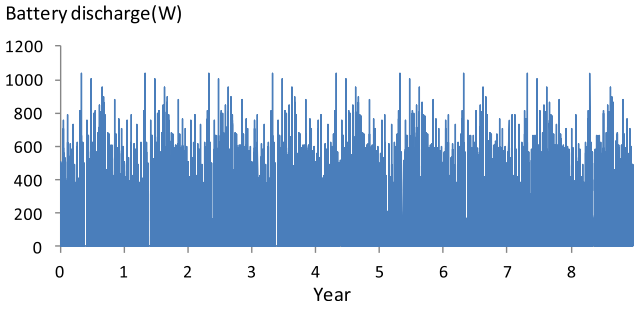

Fig. A5. Battery bank discharge power.

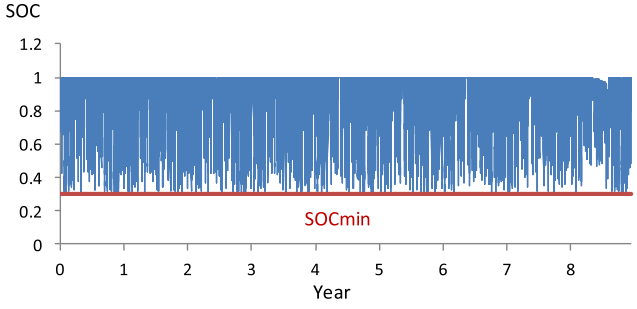

Fig. A6. Battery bank SOC.

Annex 2. PDF of some relevant results of the optimal system found in the stochastic optimisation.

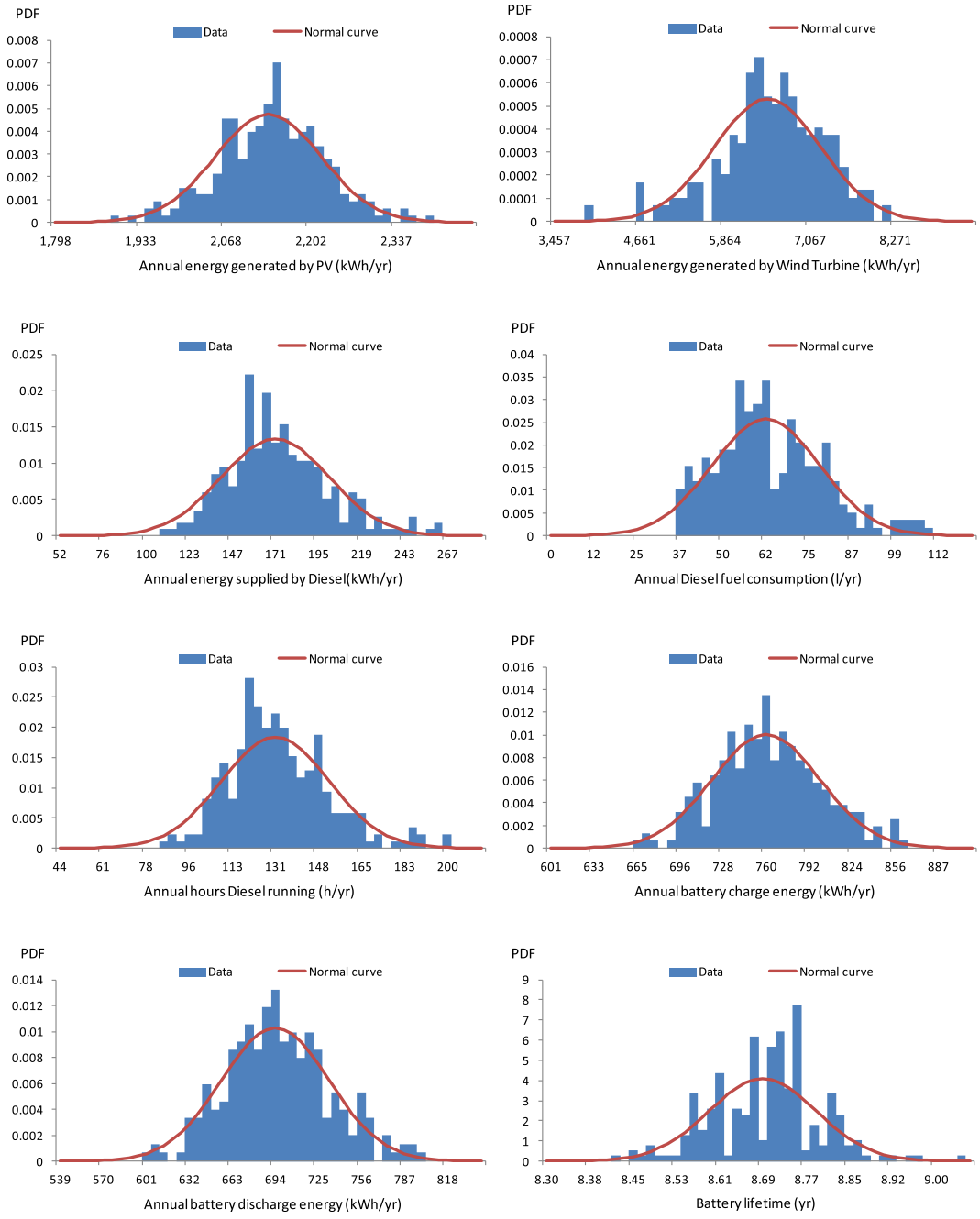

Fig. A7. PDF of some results of the optimal system.9

References

[1] U. Nations, United Nations Development Programme, Human Development Report, 2015 n.d, http://hdr.undp.org/sites/default/files/2015_human_development_report_1.pdf.
[2] P. Bajpai, V. Dash, Hybrid renewable energy systems for power generation in stand-alone applications: a review, Renew. Sustain. Energy Rev. 16 (2012) 2926–2939, http://dx.doi.org/10.1016/j.rser.2012.02.009.
[3] Y.S. Mohammed, M.W. Mustafa, N. Bashir, Hybrid renewable energy systems for off-grid electric power: review of substantial issues, Renew. Sustain. Energy Rev. 35 (2014) 527–539, http://dx.doi.org/10.1016/j.rser.2014.04.022.
[4] P. Nema, R.K. Nema, S. Rangnekar, A current and future state of art development of hybrid energy system using wind and PV-solar: a review, Renew. Sustain. Energy Rev. 13 (2009) 2096–2103, http://dx.doi.org/10.1016/j.rser.2008.10.006.
[5] R.K. Akikur, R. Saidur, H.W. Ping, K.R. Ullah, Comparative study of stand-alone and hybrid solar energy systems suitable for off-grid rural electrification: a review, Renew. Sustain. Energy Rev. 27 (2013) 738–752, http://dx.doi.org/10.1016/j.rser.2013.06.043.
[6] S. Sinha, S.S. Chandel, Review of software tools for hybrid renewable energy

systems, Renew. Sustain. Energy Rev. 32 (2014) 192–205, http://dx.doi.org/10.1016/j.rser.2014.01.035.
[7] J.L. Bernal-Agustín, R. Dufo-López, Simulation and optimization of stand-alone hybrid renewable energy systems, Renew. Sustain. Energy Rev. 13 (2009) 2111–2118, http://dx.doi.org/10.1016/j.rser.2009.01.010.
[8] H. Belmili, M. Haddadi, S. Bacha, M.F. Almi, B. Bendib, Sizing stand-alone photovoltaic-wind hybrid system: techno-economic analysis and optimization, Renew. Sustain. Energy Rev. 30 (2014) 821–832, http://dx.doi.org/10.1016/j.rser.2013.11.011.
[9] O. Erdinc, M. Uzunoglu, Optimum design of hybrid renewable energy systems: overview of different approaches, Renew. Sustain. Energy Rev. 16 (2012) 1412–1425, http://dx.doi.org/10.1016/j.rser.2011.11.011.
[10] N.D. Nordin, H. Abdul Rahman, A novel optimization method for designing stand alone photovoltaic system, Renew. Energy 89 (2016) 706–715, http://dx.doi.org/10.1016/j.renene.2015.12.001.
[11] I.G. Mason, A.J.V. Miller, Energetic and economic optimisation of islanded household-scale photovoltaic-plus-battery systems, Renew. Energy 96 (2016) 559–573, http://dx.doi.org/10.1016/j.renene.2016.03.048.
[12] S. Mandelli, C. Brivio, E. Colombo, M. Merlo, A sizing methodology based on levelized cost of supplied and lost energy for off-grid rural electrification systems, Renew. Energy 89 (2016) 475–488, http://dx.doi.org/10.1016/j.renene.2015.12.032.
[13] R. Dufo-López, J.L. Bernal-Agustín, Design and control strategies of PV-diesel systems using genetic algorithms, Sol. Energy 79 (2005) 33–46, http://dx.doi.org/10.1016/j.solener.2004.10.004.
[14] J.L. Bernal-Agustín, R. Dufo-López, Efficient design of hybrid renewable energy systems using evolutionary algorithms, Energy Convers. Manag. 50 (2009) 479–489, http://dx.doi.org/10.1016/j.enconman.2008.11.007.
[15] R. Dufo-López, J.L. Bernal-Agustín, J. Contreras, Optimization of control strategies for stand-alone renewable energy systems with hydrogen storage, Renew. Energy 32 (2007) 1102–1126, http://dx.doi.org/10.1016/j.renene.2006.04.013.
[16] D. Tsuanyo, Y. Azoumah, D. Aussel, P. Neveu, Modeling and optimization of batteryless hybrid PV (photovoltaic)/diesel systems for off-grid applications, Energy 86 (2015) 152–163, http://dx.doi.org/10.1016/j.energy.2015.03.128.
[17] D.E. Goldberg, Genetic Algorithms in Search, Optimization, and Machine Learning, 1989th ed., Addison-Wesley Publishing Company, 1989.
[18] S. Sinha, S.S. Chandel, Review of recent trends in optimization techniques for solar photovoltaic–wind based hybrid energy systems, Renew. Sustain. Energy Rev. 50 (2015) 755–769, http://dx.doi.org/10.1016/j.rser.2015.05.040.
[19] S. Rajanna, R.P. Saini, Modeling of integrated renewable energy system for electrification of a remote area in India, Renew. Energy 90 (2016) 175–187, http://dx.doi.org/10.1016/j.renene.2015.12.067.
[20] S. Sanajaoba, E. Fernandez, Maiden application of Cuckoo search algorithm for optimal sizing of a remote hybrid renewable energy system, Renew. Energy 96 (2016) 1–10, http://dx.doi.org/10.1016/j.renene.2016.04.069.
[21] P. Hajela, C.Y. Lin, Genetic search strategies in multi-criterion optimal design, Struct. Optim. 4 (1992) 99–107.
[22] C.A. Coello, D.A.V. Veldhuizen, G.B. Lamont, Evolutionary Algorithms for Solving Multi-Objective Problems, Kluwer Aca, New York, 2002.
[23] M. Fadaee, M.A.M. Radzi, Multi-objective optimization of a stand-alone hybrid renewable energy system by using evolutionary algorithms: a review, Renew. Sustain. Energy Rev. 16 (2012) 3364–3369, http://dx.doi.org/10.1016/j.rser.2012.02.071.
[24] P. Paliwal, N.P. Patidar, R.K. Nema, A novel method for reliability assessment of autonomous PV-wind-storage system using probabilistic storage model, Int. J. Electr. Power Energy Syst. 55 (2014) 692–703, http://dx.doi.org/10.1016/j.ijepes.2013.10.010.
[25] P. Arun, R. Banerjee, S. Bandyopadhyay, Optimum sizing of photovoltaic battery systems incorporating uncertainty through design space approach, Sol. Energy 83 (2009) 1013–1025, http://dx.doi.org/10.1016/j.solener.2009.01.003.
[26] A. Kamjoo, A. Maheri, G. a. Putrus, Chance constrained programming using non-Gaussian joint distribution function in design of standalone hybrid renewable energy systems, Energy 66 (2014) 677–688, http://dx.doi.org/10.1016/j.energy.2014.01.027.
[27] A. Kamjoo, A. Maheri, A.M. Dizqah, G. a. Putrus, Multi-objective design under uncertainties of hybrid renewable energy system using NSGA-II and chance constrained programming, Int. J. Electr. Power Energy Syst. 74 (2016) 187–194, http://dx.doi.org/10.1016/j.ijepes.2015.07.007.
[28] A. Maheri, A critical evaluation of deterministic methods in size optimisation of reliable and cost effective standalone hybrid renewable energy systems, Reliab. Eng. Syst. Saf. 130 (2014) 159–174, http://dx.doi.org/10.1016/j.ress.2014.05.008.
[29] A. Maheri, Multi-objective design optimisation of standalone hybrid wind-PV-diesel systems under uncertainties, Renew. Energy 66 (2014) 650–661, http://dx.doi.org/10.1016/j.renene.2014.01.009.
[30] W. Alharbi, K. Raahemifar, Probabilistic coordination of microgrid energy resources operation considering uncertainties, Electr. Power Syst. Res. 128 (2015) 1–10, http://dx.doi.org/10.1016/j.epsr.2015.06.010.
[31] K.-H. Chang, G. Lin, Optimal design of hybrid renewable energy systems using simulation optimization, Simul. Model. Pract. Theory 52 (2015) 40–51, http://dx.doi.org/10.1016/j.simpat.2014.12.002.
[32] I. Falconett, K. Nagasaka, Comparative analysis of support mechanisms for renewable energy technologies using probability distributions, Renew. Energy 35 (2010) 1135–1144, http://dx.doi.org/10.1016/j.renene.2009.11.019.
[33] G.M. Tina, S. Gagliano, Probabilistic modelling of hybrid solar/wind power system with solar tracking system, Renew. Energy 36 (2011) 1719–1727, http://dx.doi.org/10.1016/j.renene.2010.12.001.
[34] E.J.D.S. Pereira, J.T. Pinho, M.A.B. Galhardo, W.N. Macêdo, Methodology of risk analysis by Monte Carlo Method applied to power generation with renewable energy, Renew. Energy 69 (2014) 347–355, http://dx.doi.org/10.1016/j.renene.2014.03.054.
[35] R. Dufo-López, J.M. Lujano-Rojas, J.L. Bernal-Agustín, Comparison of different lead–acid battery lifetime prediction models for use in simulation of stand-alone photovoltaic systems, Appl. Energy 115 (2014) 242–253, http://dx.doi.org/10.1016/j.apenergy.2013.11.021.
[36] L.M. Carrasco, L. Narvarte, F. Martínez-Moreno, R. Moretón, In-field assessment of batteries and PV modules in a large photovoltaic rural electrification programme, Energy 75 (2014) 281–288, http://dx.doi.org/10.1016/j.energy.2014.07.074.
[37] J. Schiffer, D.U. Sauer, H. Bindner, T. Cronin, P. Lundsager, R. Kaiser, Model prediction for ranking lead-acid batteries according to expected lifetime in renewable energy systems and autonomous power-supply systems, J. Power Sources 168 (2007) 66–78, http://dx.doi.org/10.1016/j.jpowsour.2006.11.092.
[38] J. Kenney, E.S. Keeping, Mathematics of Statistics, Van Nostrand, New York, 1963.
[39] B.S. Everitt, The Cambridge Dictionary of Statistics, Cambridge University Press, 2003.
[40] M. Gilli, D. Maringe, E. Schumann, Numerical Methods and Optimization in Finance, Academic Press, 2011.
[41] M.H. Kalos, P. a. Whitlock, Monte Carlo Methods, 2008th ed., WILEY-VCH, 2008 http://dx.doi.org/10.1002/9783527626212.
[42] L. Mendo, J.M. Hernando, A simple sequential stopping rule for Monte Carlo simulation, IEEE Trans. Commun. 54 (2006) 231–241.
[43] J.-C. Chen, D. Lu, J.S. Sadowsky, K. Yao, On importance sampling in digital communications. I. Fundamentals, IEEE J. Sel. Areas Commun. 11 (1993), http://dx.doi.org/10.1109/49.219542.
[44] O. Skarstein, K. Uhlen, Design considerations with respect to long-term diesel saving in wind/diesel plants, Wind Eng. 13 (1989) 72–87.
[45] J. Bleijs, C. Nightingale, D. Infield, Wear implications of intermittent diesel operation in wind/diesel systems, Wind Energy 17 (1993) 206–218.
[46] International Electrotechnical Commission, IEC 60896-1:1987 Stationary Lead-acid Batteries. General Requirements and Methods of Test. Vented Types, 1987.
[47] Prices of petroleum products: Spain, (2015). http://www.datosmacro.com/energia/precios-gasolina-diesel-calefaccion/espana.
[48] Meteorology and climatology of Navarra. Government of Navarra, Spain, (n.d.). http://meteo.navarra.es/estaciones/mapadeestaciones.cfm.
[49] Spanish Ministry of Industry, Energy and Tourism. Evolution of diesel price in Spain during the last half century ("Ministerio de Industria Energía y Turismo de España. Evolución del precio del gasóleo España durante el último medio siglo"), 2011. http://www.minetur.gob.es/Publicaciones/Publicacionesperiodicas/EconomiaIndustrial/RevistaEconomiaIndustrial/387/NOTAS.pdf.

3. MEMORIA

3.1 OBJETIVOS DE LA INVESTIGACIÓN

Los objetivos del presente trabajo de investigación han sido:

1. Analizar los modelos existentes de los distintos componentes de los sistemas híbridos aislados con alimentación renovable (energía solar y energía eólica) y generación convencional (generadores diésel) y con almacenamiento de baterías tipo plomo-ácido.
2. Analizar las distintas estrategias de control que se utilizan en la optimización de los sistemas híbridos aislados con alimentación renovable (energía solar y energía eólica) y generación convencional (generadores diésel) y con almacenamiento de baterías tipo plomo-ácido.
3. Analizar las distintas técnicas determinísticas, heurísticas y probabilísticas utilizadas para la simulación y optimización de sistemas híbridos aislados con alimentación renovable (energía solar y energía eólica) y generación convencional (generadores diésel) y con almacenamiento de baterías tipo plomo-ácido.
4. Analizar la influencia del modelo de batería tipo plomo-ácido utilizado en la optimización de sistemas híbridos aislados con alimentación renovable.
5. Diseñar un nuevo modelo para optimizar sistemas híbridos aislados temporales con alimentación renovable, durante el periodo específico en el que estará instalado el sistema, optimizando el peso y/o el coste de la instalación temporal.
6. Diseñar un nuevo método para optimizar sistemas híbridos aislados con alimentación renovable, minimizando el coste actual neto y maximizando el índice de desarrollo humano y la creación de empleo.
7. Diseñar una nueva metodología estocástica-heurística para optimizar sistemas híbridos aislados con alimentación renovable.

3.2 METODOLOGÍA UTILIZADA

La metodología empleada para alcanzar los objetivos propuestos en este trabajo de investigación, ha sido:

1. Revisión bibliográfica de los diferentes modelos matemáticos existentes de paneles fotovoltaicos, aerogeneradores, generadores diésel, banco de baterías de plomo ácido, inversores, cargadores y controladores de carga.
2. Revisión bibliográfica de las distintas estrategias de control para la simulación y optimización de sistemas híbridos aislados con alimentación renovable.
3. Revisión bibliográfica de las distintas técnicas determinísticas, heurísticas y probabilísticas para la simulación y optimización de sistemas híbridos aislados con alimentación renovable.
4. Diseño de la estrategia e implementación del modelo del *Criterio ponderado del flujo de Ah* para analizar la influencia del modelo de batería en la optimización de sistemas híbridos aislados con alimentación renovable. Simulación de distintos casos empleando distintos modelos para poder comparar los resultados obtenidos.
5. Revisión bibliográfica de costos (incluido el transporte) y pesos de los componentes de los sistemas híbridos. Diseño e implementación del nuevo modelo para optimizar en peso y/o coste del sistema híbrido aislado temporal con alimentación renovable. Aplicación a un caso concreto.
6. Revisión bibliográfica en referencia al HDI y al JC de los componentes de los sistemas híbridos. Diseño e implementación del nuevo modelo para minimizar el coste actual neto y maximizar el índice de desarrollo humano y la creación de empleo del sistema híbrido aislado con alimentación renovable. Aplicación a un caso concreto.
7. Diseño e implementación de una nueva metodología estocástica-heurística para optimizar sistemas híbridos aislados con alimentación renovable. Aplicación a un caso concreto.

3.3 REVISIÓN BIBLIOGRÁFICA

3.3.1 *Influence of the battery model in the optimisation of stand-alone renewable systems*.

Los mecanismos de envejecimiento de las baterías plomo-ácido han sido estudiados previamente, y se han planteado distintos modelos para el cálculo de su vida útil [6,18-21].

Se han publicado numerosos estudios sobre la simulación y optimización de sistemas autónomos renovables, incluidas las baterías. Sin embargo, la duración de las baterías muchas veces se estima sobre la base de la experiencia del investigador [22-26], o mediante el cálculo de los ciclos completos equivalentes hasta el fallo [4,27,28], o en el mejor de los casos, utilizando el conteo de ciclos Rainflow [29-31]. Además, muchas herramientas de simulación y optimización utilizan estas metodologías para estimar la duración de las baterías [5,32-34].

Wenzl et al. [35] describieron un procedimiento para la predicción de la vida útil que incluía las relaciones entre los factores de stress y la vida útil. Cherif et al. [19] propusieron un modelo para el cálculo para sistemas fotovoltaicos aislados basado en el modelo inicial de Shepherd [36].

En 2008, Sauer y Wenzl [21] compararon distintos enfoques para la predicción de la vida útil de las baterías de plomo-ácido. Los modelos comparados fueron: (i) el modelo de envejecimiento físico-químico, que tiene alta precisión pero también alta complejidad y alta dificultad para obtener los parámetros del modelo, por tanto baja velocidad de cálculo; (ii) el modelo de envejecimiento basado en el criterio ponderado del flujo de Ah, propuesto por Schiffer et al. [20], que tiene precisión media, complejidad media y velocidad de cálculo media. Y los modelos de envejecimiento orientados a eventos (iii) que tienen baja precisión, baja complejidad y alta velocidad de cálculo.

3.3.2. *Optimisation of photovoltaic–diesel–battery stand-alone systems minimising system weight*.

Para la realización de este artículo, además de la revisión bibliográfica de los artículos de investigación relacionados con el mismo, se hizo una amplia revisión del coste y peso de los distintos: paneles fotovoltaicos, modelos de baterías, generadores diésel e inversores/cargadores presentes en el mercado.

El coste del transporte en camión (en € por tonelada y km) es diferente en cada país, y depende principalmente del tipo de carretera y del precio del combustible. En Europa, Bina et al. [37] informaron de costes entre 0,059 y 0,094 €/(t·km). En [38] se muestra una visión general de las estadísticas relacionadas con el transporte en la Unión Europea. En los Estados Unidos de América, se presentan valores alrededor de 0,1 €/(t·km), que se muestran en [39]. En África, se informan valores de 0,036 (Kenia) a 0,109 €/(t·km) (República del Congo) para corredores internacionales [40]. El transporte en las carreteras nacionales suele ser más caro; por ejemplo, en Etiopía, Rancourt et al. [41] informaron de una media de 0,109 €/(t·km), mientras que los corredores internacionales presentan una media de 0,089 €/(t·km). El transporte por avión es mucho más caro: en Estados Unidos se informa de un valor de alrededor de 0,65 €/(t·km) [39]. En el transporte en helicóptero se pueden observar valores superiores a 2 €/(t·km). En áreas peligrosas, el coste del transporte puede ser mucho mayor.

Algunos estudios previos muestran los problemas relacionados con las energías renovables y la electrificación rural en algunas regiones. Ahlborg y Hammar [42] muestran los puntos a favor y en contra de la electrificación rural mediante energías renovables en Tanzania y Mozambique. Borhanazad et al. [43] estudian la aplicación de fuentes renovables para la electrificación rural en las zonas más pobres de Malasia. Adaramola et al. [44] presentan un análisis económico de un sistema híbrido fotovoltaico-eólico-diésel para su aplicación en zonas remotas del sur de Ghana. Ismail et al. [45] muestran un análisis tecno-económico de un sistema híbrido formado por paneles fotovoltaicos y un micro-aerogenerador para una comunidad remota ubicada en Palestina; los mismos autores presentan un análisis similar de un sistema fotovoltaico-diésel para

suministrar a una pequeña comunidad en Malasia [46]. Kumar y Manoharan [47] analizan la viabilidad económica de sistemas híbridos fotovoltaico-diésel en diferentes áreas de Tamil Nadu (India) con conexión de red inestable.

Estudios previos muestran también aplicaciones específicas de sistemas renovables aislados. Por ejemplo, Campana et al. [48] muestran la optimización económica de sistemas fotovoltaicos para el bombeo de agua para el riego. Edwin y Sekhar estudian el uso de biomasa y biogás para el enfriamiento y la preservación de leche en la India [49]. En un trabajo reciente Dufo-López et al. [50] presentan la optimización estocástica de un sistema fotovoltaico-diésel para abastecer a un hospital (aislado de la red) ubicado en la República Democrática del Congo.

Existen muchos trabajos anteriores que muestran la optimización de sistemas híbridos aislados (fotovoltaicos y/o aerogeneradores y/o hidroeléctricos y/o diésel, normalmente usando baterías como sistema de almacenamiento) minimizando el coste actual neto del sistema (incluyendo todos los costes a lo largo de la vida del sistema) o el coste normalizado de la energía. Akikur et al. [51] presentan una revisión de sistemas fotovoltaicos y sistemas híbridos fotovoltaicos utilizados para electrificar ubicaciones aisladas de la red eléctrica. Mohammed et al. [52] muestran una revisión de los beneficios de los sistemas híbridos (considerando energía solar fotovoltaica, eólica, hidroeléctrica y biomasa), incluyendo los factores a considerar para su diseño e implementación. Bajpai y Dash [53] muestran una revisión sobre el dimensionamiento, optimización, gestión y modelado de los componentes de los sistemas híbridos. Bernal-Agustín y Dufo-López [5] presentan una revisión de los trabajos previos más relevantes de simulación y optimización de sistemas autónomos híbridos con energías renovables, incluyendo una revisión de las herramientas de software. Sinha y Chandel también muestran una revisión de las herramientas de software más relevantes para la simulación y/o optimización de sistemas renovables híbridos [54].

En algunos casos, si el número de combinaciones posibles del sistema híbrido renovable implica un tiempo de cálculo inaceptable, algunos autores aplican

técnicas heurísticas, como algoritmos genéticos (*Genetic Algorithms*, GA) [55] en la optimización. Por ejemplo, en [4] se aplican algoritmos genéticos en la optimización de sistemas fotovoltaicos-diésel-baterías mientras que en [56] se optimiza un sistema fotovoltaico-micro-aerogenerador-baterías mediante GA. La mayoría de las obras consideran sólo una variable a ser optimizada (el costo del sistema). Sin embargo, en algunos casos, las emisiones de CO_2 y/o la carga no satisfecha, o la probabilidad de pérdida de potencia, son también variables que se utilizan en la optimización, aplicando algoritmos evolutivos multiobjetivo [57]. Fadaee y Radzi [34] muestran una revisión de los trabajos más importantes relacionados con la optimización de sistemas autónomos híbridos renovables utilizando algoritmos evolutivos multiobjetivo.

El diseño y desarrollo de la alimentación eléctrica de una clínica médica móvil mediante un sistema renovable híbrido en la República Dominicana se muestra en [58], compuesto por paneles fotovoltaicos, aerogeneradores, banco de baterías y un generador diésel. Los autores muestran el funcionamiento de un día completo; sin embargo, no se realiza ninguna optimización.

3.3.3. *Optimisation of PV-wind-diesel-battery stand-alone systems to minimise cost and maximise human development index and job creation*.

Estudios previos muestran las ventajas e inconvenientes de la electrificación rural mediante sistemas de energías renovables sin conexión a la red eléctrica [42-47]. Otros trabajos muestran la optimización de sistemas híbridos aislados minimizando el coste actual neto del sistema o el coste normalizado de la energía [5,51-54,59,60]. En algunos trabajos anteriores, los autores aplican técnicas heurísticas como algoritmos genéticos [55,61] con el fin de reducir el tiempo de cálculo de la optimización. La mayoría de estos estudios sólo optimizan el costo (costo actual neto del sistema y/o el costo normalizado de la energía), pero algunos trabajos previos también consideran otros objetivos, como la minimización de las emisiones de CO_2 y/o cargas no satisfechas, aplicando una optimización de Pareto mediante algoritmos evolutivos multiobjetivo [30,34,57,62-65].

Rojas-Zerpa y Yusta [66,67] propusieron una aplicación combinada de dos métodos de decisión multicriterio (*Analytical Hierarchy Process* y *Compromise Ranking method*) para facilitar la selección de la mejor solución para el suministro eléctrico de zonas rurales remotas, considerando criterios técnicos, económicos, medioambientales y sociales (incluyendo el *índice de desarrollo humano* y la *creación* de *empleo*). Su trabajo utiliza pesos para cada criterio, que se seleccionan sobre la base de las opiniones de los expertos, y utiliza métodos multicriterio, no metodologías de optimización multiobjetivo.

Salas et al. [68] estudiaban las posibles configuraciones de sistemas fotovoltaicos-diésel-baterías para alimentar a sistemas con cargas AC aislados de la red eléctrica.

Las Naciones Unidas [8] clasifican a los países con un índice de desarrollo humano bajo, medio, alto o muy alto. Este índice depende del uso *per cápita* de la electricidad con una dependencia logarítmica introducida por Pasternak [69] con datos de 60 países obtenidos del *United Nations Human Development Report* 1999 [70]. Posteriormente Rojas-Zerpa [17] mostró también una dependencia logarítmica (con diferentes parámetros de ajuste) con datos de 128 países [71].

3.3.4. *Stochastic-heuristic methodology for the optimisation of components and control variables of PV-wind-diesel-battery stand-alone systems.*

Muchos estudios previos han examinado el rendimiento y la optimización del suministro eléctrico de sistemas autónomos, generalmente integrando paneles fotovoltaicos y/o aerogeneradores y/o generadores diésel con almacenamiento mediante bancos de baterías. Las revisiones de trabajos relevantes relacionados con sistemas híbridos autónomos se pueden encontrar en las referencias [52,53,60]. Un estudio comparativo de sistemas de energía solar híbridos autónomos se muestra en [51]. Las revisiones más relevantes de las herramientas de software utilizadas para la optimización de sistemas híbridos se muestran en [5,54]. La optimización de los sistemas fotovoltaicos-aerogeneradores se discute en [72], mientras que una revisión de los artículos más relevantes en la

optimización de los sistemas autónomos se muestra en [73].Un nuevo método de optimización para los sistemas fotovoltaicos aislados se ha mostrado recientemente en [74]. En la referencia [75] se muestra la optimización energética y económica de un sistema fotovoltaico (con almacenamiento mediante baterías). Una metodología basada en el costo normalizado de la energía suministrada y perdida para el diseño de sistemas autónomos se muestra en [76]. Trabajos anteriores relacionados con las estrategias de control de los sistemas autónomos híbridos se pueden encontrar en [4,77,78].

En algunos casos el sistema autónomo no incluye el almacenamiento mediante baterías [79], pero el almacenamiento es necesario (y rentable) en la mayoría de las aplicaciones que se encuentran aisladas de la red. En la mayoría de los trabajos anteriores, la optimización intenta obtener la combinación de componentes (y/o, en algunos casos, de estrategias de control), lo que minimiza el coste actual neto del sistema (NPC), el coste normalizado de la energía (LCE, calculado como NPC dividido por el total de energía consumida por la carga durante la vida útil del sistema) o el coste de operación de un intervalo corto. Algunos de estos trabajos utilizan técnicas heurísticas, como algoritmos genéticos [55,61] en la optimización. Una aplicación reciente de algoritmos genéticos en la optimización de sistemas autónomos híbridos se muestra en [80]. En [81] un algoritmo meta-heurístico (Cuckoo Search) se aplica en la optimización de sistemas autónomos híbridos. Otros trabajos consideran que se deben minimizar varias variables, generalmente LCE, emisiones de CO_2 y la carga no satisfecha o la probabilidad de pérdida de potencia, la mayoría utilizando algoritmos evolutivos multiobjetivo (*Multi Objective Evolutionary Algorithms*, MOEA) [34,57,62] para obtener el conjunto óptimo de Pareto.

La optimización en los estudios previos se llevó a cabo habitualmente utilizando un enfoque determinístico, aunque algunos utilizaron un enfoque estocástico, teniendo en cuenta las incertidumbres de las fuentes renovables.

En [82], Paliwal et al. muestran un modelo probabilístico para los sistemas de almacenamiento mediante baterías para facilitar la evaluación de la fiabilidad de los sistemas autónomos renovables. Los autores comparan mediante

simulaciones de Monte Carlo (*Monte Carlo Simulation*, MCS), obteniendo mejores resultados con su modelo probabilístico. Sin embargo, en este trabajo no se obtiene la estimación de la vida útil de las baterías y no se realiza ninguna optimización.

Arun et al. [83] optimizaron un sistema fotovoltaico con baterías utilizando MCS, incluyendo la incertidumbre de la irradiación solar. Kamjoo et al. [84] mostraron un método basado en *Chance-Constrained Programming* (CCP) para la optimización de un sistema fotovoltaico-aerogeneradores-baterías, incluyendo las incertidumbres de la velocidad del viento y de la irradiación. En [85], Kamjoo et al. utilizan algoritmos genéticos en la optimización multiobjetivo de sistemas fotovoltaicos-aerogeneradores-baterías, considerando incertidumbres por medio del CCP y comparando los resultados con MCS. Maheri [86] evalúa la fiabilidad de diferentes sistemas fotovoltaicos-aerogeneradores-diésel-baterías obtenidos mediante un diseño determinista, y posteriormente [87], utiliza dos algoritmos (con MCS) en la optimización del margen de seguridad.

Recientemente, Alharbi y Raahemifar [88] presentaron un modelo estocástico para la coordinación de recursos energéticos distribuidos en una microred aislada considerando las incertidumbres de la carga, el viento y la irradiación. Chang y Lin [89] también consideraron las incertidumbres de la carga, el viento y la irradiación y propusieron el diseño óptimo de sistemas híbridos de energía renovable usando MCS con técnicas de optimización de la simulación (*stochastic trust-region response-surface method*). El efecto de las incertidumbres en los resultados económicos de generadores (alimentados por energías renovables) conectados a la red se ha estudiado en [90] donde Falconett y Nagasaka muestran un modelo probabilístico para evaluar los efectos de diferentes mecanismos de apoyo (subvención gubernamental, *Feed-In Tariff* y certificados de energía renovable) sobre el valor actual neto de pequeñas centrales hidroeléctricas, parques eólicos y parques fotovoltaicos. Tina y Gagliano [91] estudiaron el impacto del sistema de seguimiento en la función de densidad de probabilidad (Probability Density Function, PDF) de la potencia producida por el sistema fotovoltaico mientras Pereira et al. [92] utilizaron MCS en el análisis de riesgo en pequeños sistemas renovables.

En todos los estudios anteriores, los modelos utilizados para el cálculo de la vida útil de las baterías eran modelos clásicos simples. La utilización de modelos simples para las baterías puede implicar una estimación demasiado optimista de la vida útil de las mismas (varias veces la vida real [7]) y, por tanto, resultados erróneos para el NPC y el LCE, dado que el coste total del banco de baterías (coste de adquisición más coste de mantenimiento más coste de reposición al final de su vida útil) es generalmente el coste más alto del sistema [93].

3.4 METODOLOGÍA EMPLEADA EN CADA ARTÍCULO

3.4.1 *Influence of the battery model in the optimisation of stand-alone renewable systems*.

En este artículo se aplica el modelo para el banco de baterías *Criterio ponderado del flujo de Ah*, propuesto por Schiffer et al. [20], y que tiene en consideración las condiciones reales de operación del banco de baterías. El flujo actual de Ah es continuamente multiplicado por un factor de peso que representa las condiciones reales de funcionamiento.

Se toma en consideración la influencia del estado de carga, el tiempo que las baterías están en un bajo estado de carga, el tiempo desde la última carga completa, la corriente, la estratificación del ácido, la tensión de las celdas, la temperatura y otros factores. Además, mediante el uso de este modelo, se puede aplicar el efecto de los distintos límites de tensión de corte en el controlador de carga las baterías [7], cuestión que con otros modelos no es posible.

Es un modelo complejo que utiliza muchas ecuaciones, cuya información detallada se puede consultar en [20] y [7]. En [7] se demostró que este modelo es mucho más preciso y que predice la vida útil de las baterías mucho mejor que otros modelos. Los modelos clásicos (Ciclos completos equivalentes hasta el fallo y Conteo de ciclos Rainflow) no estiman correctamente el envejecimiento de las baterías; en muchos casos, el tiempo de vida previsto es dos o tres veces mayor que el tiempo de vida obtenido en sistemas reales. Sin embargo, usando el *Criterio ponderado del flujo de Ah* las predicciones son muy similares a los resultados obtenidos en sistemas reales.

En este modelo, la potencia de entrada del banco de baterías P_{bat} (t) (es mayor que cero si las baterías se están cargando y menor que cero si las baterías se están descargando) depende de la potencia de salida de las fuentes renovables, de la carga, de la estrategia de control, de la potencia de salida del generador diésel y del *SOC* del banco de baterías. El *SOC* (por unidad de la capacidad nominal) se calcula sumando la carga efectiva que entra en la batería al *SOC* de

la hora anterior. Para ello, se tiene en cuenta la capacidad nominal, la corriente de entrada a la batería y la corriente de gasificación (que será cero durante la descarga) en ese instante de tiempo.

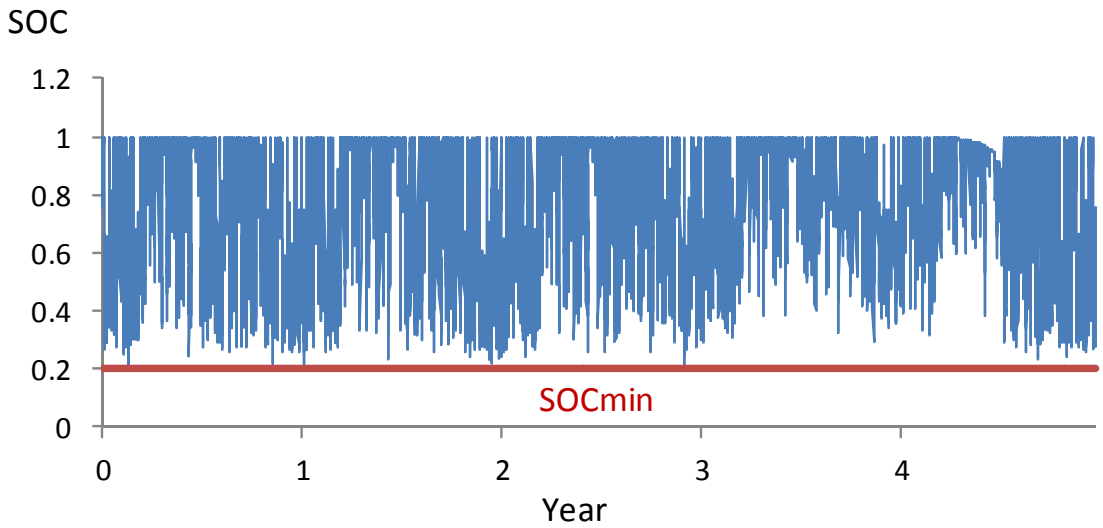

Figura 3. Ejemplo del estado de carga (*SOC*) durante una simulación.

La tensión de las baterías se calcula mediante las ecuaciones modificadas de Sheperd [20]. Esta tensión depende de la tensión en equilibrio de la celda a circuito abierto cuando está plenamente cargada, de una constante de proporcionalidad del electrolito, de la profundidad de descarga, de unas resistencias internas agregadas durante la carga o la descarga, de la capacidad de la batería a 10 horas y de la capacidad normalizada de la batería durante la carga y la descarga.

La eficiencia de la batería está implícitamente considerada, ya que la corriente de gasificación afecta al *SOC* durante la carga. También está implícitamente considerada en la tensión de la batería. Durante la carga, la tensión de la batería aumenta su valor, pero la potencia requerida para ello debe ser mayor, ya que no toda la potencia es convertida en energía almacenada. Durante la descarga, la tensión de la batería disminuye, pero la potencia suministrada por el banco de baterías es menor, ya que no toda la potencia extraída de las baterías se convierte en energía que se suministra a la carga.

El modelo calcula la pérdida de capacidad por corrosión y por degradación. Cada hora la capacidad remanente de la batería se calcula como la capacidad inicial normalizada de la batería menos la capacidad perdida por corrosión y por degradación. Cuando la capacidad remanente sea el 80% de la capacidad nominal de la batería, se considera que ha finalizado su vida útil.

En el cálculo de la pérdida de capacidad por degradación, que tiene en cuenta básicamente la manera en la que la energía es ciclada, se tiene en cuenta el número ponderado de ciclos y el número de ciclos según las normas IEC. Para calcular el número ponderado de ciclos se tiene en cuenta la corriente de descarga de la batería, el estado de carga, la corriente, el impacto de la estratificación del ácido en la degradación de la masa activa, el tiempo desde la última carga completa, el estado de carga mínimo desde la última carga completa y el número de malas cargas (cargas incompletas). Este tipo de cargas tiene lugar cuando la carga finaliza entre un 0,9 y un 0,9998 del *SOC*.

La pérdida de capacidad por corrosión se modela utilizando el concepto de una capa de corrosión, que crece durante la vida útil de la batería. El espesor efectivo de la capa de corrosión se calcula durante cada hora dependiendo de la tensión de corrosión del electrodo positivo y de la temperatura [20]. La pérdida de capacidad por corrosión es proporcional al espesor de capa efectivo en cada instante

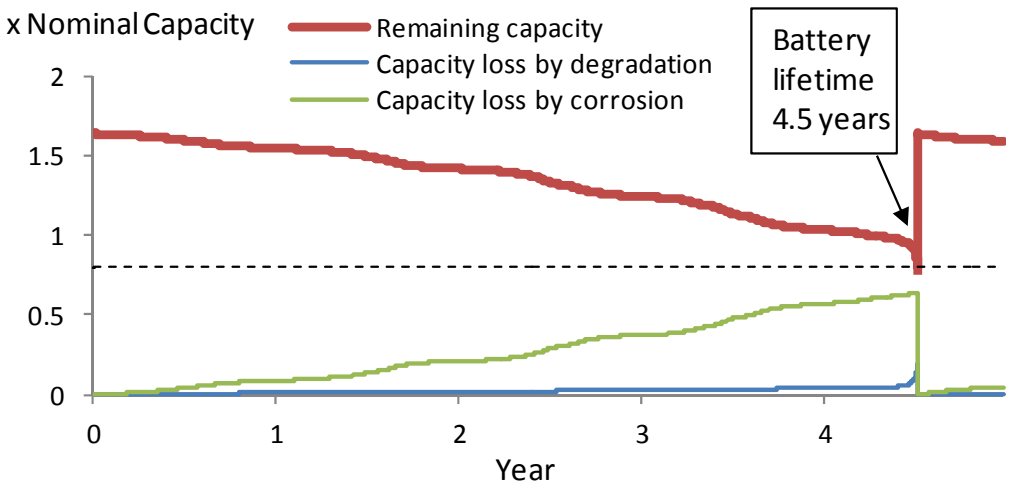

Figura 4. Ejemplo de la pérdida de capacidad por degradación y corrosión de las baterías durante una simulación.

También se ha modelado un inversor/cargador, que se podría denominar convertidor bidireccional. Es un controlador PWM (modulación de la anchura de pulso) con un proceso de carga en tres etapas (carga, absorción y flotación) con control del estado de carga mediante una compleja estrategia de control. El inversor/cargador incluye un inversor de salida (DC/AC) para alimentar a la carga AC desde el bus de DC. También incluye un rectificador (AC/DC), que en realidad es el cargador de las baterías, de tal manera que desde las fuentes de AC se puede cargar el banco de baterías. La potencia de entrada al banco de baterías, estará afectada, al igual que ocurre en la realidad, por la eficiencia del cargador, que a su vez depende de la potencia de salida.

La unidad de control está normalmente incluida en el inversor/cargador. El inversor/cargador realiza una gestión completa aislado de la red. Controla la carga y la descarga, calculando el *SOC* del banco de baterías. Cuando el *SOC* es inferior a un límite especificado, conecta el generador diésel. La potencia de salida del generador diésel puede ser controlada por el inversor/cargador y también el límite del *SOC* para detenerlo. Muchos inversores/cargadores incluyen un MPPT (sistema de seguimiento de punto de máxima potencia) para obtener la máxima potencia de los paneles fotovoltaicos.

Los paneles fotovoltaicos generan electricidad en corriente continua, por lo que el bus fotovoltaico está en DC, utilizando en este caso un inversor/cargador acoplado a DC. Si se quisiera utilizar un inversor/cargador acoplado en AC, el generador fotovoltaico debería incluir un inversor, de tal manera que su salida fuera al bus de AC. Se puede aplicar lo mismo para los aerogeneradores. La potencia de salida es normalmente en DC para los de poca potencia y AC para los de mayor potencia. Existen diferentes inversores/cargadores comerciales que permiten distinto tipo de tensión en el bus (acoplamiento DC o AC) para los paneles fotovoltaicos y para los aerogeneradores.

De las ocho variables utilizadas para diseñar la estrategia de control del sistema, cuatro se utilizan para modelar el inversor/cargador PWM que controla el estado de carga (*SOC*) de las baterías [7]. Las etapas de carga utilizadas por la mayoría de los cargadores PWM han sido incluidas en la simulación. La carga se

lleva a cabo en tres etapas: carga, absorción y flotación (también se realiza una etapa de ecualización bajo ciertas condiciones). Durante la fase de carga, la batería se carga a la máxima corriente. Más tarde, cuando la batería alcanza la tensión de absorción, la corriente de carga va disminuyendo, manteniéndose ese valor de tensión constante. Entonces, cuando la corriente de carga cae a un cierto nivel, o ha pasado un tiempo especificado en la etapa absorción, el tensión se fija en un valor menor, la tensión de flotación. Este tipo de controladores sobrecargan las baterías a intervalos regulares de tiempo (ecualización), aplicando una tensión de ecualización durante un tiempo especificado.

El control del proceso de descarga se realiza mediante el control de la tensión: cuando se alcanza la tensión de desconexión, la carga se desconecta de la batería (evitando la sobre-descarga). Una vez que la batería se recarga y alcanza la tensión de re-conexión, la carga se vuelve a conectar. Algunos controladores PWM modernos incluyen algoritmos para calcular el *SOC* real de la batería, de tal manera que la batería pueda ser protegida óptimamente. Lo hacen mediante puntos de ajuste del *SOC*. Estos valores pueden ser optimizados (dependiendo de las condiciones de operación) ya que los valores óptimos de estos puntos de ajuste pueden ser diferentes de los valores por defecto ajustados en el controlador.

Estos valores son:

- $SOC_{min\_disconnect}$: Es el mínimo estado de carga de la batería. Cuando la batería se está descargando y alcanza este valor, la carga se desconecta de la batería, evitando la sobre-descarga.
- $SOC_{min\_reconnect}$: Después de desconectar la carga de la batería, si la batería se recarga, la carga se re-conecta cuando se alcanza este *SOC*.
- SOC_{boost}: Si la batería ha caído, desde la última plena carga, por debajo este estado de carga, la próxima carga incluirá una etapa de absorción. De lo contrario, no se realizará esta etapa.
- SOC_{equal}: Si la batería ha caído, desde la última plena carga, por debajo este estado de carga, se realizará una etapa de ecualización según esté programada. De lo contrario, no se realizará esta etapa.

3.4.2. *Optimisation of photovoltaic–diesel–battery stand-alone systems minimising system weight*.

En este trabajo se optimizan por primera vez sistemas híbridos aislados con alimentación renovable (fotovoltaica y/o diésel, con o sin acumulación de baterías) para suministrar la carga eléctrica durante un periodo de tiempo específico, es decir, se tratará de una instalación temporal.

Por tanto, cada combinación de componentes y estrategias de control deben ser simuladas y optimizadas para el periodo de tiempo en el que esa instalación temporal va a estar en funcionamiento, con el fin de conocer su rendimiento. Después de la simulación, se puede saber si esa combinación puede suministrar toda la carga, y también se conocerá el combustible consumido y otras variables como el número de horas de funcionamiento del generador diésel, le energía ciclada por las baterías, la pérdida de capacidad de las mismas, etc. Con estos resultados, es posible calcular el peso del sistema (componentes + combustible) y el coste del sistema (combustible + operación y mantenimiento + envejecimiento de los componentes).

La simulación del sistema se realiza en pasos de hora a hora, desde la primera hora (t = 0) hasta la última hora ($t = 24 \cdot N_{days}$), donde N_{days} es el número de días que la instalación temporal está trabajando en el lugar que ha sido instalada.

Sin entrar a describir aquí los modelos matemáticos mediante los que modela el sistema, las pautas básicas que debe cumplir el balance de energía del sistema son:

- Si la potencia de salida de los paneles fotovoltaicos es superior a la demandada por la carga, la diferencia se utilizará para cargar las baterías.

- Si la potencia de salida de los paneles fotovoltaicos no es suficiente para cubrir la demandada por la carga, el banco de baterías y/o el generador diésel deben suministrar el resto. Como se gestiona ese caso depende del estado de carga

(SOC) del banco de baterías y de la estrategia de control (comentada más adelante).

Se pueden considerar muchas combinaciones de componentes y estrategias de control. Si el número de posibles combinaciones de componentes y estrategias de control es demasiado alto, implicaría un tiempo de computación inadmisible. Por tanto, se utilizan algoritmos genéticos para realizar la optimización cuando se tiene un solo objetivo (es decir, minimizar por ejemplo o el peso o el coste). Se utilizan dos algoritmos genéticos: el algoritmo principal se utiliza para la optimización de los componentes y el segundo algoritmo para la optimización de la estrategia de control (para cada combinación de componentes).

El algoritmo principal utiliza un vector de enteros con el código del tipo de panel fotovoltaico (a), el número de paneles fotovoltaicos en paralelo (b), el código del tipo de batería (c), el número de baterías en paralelo (d), el código del tipo de generador diésel (e), y el código del tipo de inversor/cargador (f):

$$\{ a \mid b \mid c \mid d \mid e \mid f \}$$

El segundo algoritmo utiliza también un vector de enteros, con cuatro variables relativas a la estrategia de control:

$$\{ \textit{Estrategia} \mid P_{min\_gen} \mid SOC_{min\_disconnect} \mid P_{stp\_gen} \}$$

Estrategia: Esta variable tiene seis valores posibles, ya que existen tres estrategias generales de control que pueden aplicarse [4] y para cada estrategia existen dos posibilidades de prioridad en el suministro de la carga que no puede ser cubierta por los paneles fotovoltaicos, que son, prioridad del banco de baterías o prioridad del generador diésel. Las tres estrategias generales de control son:

- Estrategia *seguimiento de la carga*: cuando el generador diésel debe funcionar, solamente trabaja para satisfacer la demanda de la carga; no trabaja para cargar las baterías (a menos que su potencia de salida mínima sea más alta que la potencia requerida por la carga).

• Estrategia *ciclo de carga*: cuando el generador diésel debe funcionar, trabajará a su potencia nominal, no sólo para satisfacer la demanda, sino también para cargar las baterías, sólo durante esa hora (unidad mínima de tiempo).

• Estrategia *ciclo de carga hasta el punto de ajuste*: cuando el generador diésel debe funcionar, trabajará a su potencia nominal hasta que el banco de baterías alcance un estado específico de carga, SOCstp_gen.

P_{min_gen}: Es la potencia de salida mínima del generador diésel. El consumo específico (l/kWh) para una potencia de salida baja es siempre mayor que para una potencia alta [4], por lo que la P_{min_gen} óptima podría ser mayor al valor recomendado por el fabricante. Esta variable puede variar desde el valor recomendado por el fabricante hasta la potencia nominal, en un número específico de pasos.

$SOC_{min\_disconnect}$: SOC mínimo de la batería. Cuando la batería se está descargando y alcanza este valor, la carga se desconecta de la batería, evitando una descarga excesiva. Puede variar desde el valor recomendado por el fabricante hasta el 80%, en un número determinado de pasos.

P_{stp_gen}: Cuando se selecciona la estrategia ciclo de carga hasta el punto de ajuste, el generador diésel funciona a potencia nominal, cargando el banco de baterías hasta que se alcanza este punto de SOC. Puede variar desde $SOC_{min\_disconnect}$ hasta el 100%, en un número específico de pasos.

Para cada combinación de componentes *i* que es evaluada por el algoritmo genético principal, se utiliza el denominado algoritmo genético secundario para obtener la estrategia de control óptima *k* y minimizar la variable objetivo (peso total o coste total). El algoritmo principal se utiliza para obtener la combinación óptima de los componentes i (con la combinación óptima de variables de control obtenidas por el algoritmo secundario), lo que minimiza la variable objetivo (peso total o coste total).

Para cada uno de los algoritmos, se obtiene aleatoriamente una población inicial de *N* vectores o individuos (primera generación). Cada vector del algoritmo secundario se evalúa mediante una simulación horaria del sistema durante el periodo de tiempo en el que la instalación está funcionando (un número de días N_{days}). Al final de la simulación de cada individuo (combinación de componentes y estrategia de control), si la carga insatisfecha es superior a un valor específico (por ejemplo, 0,01%), ese individuo se descarta. El conjunto de vectores se ordena en función del objetivo. El primero (posición 1) es el mejor individuo, mientras que el último (posición *N*) es el peor. A cada uno de los individuos se le asigna una aptitud con la función de aptitud.

Los mejores individuos (mejor aptitud) tendrán una probabilidad mayor de reproducirse, mediante cruce con otros vectores. En cada cruce, se obtienen dos nuevos vectores. Algunos individuos aleatoriamente cambian alguno de sus componentes, por ejemplo, un componente del vector de enteros es seleccionado aleatoriamente y su valor se cambia aleatoriamente (mutación, con el fin de mantener la diversidad de la población) y así evitar mínimos locales y evitar la convergencia prematura. Estos individuos obtenidos mediante reproducción y mutación, reemplazan a los peores individuos de la generación previa, de tal manera que se obtiene la siguiente generación. El proceso continúa hasta que se ha evaluado un número específico de generaciones N_{gen_max}. La mejor solución es la que minimiza el objetivo elegido.

Se han considerado dos tipos de optimización mono-objetivo: minimización del peso total y minimización del coste total.

- *Minimización del peso total*

El objetivo en este caso es minimizar el peso total del sistema, W_{TOTAL} (Kg), calculado como el peso total de los componentes desplazados más el combustible diésel utilizado durante el periodo de N_{days} que tiene que ser transportado.
Si el combustible a utilizar (W_{fuel}) fuera inferior a un número mínimo de litros (W_{fuel_min}), valor mínimo decidido por el diseñador que debe ser transportado al principio, la diferencia (W_{fuel_min} - W_{fuel}) deberá ser transportada de regreso a la

sede cuando se desmonte la instalación. Ese valor mínimo de combustible, que debe ser transportado al principio, tiene como objetivo cubrir un porcentaje de la carga total, en el caso de cualquier incidencia en los paneles fotovoltaicos o en el banco de baterías, o en el caso de que la radiación solar sea inferior a la esperada.

El peso por kWh se calculará dividiendo el peso total entre la carga total, L_{TOTAL} (kWh) consumida durante el periodo.

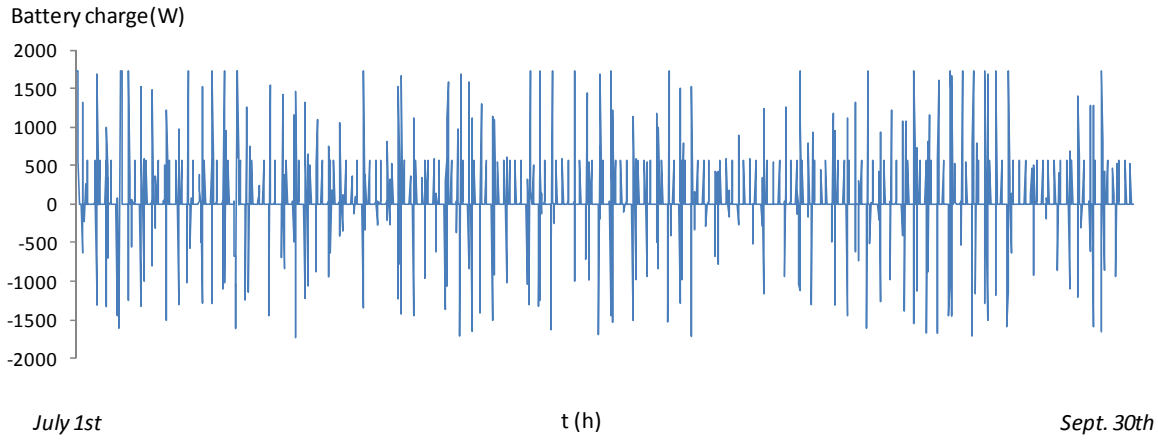

Figura 5. Ejemplo de la carga de las baterías, en una simulación horaria de la configuración óptima, minimización del peso, caso de N_{days} = 90 días.

- *Minimización del coste total*

El objetivo en este caso es minimizar el coste total del sistema C_{total} (€) durante el período considerado (N_{days}), que incluye:

- El coste del combustible diésel durante el periodo considerado.
- El coste de O&M del generador durante el periodo considerado.
- El coste del transporte del peso total.
- El coste de envejecimiento de los paneles fotovoltaicos durante el periodo.
- El coste de envejecimiento de las baterías durante el periodo.
- El coste de envejecimiento del generador diésel durante el periodo.
- El coste de envejecimiento del inversor/cargador durante el periodo.

El coste por kWh se calculará dividiendo el coste total entre la carga total, L_{TOTAL} (kWh) consumida durante el periodo.

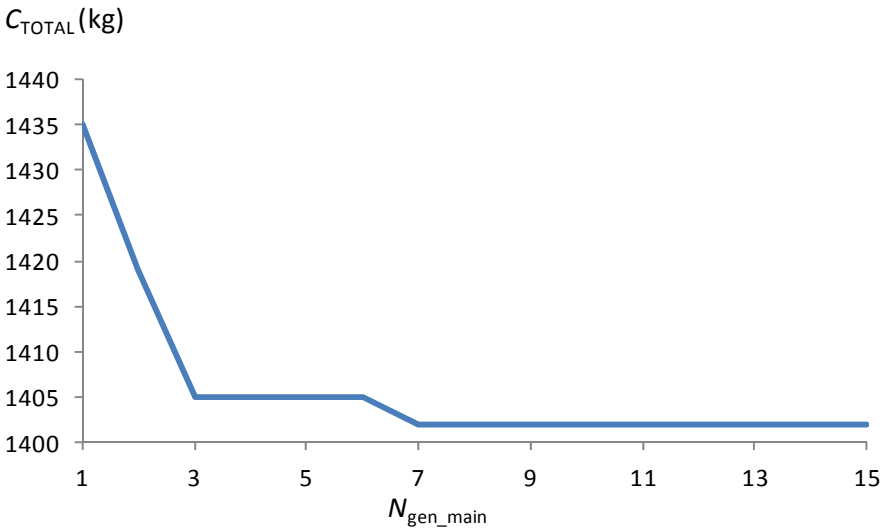

Figura 6. Ejemplo de la evolución del algoritmo principal, minimización del coste total, caso de N_{days} = 30 días.

- *Optimización multiobjetivo*

Cuando los objetivos son dos (minimización del coste total y también minimización del peso total), como algoritmo principal se aplica una optimización de Pareto mediante algoritmos evolutivos multiobjetivo para optimizar los componentes [30,63]. Al final del proceso de optimización, se tendrá un conjunto de soluciones "no dominadas", que constituyen el *Conjunto Óptimo de Pareto* (no hay otros individuos que sean mejores en ambos objetivos).

Como algoritmo secundario se aplica el mismo utilizado en la optimización de un solo objetivo, pero en este caso el objetivo para este algoritmo es minimizar el consumo de combustible (que es la variable que más afecta tanto al coste como al peso).

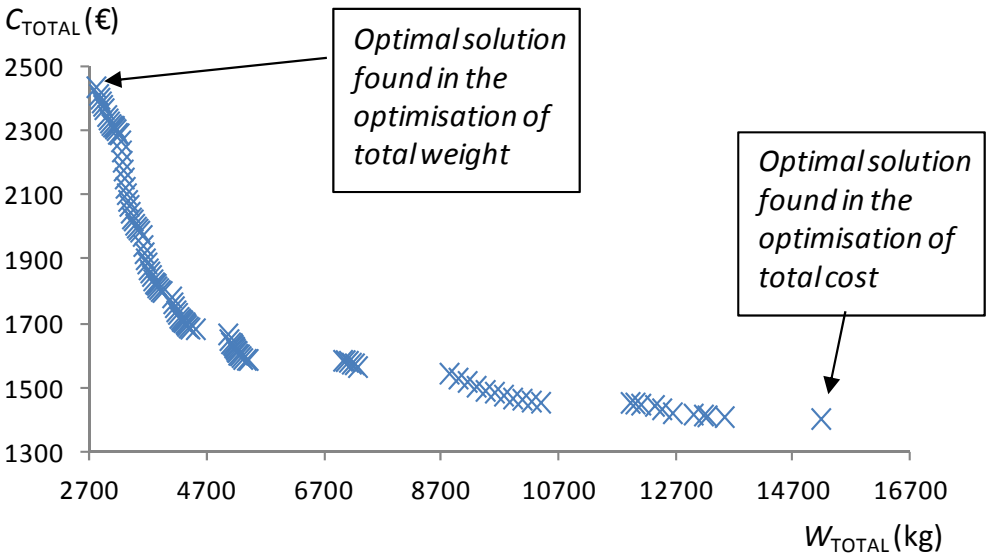

Figura 7. Ejemplo del conjunto óptimo de Pareto de la última generación (decimoquinta), caso de N_{days} = 30 días.

3.4.3. *Optimisation of PV-wind-diesel-battery stand-alone systems to minimise cost and maximise human development index and job creation*.

Al igual que en los trabajos anteriores, evaluar cada combinación de componentes y estrategia de control implica que el comportamiento de esa combinación debe ser simulado en su totalidad. La simulación se realiza en pasos de una hora, durante un número de años n_y (que no se conocen a priori) hasta que la capacidad remanente del banco de baterías cae hasta el 80% de su capacidad nominal (en ese momento se considera que el banco de baterías ha llegado al final de su vida útil y un nuevo banco de baterías reemplazará al antiguo). Se supone que la carga, la irradiación solar y la velocidad del viento mantienen los mismos valores para los diferentes años; es decir, los valores horarios de un año se repiten al año siguiente. Sin embargo, el rendimiento del banco de baterías no será el mismo para los diferentes años, ya que la capacidad remanente del banco de baterías se reduce continuamente. Una vez conocido el comportamiento hora a hora del sistema durante los primeros n_y años, se supone que los siguientes n_y años el sistema se comportará de la misma manera y así sucesivamente hasta que finalice la vida útil del sistema (normalmente 20 ó 25 años).

Después de la simulación, se sabrá si esa combinación de componentes y estrategia de control puede suministrar toda la carga demandada, y también se conocerá la energía cargada y descargada por el banco de baterías a lo largo de los años, la duración de las baterías en años, el número de horas que el generador diésel está trabajando, el consumo anual de combustible, la energía anual suministrada por el generador diésel, el exceso de energía generado por las fuentes renovables, el coste anual de O&M, los costes de sustitución de los componentes durante el período de vida del sistema, etc. Con estos resultados se podrá calcular el coste actual neto (*Net Present Cost*, NPC), el índice de desarrollo humano ((*Human Development Index*, HDI) y la creación de empleo (*Job Creation*, JC).

La simulación del sistema se realiza en pasos de hora a hora, desde la primera hora (t = 0) hasta la última hora (t = 8760 · n_y). Durante cada hora se debe satisfacer el equilibrio de potencia del sistema:

- Si la potencia de salida renovable es superior a la demanda de la carga, la diferencia se utilizará para cargar el banco de baterías. Si todavía hay exceso de energía, puede ser utilizado o almacenado por la carga extra (adicional) de CA (utilizando la energía en nuevos negocios o servicios o almacenándola con su propio banco de baterías).

- Si la potencia de salida renovable no es suficiente para suministrar la demanda de carga, el banco de baterías y/o el generador diésel deben suministrar el resto. Depende del estado de carga (SOC) del banco de baterías y de la estrategia de control que se haga mediante uno u otro.

Al igual que en los trabajos presentados anteriormente, dado que el número de posibles combinaciones de componentes y estrategias de control es demasiado alto, y que la evaluación de todas ellas implicaría un tiempo de computación inadmisible, se han aplicado técnicas heurísticas combinando dos algoritmos:

• El principal es un algoritmo evolutivo multiobjetivo MOEA (por sus siglas en inglés). Es utilizado para la optimización de los componentes (considerando los

tres objetivos: minimización del NPC, maximización del HDI y maximización del JC).

• El secundario es un algoritmo genético utilizado para la optimización de la estrategia de control (para cada combinación de componentes considerada en el algoritmo principal), teniendo en cuenta únicamente la minimización del NPC.

El algoritmo principal (MOEA) considera los tres objetivos y obtiene el conjunto de Pareto de las combinaciones de componentes no dominadas (con la mejor estrategia de control encontrada para cada una por el algoritmo secundario). Al tratarse de una optimización de 3 objetivos, el *conjunto de Pareto* puede ser mostrado en un gráfico en tres dimensiones.

El MOEA (algoritmo principal) implementado en este trabajo utiliza un vector de enteros con el código del tipo de panel fotovoltaico (a), el número de paneles fotovoltaicos en paralelo (b), el código del tipo de aerogenerador (c), el número de aerogeneradores en paralelo (d), el código del tipo de batería (e), el número de baterías en paralelo (f), el código del tipo de generador diésel (g) y el código del tipo de inversor/cargador (h):

$$\{ a \mid b \mid c \mid d \mid e \mid f \mid g \mid h \}$$

En primer lugar, se genera una población aleatoria de N_{MAIN} vectores (también llamados individuos o soluciones, es decir, combinaciones de componentes) (i = 1 ... N_{MAIN}), constituyendo la primera generación (N_{gen_main} = 1). Para cada combinación de componentes i, se utiliza el algoritmo secundario para obtener la estrategia de control óptima k, de manera que el NPC de esa combinación de componentes se minimice. Una vez que se encuentra la mejor estrategia de control para cada combinación de componentes, se clasifican en función del número de soluciones por las que son dominados, considerando los tres objetivos (minimización de NPC, maximización de HDI y maximización de JC). La aptitud de la combinación i del MOEA se asigna (mediante la función de aptitud) en función de su posición dentro de la población, ordenada según se ha comentado. Las

soluciones que están dominadas por el mismo número de soluciones deben tener la misma aptitud, que será la aptitud promedio de estas soluciones.

Si hay un elevado número de soluciones no dominadas (N_{non_dom}) cerca del número total de soluciones N_{MAIN}, esto significa que hay soluciones muy cercanas entre sí en el conjunto de Pareto, lo cual no proporciona variedad. Entonces, para mejorar la evolución del MOEA, algunas de ellas deben ser eliminadas, reduciendo el número de soluciones no dominadas. Existen técnicas relativamente complejas para eliminar las soluciones ineficientes del conjunto de Pareto [94], pero en este trabajo se ha utilizado una técnica de truncamiento simple: si N_{non_dom} es mayor que un valor máximo permitido ($N_{non\_dom\_max}$), se selecciona para ser eliminada la solución que tiene la distancia mínima a otra solución en el conjunto de Pareto no dominado. Las soluciones en los extremos del frente de Pareto nunca serán eliminadas.

Se realiza la selección, el cruce y la mutación de los vectores para obtener una nueva generación de individuos. Los mejores vectores tendrán una mayor probabilidad de reproducirse, cruzándose con otros vectores. Los individuos son seleccionados por el método de selección de rueda de la ruleta. En cada cruce de dos vectores, se aplica un *crossover* de punto único y se obtienen dos nuevos vectores. También se aplica el operador de mutación (mutación uniforme). El proceso continúa hasta que se ha evaluado un número determinado de generaciones, $N_{gen\_main\_max}$.

El algoritmo secundario también utiliza un vector de enteros, con cinco variables relacionadas con la estrategia de control.

$$\{ P_{min\_gen} \mid P_{limit\_disch} \mid P_{critical\_gen} \mid SOC_{stp\_gen} \mid SOC_{minimun} \}$$

P_{min_gen}: Potencia de salida mínima del generador diésel. El consumo específico de combustible del generador diésel (l/kWh) para potencias de salida bajas es mayor que para altas potencias [95], por lo que el P_{min_gen} óptimo podría ser más alto que el recomendado por el fabricante.

P_{limit_disch}: Cuando la carga de CA no puede ser cubierta por las fuentes renovables, debe ser suministrada por el banco de baterías o por el generador diésel. Generalmente, a baja potencia, el coste de suministro de energía por las baterías es menor que el suministro de energía por el generador diésel. Si la potencia es inferior a P_{limit_disch}, se suministrará con el banco de baterías; de lo contrario se utilizará el generador diésel. El valor óptimo de P_{limit_disch} depende de las condiciones de funcionamiento reales, que no se conocen a priori, por lo que esta variable es parte de la estrategia de control a optimizar.

$P_{critical\_gen}$ y SOC_{stp_gen}: Debido al citado elevado consumo específico del generador diésel a baja potencia, cuando la potencia que el diésel debe suministrar es inferior a un límite crítico, $P_{critical\_gen}$, puede ser óptimo trabajar a potencia nominal, utilizando la potencia extra para cargar las baterías hasta un SOC denotado como SOC_{stp_gen}.

$SOC_{minimun}$: mínimo SOC de la batería. Cuando la batería se está descargando y alcanza este valor, la carga se desconecta de la batería, evitando una descarga excesiva. El fabricante recomienda un valor (usualmente entre el 20 y el 40%); Sin embargo, el valor óptimo puede ser mayor.

Para cada combinación de componentes evaluada por el MOEA, el algoritmo secundario busca la mejor estrategia de control. Se obtiene aleatoriamente una primera generación de vectores o individuos (combinaciones de variables de control, es decir, estrategias de control). Cada vector del algoritmo secundario se evalúa mediante una simulación horaria del sistema durante un número de años n_y hasta que la capacidad remanente del banco de baterías cae al 80% (fin de la vida de la batería). Entonces, se espera que el rendimiento de los primeros años n_{years} se repita durante los siguientes n_{years}, y así sucesivamente hasta que termine la vida del sistema. Al final de la simulación de cada individuo (combinación de componentes y estrategia de control), si la carga insatisfecha es superior a un valor fijado (por ejemplo, 0 ó 0,1%), ese individuo se descarta. Si no es descartado, se calcula el NPC de esa solución. Entonces los vectores (combinaciones de variables de control) son ordenados por su NPC. El primero

(posición 1) es el mejor individuo, mientras que el último (posición N) es el peor. A cada uno de los individuos se le asigna una aptitud con la función de aptitud.

A continuación se realiza la selección (rueda de ruleta), cruce (cruce de punto único) y mutación (uniforme) para obtener una nueva generación de individuos (estrategias de control). El proceso continúa hasta que se ha evaluado un número determinado de generaciones $N_{gen\_sec\_max}$.

Evaluar cada combinación de componentes y estrategias implica calcular los tres objetivos planteados: minimizar el NPC, y maximizar el HDI y el JC.

El NPC de una combinación de componentes y estrategia se calcula considerando el coste de adquisición de todos los componentes (paneles fotovoltaicos, aerogeneradores, banco de baterías, generador diésel e inversor/cargador), el coste de instalación y de reposición de los componentes, el coste de O&M y el coste del combustible diésel durante la vida útil del sistema, $Life_{system}$ (años). Se tiene en cuenta la vida esperada de cada uno de los componentes (datos del fabricante) y el coste residual de los componentes al final de la vida útil del sistema. Todos los flujos de caja se convierten al momento inicial del sistema (hora 0, año 1) considerando la inflación y la tasa de interés.

El HDI de una combinación de componentes y estrategia de control se calcula sobre la base de la ecuación introducida por Rojas-Zerpa (2012). Se considera que una fracción del excedente anual de energía puede ser utilizada por nuevas empresas, servicios o pequeños talleres, lo que puede mejorar el nivel de vida y por lo tanto el HDI. El exceso de energía es la energía generada por las fuentes renovables que no puede usarse; es decir, es la energía generada cada hora por los paneles fotovoltaicos y por los aerogeneradores y que no puede ser consumida por la carga porque la carga es menor y ya está cubierta. Si dicho exceso de energía no puede almacenarse en el banco de baterías del sistema porque está completamente cargado, el exceso de energía puede ser utilizado por cargas adicionales de CA (nuevos negocios o servicios con sus propios sistemas de almacenamiento) que no fueron considerados cuando se definió la carga. Estos nuevos negocios o servicios pueden utilizar el exceso de energía

directamente (en las horas que el exceso de energía está disponible) o almacenarlo en sus propias baterías para usarlo más tarde cuando no haya exceso de energía. Para el cálculo se tiene en cuenta la energía del sistema, el exceso anual de energía del sistema y distintos factores que limitan el aprovechamiento máximo de esa energía sobrante.

En cuanto al cálculo de JC, se realiza en función de la creación de trabajo de las diferentes tecnologías (fotovoltaica, eólica, generador diésel y baterías) y de la potencia instalada o energía suministrada por cada una de ellas.

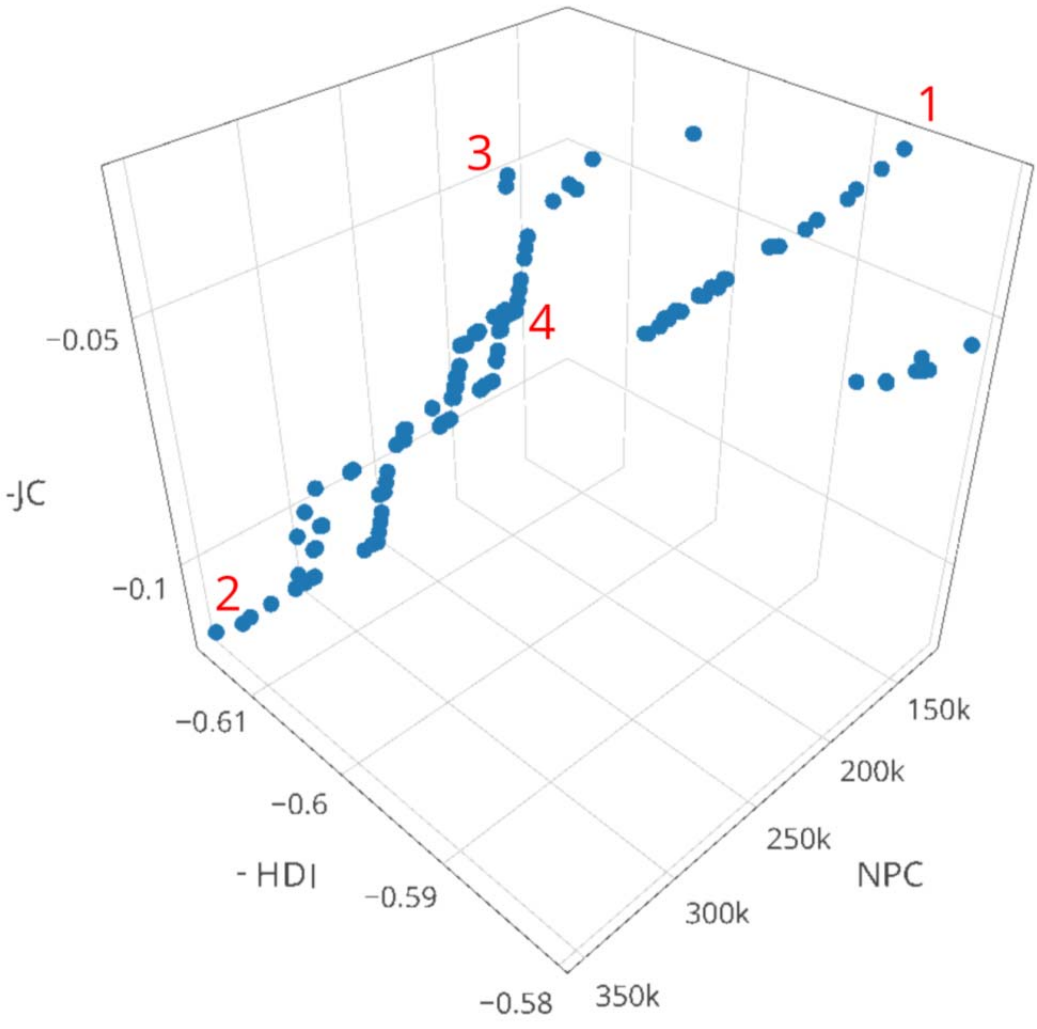

Figura 8. Conjunto óptimo de Pareto de la última generación del MOEA en un caso estudiado.

3.4.4. *Stochastic-heuristic methodology for the optimisation of components and control variables of PV-wind-diesel-battery stand-alone systems.*

En este trabajo se ha utilizado una metodología que combina los algoritmos genéticos (*Genetic Algorithms*, GA) con la simulación de Monte Carlo (*Monte Carlo Simulation*, MCS) para conseguir la optimización de la combinación de componentes y de variables de control (estrategias) de sistemas híbridos aislados con alimentación renovable. En general, el número de combinaciones posibles de componentes y estrategias de control es tan alto, que implicaría un tiempo de computación inadmisible. Ello implica que deben utilizarse modelos heurísticos en la optimización (algoritmos genéticos en este caso).

Se aplican dos GA, uno para la optimización de los componentes (algoritmo principal) y otro (algoritmo secundario) para la optimización de las variables de control (estrategia de control).

El algoritmo principal trabaja mediante un vector de enteros, que utiliza como variables el número de paneles fotovoltaicos en paralelo (a), el código del tipo de panel fotovoltaico (b), el número de aerogeneradores en paralelo (c), el código del tipo de aerogenerador (d), el código del tipo de batería (e), el número de baterías en paralelo (f), el código del tipo de generador diésel (g) y el código del tipo de inversor/cargador (h):

$$\{ a \mid b \mid c \mid d \mid e \mid f \mid g \mid h \}$$

El algoritmo secundario, también utiliza un vector de enteros, en este caso con ocho variables de control que ya han sido comentadas en los trabajos anteriores:

$$\{ P_{min\_gen} \mid P_{limit\_disch} \mid P_{critical\_gen} \mid SOC_{stp\_gen} \mid SOC_{min\_disconnect} \mid SOC_{min\_reconnect} \mid SOC_{boost} \mid SOC_{equal} \}$$

Para cada combinación de componentes *i* que es evaluada por el algoritmo principal, se utiliza el algoritmo secundario para obtener la estrategia de control óptima *k*, denominada *k(opt)* (combinación óptima de las variables de control), que minimiza la media de la distribución del NPC para esa combinación *i*.

Después el algoritmo principal se utiliza para obtener la combinación óptima de los componentes i, denominada *i(opt)* (con su combinación óptima de variables de control ya obtenida por el algoritmo secundario), lo que minimiza la media de la distribución del NPC con *i(opt)* y *k(opt).*

Para cada algoritmo, al inicio, se obtiene aleatoriamente una población de *N* vectores (o individuos) que forman la primera generación. Cada vector se evalúa mediante una simulación horaria del sistema durante los años de vida de las baterías, y se repite $MCS_{samples}$ veces para obtener el enfoque probabilístico. Entonces, se conocerá la función de densidad de probabilidad (PDF) de las variables que interesan como resultados. Se descartan los individuos con una media de carga insatisfecha superior a un valor específico (por ejemplo, 0,01%). El resultado principal es la media de la distribución de NPC, que es la variable utilizada para ordenar el conjunto de vectores. El primero (posición 1) será el mejor individuo, el que tenga la media de NPC más baja, mientras que el último (posición *N*) será el peor, el que tenga la media de NPC más alta. Una vez ordenados, se le asigna una aptitud a cada uno en función de este orden.

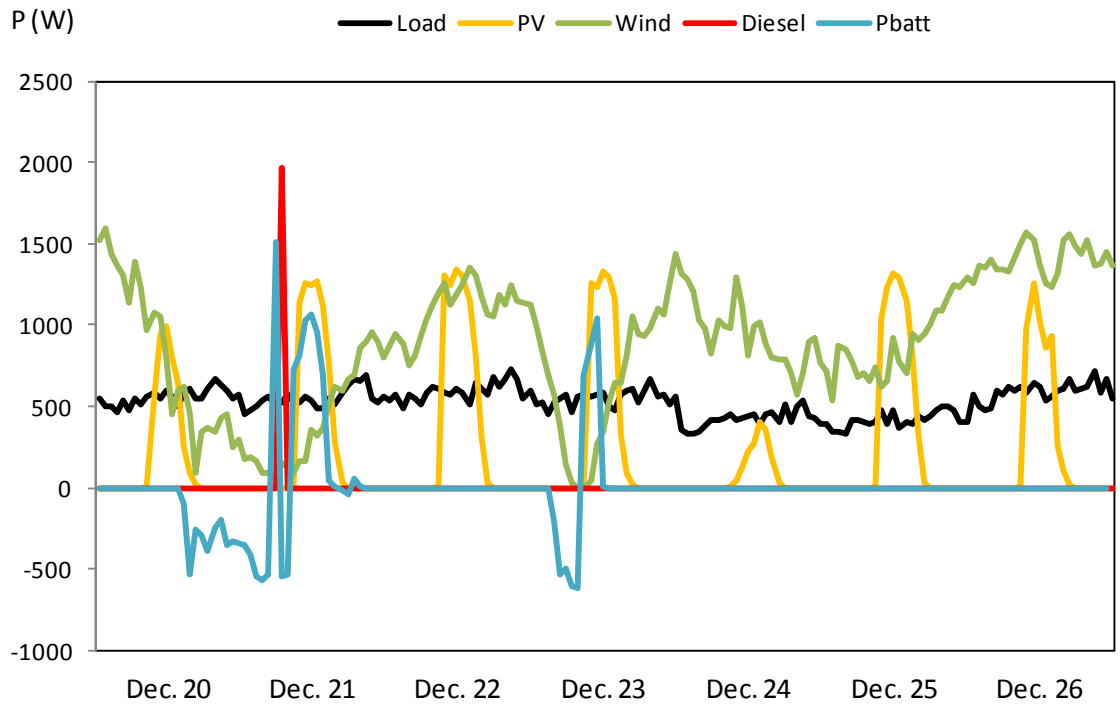

Figura 9. Evolución de algunas variables durante la simulación de una semana al final de un año.

Los mejores individuos (más aptos) tendrán una probabilidad mayor de reproducirse, mediante cruce con otros vectores. En cada cruce se obtendrán dos nuevos vectores. Algunos individuos aleatoriamente cambian alguno de sus componentes (mutarán), con el fin de mantener la diversidad de la población y así evitar mínimos locales y la convergencia prematura. Estos individuos obtenidos mediante reproducción y mutación reemplazarán a los peores individuos de la generación previa, de tal manera que se obtiene la siguiente generación. El proceso continuará hasta que se ha evaluado un número específico de generaciones N_{gen_max}. La mejor solución obtenida es aquella que tiene el valor más bajo de la media de la distribución de NPC.

Como se ha mencionado anteriormente, el algoritmo secundario, que se utiliza para optimizar las variables de control, incluye una optimización de Monte Carlo (MCS). Para aplicarla, para cada combinación de componentes *i* y estrategias de control *k*, y para cada año, se obtiene un vector de variables aleatorias gaussianas correlacionadas $\boldsymbol{Z}$. Este vector contiene los factores por los que se modificarán los valores horarios de carga, irradiación, temperatura y velocidad del viento, con respecto a la media y para ese año concreto. Este vector, por ejemplo del año 1, $\boldsymbol{Z}_{\mathbf{year1}}$= [$E_{year1}$, G_{year1}, T_{year1}, W_{year1}] está normalmente distribuido entre el vector de los valores medios y la matriz varianza-covarianza.

Una vez hallado este vector Z de ese año, la serie horaria de ese año de cada una de las variables, se puede calcular como el producto de la serie horaria de esa variable por su factor correspondiente (por ejemplo: E_{year1}/E_{mean} en el caso de la carga demandada).

Conocidos los datos del primer año, se realiza la simulación horaria del sistema durante este primer año. Al final del primer año, si la capacidad remanente del banco de baterías es aún superior al 80% de su valor nominal, esto significa que la batería aún no ha llegado al final de su vida útil, por lo que la simulación debe continuar durante el año 2. Se calculan los valores de las variables aleatorias gaussianas correlacionadas de E_{year2}, G_{year2}, T_{year2} y W_{year2}, y se calculan las series horarias como se hizo para el año 1. El proceso continúa hasta el año en que la capacidad restante del banco de baterías alcanza el 80% de su valor

nominal. Entonces se conoce la duración de la batería para esa combinación de componentes *i* y estrategia de control *k*, y el rendimiento del sistema durante ese tiempo. Se asume que este rendimiento del sistema se repite hasta el final de la vida útil del mismo. Con lo que ya se pueden calcular todos los demás resultados, incluyendo $NPC_{i,k}$ y $LCE_{i,k}$.

El proceso explicado anteriormente se repite $MCS_{samples}$ veces ($MCS_{samples}$ es el número de muestras o ensayos o tamaño de la muestra de la MCS) o hasta que se alcance la regla de detención de la MCS. Entonces, los resultados se podrán mostrar en forma de curvas de distribución PDF. La media del PDF del $NPC_{i,k}$, que se ha llamado NPC_{i,k_mean}, será el valor utilizado para evaluar la aptitud de la combinación de los componentes *i* y la estrategia de control *k*.

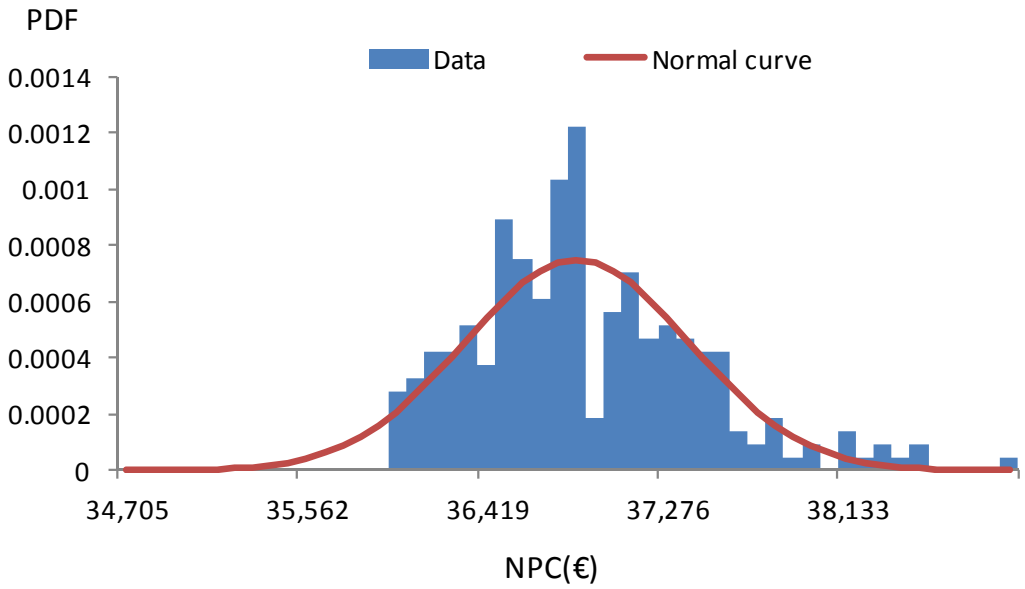

Figura 10. Ejemplo de la función de distribución de probabilidad del NPC.

Existen bastantes reglas para detener la MCS [96,97]. Algunas permiten que la simulación continúe mientras que el error relativo estándar del NPC no disminuye de un determinado valor (0,1 % por ejemplo). Otras, también ampliamente utilizadas [98], permiten que la simulación continúe hasta que se obtiene una determinada precisión (por ejemplo 1%) bajo un nivel de confianza determinado (95% por ejemplo).

Dado que la optimización mediante algoritmos genéticos es una técnica heurística, que no evalúa todas las combinaciones, no es posible asegurar que siempre obtendrá la solución óptima. En algunos casos se puede obtener una solución muy cerca del óptimo.

3.5 APORTACIONES DEL DOCTORANDO

3.5.1 *Influence of the battery model in the optimisation of stand-alone renewable systems*.

En este artículo realicé la revisión bibliográfica de los distintos modelos de baterías existentes, participé en el planteamiento y objetivos del artículo, definí el sistema y las distintas configuraciones a simular y optimizar, participé en los modelos y metodología a emplear, preparé los casos a evaluar, realicé los cálculos, obtuve los resultados y participé en la obtención de conclusiones.

3.5.2. *Optimisation of photovoltaic–diesel–battery stand-alone systems minimising system weight*.

En este artículo realicé un amplio estudio de costes y pesos de los distintos elementos de estos sistemas, realicé la revisión bibliográfica de los artículos relacionados, participé en el planteamiento y objetivos del artículo, definí el sistema a simular y optimizar, definí los modelos y metodología a emplear, preparé los casos a evaluar, realicé los cálculos, obtuve los resultados y participé en la obtención de conclusiones.

3.5.3. *Optimisation of PV-wind-diesel-battery stand-alone systems to minimise cost and maximise human development index and job creation*.

En este artículo realicé una revisión bibliográfica sobre la electrificación rural mediante sistemas de energías renovables sin conexión a la red eléctrica y sobre los índices de desarrollo humano y de creación de empleo de las distintas tecnologías de generación. Participé en el planteamiento y objetivos del artículo, definí el sistema a simular y optimizar, definí los modelos y metodología a emplear, preparé el caso a evaluar, participé en la realización de los cálculos, obtuve los resultados y participé en la obtención de conclusiones.

3.5.4. *Stochastic-heuristic methodology for the optimisation of components and control variables of PV-wind-diesel-battery stand-alone systems.*

En este artículo realicé una exhaustiva revisión bibliográfica sobre los trabajos previos que utilizaban enfoques estocásticos y modelos probabilísticos. Participé en el planteamiento y objetivos del artículo, definí el sistema a simular y optimizar, participé en la elección de los modelos y metodología a emplear, preparé los casos a evaluar, participé en la realización de los cálculos, obtuve los resultados y participé en la obtención de conclusiones.

3.6 RESULTADOS Y CONCLUSIONES FINALES

En el primer trabajo, se han optimizado tres tipos distintos de sistemas híbridos aislados con energías renovables, alimentando a dos tipos distintos de cargas (una de corriente continua y otra de corriente alterna) y utilizando tres modelos distintos de cálculo para la vida útil de las baterías del sistema. Se puede concluir, comparando los resultados de las distintas optimizaciones, que los modelos clásicos (Ciclos equivalentes y Rainflow) obtienen una estimación muy similar para la vida de las baterías y por lo tanto valores muy similares para el coste actual neto (NPC) y el coste normalizado de la energía (LCE). Sin embargo el modelo de *Criterio ponderado del flujo de Ah* obtiene resultados más realistas sobre la vida esperada de la batería, siendo estos mucho menores que los de los modelos clásicos, y por lo tanto, obteniendo valores más realistas (mayores) del NPC y del LCE. Los modelos clásicos obtienen resultados demasiado optimistas, en algunos casos dos o tres veces mayores que los obtenidos con el modelo propuesto por Schiffer et al.

Una observación que se puede realizar, después de comparar los resultados, es que en los casos estudiados, los tres modelos de batería obtienen el mismo sistema óptimo, excepto en el caso del sistema Diésel-Baterías, donde el modelo propuesto por Schiffer et al. obtiene un banco de baterías menor. Es de mencionar que en los casos citados, todos los modelos lleguen al mismo sistema óptimo, aun cuando, como se ha comentado, los métodos clásicos llegan a costos demasiado optimistas.

En el segundo trabajo se muestra un nuevo método para la optimización de sistemas híbridos aislados con alimentación renovable para suministrar la carga eléctrica a instalaciones temporales. Por tanto, estos sistemas deben ser transportados desde una sede central a una determinada ubicación, para estar funcionando durante un periodo de tiempo específico, y pasado ese tiempo, deben ser transportados de regreso a la sede y almacenados hasta la siguiente necesidad o emergencia. Se ha estudiado el caso de un hospital en la República Centroafricana. Los periodos de tiempo simulados han sido 30, 60, 90, 180 y 365 días. Se han considerado costos de transporte relativamente bajos (transporte por

camión, costo bajo comparado con transporte aéreo o mediante helicóptero de transporte), para una distancia de 200 km.

Si el periodo de tiempo es 90 o más días, el peso mínimo se obtiene con un sistema híbrido (incluyendo paneles fotovoltaicos flexibles c-SI y un banco de baterías), con una penetración de energía renovable de más del 40%. Para los casos de 30 y 60 días, el sistema óptimo que minimiza el peso total no incluye paneles fotovoltaicos. Sin embargo, teniendo en cuenta sólo el coste total en la optimización, en todos los casos la solución óptima incluye un generador fotovoltaico (con paneles c-Si normales, obteniendo una penetración renovable superior al 88%, incluso considerando un factor de envejecimiento extra muy elevado para los paneles) y un banco de baterías de alta capacidad.

La conclusión principal es que, en muchas áreas del mundo, incluso considerando sólo la minimización del peso total, si la instalación debe trabajar más de un número específico de días, un sistema híbrido (fotovoltaico + diésel + baterías) es la solución óptima, mientras que, considerando sólo el coste, en todos los casos la solución óptima es un sistema híbrido.

En el tercer trabajo se presenta una nueva metodología para la optimización multiobjetivo de sistemas híbridos aislados con energías renovables (fotovoltaicos-eólico-diésel-baterías) maximizando el índice de desarrollo humano (HDI) y la creación de empleo (JC) y minimizando el coste actual neto (NPC).

La optimización realizada utiliza un algoritmo evolutivo multiobjetivo (MOEA) para obtener el conjunto óptimo de Pareto de las combinaciones de componentes considerando los tres objetivos. La mejor estrategia de control para cada combinación de componentes utilizada por el MOEA se obtiene por medio de un algoritmo genético, que optimiza el NPC.

El HDI y el JC no se habían considerado previamente en la optimización de este tipo de sistemas. El HDI depende de una función logarítmica del consumo eléctrico anual per cápita; por lo que se considera una carga mínima a cubrir (correspondiente a un valor específico del HDI) y se considera que el exceso de

energía generado por las fuentes renovables podría ser utilizado por nuevas cargas adicionales (nuevas empresas o servicios, con o sin sus propios sistemas de almacenamiento eléctrico), lo que aumentaría el HDI.

Cada tecnología de generación tiene un factor de creación de empleo específico, que incluye trabajos directos e indirectos en la fabricación, instalación y O&M. Se ha realizado una revisión del estado del arte de JC obteniéndose una alta variación en los factores de creación de empleo para la energía fotovoltaica y la eólica. El número de trabajos creados por un sistema híbrido dependerá de la combinación de sus componentes (mezcla de tecnologías).

Se presenta un ejemplo de aplicación a una pequeña comunidad en los campamentos de refugiados saharauis de Tindouf, para obtener un conjunto de Pareto óptimo en el que ninguna de las soluciones es mejor en los tres objetivos que cualquier otra.

Hoy en día el suministro eléctrico de estos campamentos se realiza por medio de generadores diésel para los edificios administrativos públicos, y muchas casas se abastecen de una cantidad mínima de electricidad mediante pequeños paneles fotovoltaicos. Se ha considerado una comunidad de 60 personas, y una carga media diaria de 82,14 kWh/día (diferente para cada día), con una carga total anual de 29,983 kWh/año, lo que corresponde a un HDI = 0,5756. Este será el HDI mínimo, ya que toda la carga de CA debe estar cubierta por el sistema, lo que corresponde al HDI de los países con un desarrollo medio. Se considera que como máximo el 20% del exceso de energía del sistema podrá ser utilizado por las cargas extra, y nunca podrá ser superior al 50% de la energía total consumida por el sistema, por lo que considerando el máximo de carga extra AC (nuevos negocios o servicios con su propio almacenamiento, que podrían utilizar parte del exceso de energía), el HDI máximo podría ser HDI_{max} = 0,6155. Los parámetros de creación de empleo son JC_{PV} = 2,7 empleos/MW, JC_{Wind} = 1,1 empleos/MW y JC_{Diesel} = 0,14 empleos/(GWh/año), mientras que para el banco de baterías se ha estimado un valor muy conservador de JC_{BAT} = 0,01 empleos/MWh.

Se ha considerado la posibilidad de no incluir paneles fotovoltaicos y no incluir aerogeneradores en el sistema. Sin embargo, el sistema debe contar con un generador diésel al menos para ser utilizado como reserva de emergencia. Calculando todas las posibles combinaciones de componentes y estrategias de control, y calculando el tiempo de simulación y evaluación de cada una de ellas, se necesitarían unos 216 días para evaluar todas ellas con un ordenador estándar.

Mediante el uso de algoritmos evolutivos, la optimización se puede realizar en un tiempo de cálculo razonable. El MOEA utiliza una población de 200 individuos (0,48% de las posibles combinaciones de componentes) con 15 generaciones, mientras que el algoritmo secundario utiliza una población de 20 individuos (0,64% de posibles combinaciones de variables de control) y 15 generaciones, con una tasa de cruce del 90% y una tasa de mutación del 1% para ambos algoritmos. Estos valores se seleccionaron considerando los resultados de algunas pruebas en optimizaciones similares. En aproximadamente un día y medio, los algoritmos evolutivos realizaron la optimización, obteniendo el conjunto óptimo de Pareto.

En el caso simulado, como la velocidad del viento es relativamente alta, la mayoría de las soluciones del conjunto óptimo de Pareto son sistemas híbridos fotovoltaicos-eólico-diésel-baterías, mientras que en otros lugares con menor velocidad del viento, la mayoría de las soluciones del conjunto óptimo de Pareto no incluyen aerogeneradores. Una vez que se conoce el conjunto óptimo de Pareto, el diseñador puede ver las diferencias entre los objetivos de las diferentes soluciones y puede elegir la que mejor se adapte a sus necesidades.

Para finalizar, en el último trabajo se muestra una metodología estocástica-heurística (combinando simulación Monte Carlo con algoritmos genéticos) para la optimización de componentes y variables de control de sistemas híbridos Fotovoltaicos-Eólicos-Diésel-Baterías aislados. Se ha aplicado un modelo avanzado para simular el comportamiento de las baterías que tiene en cuenta el flujo ponderado de Ah es mucho más preciso que los modelos clásicos que solo consideran la energía ciclada por la batería. También se ha incluido la

optimización de varias variables de control que actualmente se pueden configurar en los controladores de baterías modernos o en los inversores/cargadores con control del estado de carga.

La optimización estocástica utiliza como entradas las funciones de distribución de probabilidad de varias variables (carga esperada, irradiación, temperatura, velocidad del viento y tasa de interés) tomando en cuenta sus correlaciones, obteniéndose las funciones de distribución de probabilidad de los resultados. Es diseñador podrá obtener resultados que incluyen mucha más información y tener la capacidad de conocer los valores mínimos, máximos y más probables de las distintas variables de resultados, incluyendo su variabilidad, en comparación con una optimización determinista.

Sin embargo, la optimización estocástica implica tiempos de cálculo mucho mayores, dependiendo del error máximo permitido. Bajo el nivel de confianza deseado, puede ser cientos de veces mayor, lo que, en muchos casos, es inadmisible, incluso empleando algoritmos genéticos.

Como ejemplo, se ha comparado la optimización determinista de un mismo sistema (12 horas de tiempo de cálculo) con la optimización estocástica (78 horas de tiempo de cálculo, incluso reduciendo el espacio de búsqueda para las variables de control), y utilizando algoritmos genéticos para ambos casos. Se ha optimizado el sistema para abastecer a una estación de telecomunicaciones ubicada en Navarra (España) en una colina ventosa. La configuración óptima ha resultado un sistema Fotovoltaico- Eólico-Diésel-Baterías, con una penetración muy alta de las fuentes renovables. En este caso, y debido a la alta velocidad del viento en la colina, forma parte del sistema óptimo un aerogenerador. Debido al alto precio del combustible en España (y su inflación), el generador diésel solo se utiliza como sistema de respaldo, suministrando energía solamente cuando el banco de baterías alcanza el mínimo de estado de carga admitido.

Primero ha de realizarse una optimización determinista, con un tiempo de cálculo medianamente bajo. Con esos primeros resultados, se puede reducir el espacio de búsqueda alrededor del sistema óptimo, y entonces ya puede

realizarse una optimización estocástica en un tiempo de cálculo razonable. El sistema óptimo encontrado mediante el enfoque estocástico resulta muy similar al obtenido mediante el enfoque determinístico, sin embargo, la optimización estocástica ofrece mucha más información sobre el rendimiento esperado del sistema.

REFERENCIAS

[1] Global Energy Statistical Yearbook 2016.

[2] U.S. Energy Information Administration (EIA). International Energy Agency. International Energy Outlook 2016.

[3] T. Bäck; D.B. Fogel D; Z. Michalewicz. Evolutionary Computation 1: Basic Algorithms and Operators (2000). Bristol and Philadelphia: Institute of Physics Publishing.

[4] R. Dufo-López, J.L. Bernal-Agustín. Design and control strategies of PV-diesel systems using genetic algorithms. Solar Energy 79 (2005) 33–46.

[5] J.L. Bernal-Agustín, R. Dufo-López. Simulation and optimization of stand-alone hybrid renewable energy systems. Renewable and Sustainable Energy Reviews 13 (2009) 2111–2118.

[6] P. Ruetschi. Aging mechanisms and service life of lead–acid batteries. Journal of Power Sources 127 (2004) 33-44.

[7] R. Dufo-López, J.M. Lujano-Rojas, J.L. Bernal-Agustín. Comparison of different lead–acid battery lifetime prediction models for use in simulation of stand-alone photovoltaic systems. Applied Energy 115 (2014) 242–253.

[8] United Nations Development Programme. Human Development Report 2014. Sustaining Human Progress: Reducing Vulnerabilities and Building Resilience 2014. ISBN: 978-92-1-126340-4.

[9] International Energy Agency. World Energy Outlook 2014.

[10] R. Ramanathan, L.S. Ganesh. Energy resource allocation incorporating qualitative and quantitative criteria: An integrated model using goal programming and AHP. Socio-Economic Planning Sciences 29 (1995) 197–218.

[11] M. Wei, S. Patadia, D.M. Kammen. Putting renewables and energy efficiency to work: How many jobs can the clean energy industry generate in the US?. Energy Policy 38 (2010) 919–931.

[12] M. Ortega, P. Ruiz, C. Thiel. Employment effects of renewable electricity deployment . A novel methodology. Energy 91 (2015) 940–951.

[13] T.M. Sooriyaarachchi, I. Tsai, S. El Khatib, A.M. Farid. Job creation potentials and skill requirements in, PV, CSP, wind, water-to-energy and energy efficiency value chains. Renewable and Sustainable Energy Reviews 52 (2015) 653–668.

[14] IRENA. Renewable Energy Jobs & Access 2012.

[15] M. Simas, S. Pacca. Assessing employment in renewable energy technologies: A case study for wind power in Brazil. Renewable and Sustainable Energy Reviews 31 (2014) 83–90.

[16] L. Cameron, B. van der Zwaan. Employment factors for wind and solar energy technologies: A literature review. Renewable and Sustainable Energy Reviews 45 (2015) 160–172.

[17] J.C. Rojas-Zerpa. Tesis doctoral. Planificación del suministro eléctrico en áreas rurales de los países en vías de desarrollo: un marco de referencia para la toma de decisiones. Universidad de Zaragoza (2012).

[18] C. Armenta-Deu, T. Donaire. Determination of an ageing factor for lead/acid batteries. 1. Kinetic aspects. Journal of Power Sources 58 (1996) 123–133.

[19] A. Cherif, M. Jraidi, A. Dhouib. A battery ageing model used in stand alone PV systems. Journal of Power Sources 112 (2002) 49–53.

[20] J. Schiffer, D.U. Sauer, H. Bindner, T. Cronin, P. Lundsager, R. Kaiser. Model prediction for ranking lead-acid batteries according to expected lifetime in renewable energy systems and autonomous power-supply systems. Journal of Power Sources 168 (2007) 66–78.

[21] D.U. Sauer, H. Wenzl. Comparison of different approaches for lifetime prediction of electrochemical systems using lead–acid batteries as example. Journal of Power Sources 176 (2008) 534–546.

[22] O. Ekren, B.Y. Ekren. Size optimization of a PV/wind hybrid energy conversion system with battery storage using response surface methodology. Applied Energy 85 (2008) 1086–1101.

[23] A. Roy A, S.B. Kedare, S. Bandyopadhyay. Application of design space methodology for optimum sizing of wind–battery systems. Applied Energy 86 (2009) 2690–2703.

[24] Y. Hongxing, Z. Wei, L. Chengzhi. Optimal design and techno-economic analysis of a hybrid solar–wind power generation system. Applied Energy 86 (2009) 163–169.

[25] A. Roy A, S.B. Kedare, S. Bandyopadhyay. Optimum sizing of wind-battery systems incorporating resource uncertainty. Applied Energy 87 (2010) 2712–2727.

[26] M. Kalantar, G.S.M. Mousavi. Dynamic behavior of a stand-alone hybrid power generation system of wind turbine, microturbine, solar array and battery storage. Applied Energy 87 (2010) 3051–3064.

[27] G.J. Dalton, D.A. Lockington, T.E. Baldock . Feasibility analysis of stand-alone renewable energy supply options for a large hotel. Renewable Energy 33 (2008) 1475–1490.

[28] G. Bekele, B. Palm. Feasibility study for a standalone solar–wind-based hybrid energy system for application in Ethiopia. Applied Energy 87 (2010) 487–495.

[29] R. Dufo-López, J.L: Bernal-Agustín. Influence of mathematical models in design of PV–diesel systems. Energy Conversion and Management 49 (2008) 820–831.

[30] J.L. Bernal-Agustín, R. Dufo-López. Multi-objective design and control of hybrid systems minimizing costs and unmet load. Electric Power Systems Research 79 (2009) 170–180.

[31] A.T.D. Perera, R.A. Attalage, K.K.C.C. Perera, V.P.C. Dassanayake. A hybrid tool to combine multi-objective optimization and multi-criterion decision making in designing standalone hybrid energy systems. Applied Energy 107 (2013) 412–425.

[32] R. Baños, F. Manzano-Agugliaro, F.G. Montoya, C. Gil, A. Alcayde, J. Gómez. Optimization methods applied to renewable and sustainable energy: a review. Renewable and Sustainable Energy Reviews 15 (2011) 1753–1766.

[33]] R. Luna-Rubio, M. Trejo-Perea, D. Vargas-Vázquez, G.J. Ríos-Moreno. Optimal sizing of renewable hybrids energy systems: a review of methodologies. Solar Energy 86 (2012) 1077–1088.

[34] M. Fadaee, M.A.M. Radzi. Multi-objective optimization of a stand-alone hybrid renewable energy system by using evolutionary algorithms: a review. Renewable and Sustainable Energy Reviews 16 (2012) 3364–3369.

[35] H. Wenzl, I. Baring-Gould, R. Kaiser, B.Y. Liaw, P. Lundsager, J. Manwell et al. Life prediction of batteries for selecting the technically most suitable and cost effective battery. Journal of Power Sources 144 (2005) 373–384.

[36] C.M. Shepherd. Design of primary and secondary cells. An equation describing battery discharge. Journal of the Electrochemical Society 112 (1965) 657–664.

[37] L. Bína, H. Bínová, E. Brˇezina, P. Kumpošt, T.Padeˇlek. Comparative model of unit costs of road and rail freight transport for selected European countries. European Journal of Business and Social Sciences 3 (2014) 127–136.

[38] European Commission E. EU transport in figures. Statistical Pocketbook 2014.

[39] Research and Innovative Technology Administration. U.S. Department of Transportation. Bureau of Transportation Statistics. National Transportation Statistics 2015.

[40] S. Teravaninthorn, G. Raballand. Transport prices and costs in Africa: a review of the main international corridors. Afr Infraestruct Country Diagn 2008.

[41] M-È Rancourt, F. Bellavance, J. Goentzel. Market analysis and transportation procurement for food aid in Ethiopia. Socio-Economic Planning Sciences 48 (2014) 198–219.

[42] H. Ahlborg, L. Hammar. Drivers and barriers to rural electrification in Tanzania and Mozambique – grid-extension, off-grid, and renewable energy technologies. Renewable Energy 61(2014) 117–124.

[43] H. Borhanazad, S. Mekhilef, R. Saidur, G. Boroumandjazi. Potential application of renewable energy for rural electrification in Malaysia. Renewable Energy 59 (2013) 210–219.

[44] M.S. Adaramola, M. Agelin-Chaab, S.S. Paul. Analysis of hybrid energy systems for application in southern Ghana. Energy Conversion and Management 88 (2014) 284–295.

[45] M.S. Ismail, M. Moghavvemi, T.M.I. Mahlia. Design of an optimized photovoltaic and microturbine hybrid power system for a remote small community: case study of Palestine. Energy Conversion and Management 75 (2013) 271–281.

[46] M.S. Ismail, M. Moghavvemi, T.M.I. Mahlia. Techno-economic analysis of an optimized photovoltaic and diesel generator hybrid power system for remote houses in a tropical climate. Energy Conversion and Management 69 (2013) 163–173.

[47] U. Kumar Suresh, P.S. Manoharan. Economic analysis of hybrid power systems (PV/diesel) in different climatic zones of Tamil Nadu. Energy Conversion and Management 80 (2014) 469–476.

[48] P.E. Campana, H. Li, J. Zhang, R. Zhang, J. Liu, J. Yan. Economic optimization of photovoltaic water pumping systems for irrigation. Energy Conversion and Management 95 (2015) 32–41.

[49] M. Edwin, S. Joseph Sekhar. Techno-economic studies on hybrid energy based cooling system for milk preservation in isolated regions. Energy Conversion and Management 86 (2014) 1023–1030.

[50] R. Dufo-López, E. Pérez-Cebollada, J.L: Bernal-Agustín, I. Martínez-Ruiz. Optimisation of energy supply at off-grid healthcare facilities using Monte Carlo simulation. Energy Conversion and Management 113 (2016) 321–330.

[51] R.K. Akikur, R. Saidur, H.W. Ping, K.R. Ullah. Comparative study of stand-alone and hybrid solar energy systems suitable for off-grid rural electrification: a review Renewable and Sustainable Energy Reviews 27 (2013) 738–752.

[52] Y.S. Mohammed, M.W. Mustafa, N. Bashir. Hybrid renewable energy systems for off-grid electric power: review of substantial issues. Renewable and Sustainable Energy Reviews 35 (2014) 527–539.

[53] P. Bajpai, V. Dash. Hybrid renewable energy systems for power generation in stand-alone applications: a review. Renewable and Sustainable Energy Reviews 16 (2012) 2926–2939.

[54] S. Sinha, S.S. Chandel. Review of software tools for hybrid renewable energy systems. Renewable and Sustainable Energy Reviews 32 (2014) 192–205.

[55] D.E. Goldberg. Genetic algorithms in search, optimization, and machine learning. 1989th ed. Addison-Wesley Publishing Company, 1989.

[56] M.S. Ismail, M. Moghavvemi, T.M.I. Mahlia. Genetic algorithm based optimization on modeling and design of hybrid renewable energy systems. Energy Conversion and Management 85 (2014) 120–130.

[57] C.A. Coello, D.A.V. Veldhuizen, G.B. Lamont. Evolutionary algorithms for solving multi-objective problems. New York: Kluwer Aca, 2002.

[58] A. Higier, A. Arbide, A. Awaad, J. Eiroa, J. Miller, N. Munroe N, et al. Design, development and deployment of a hybrid renewable energy powered mobile medical clinic with automated modular control system. Renewable Energy 50 (2013) 847–857.

[59] M. Sharafi, T.Y. ElMekkawy. Stochastic optimization of hybrid renewable energy systems using sampling average method. Renewable and Sustainable Energy Reviews 52 (2015) 1668-1679.

[60] P. Nema, R.K. Nema, S. Rangnekar. A current and future state of art development of hybrid energy system using wind and PV-solar: a review. Renewable and Sustainable Energy Reviews 13 (2009) 2096-2103.

[61] S. Sinha, S.S. Chandel. Review of recent trends in optimization techniques for solar photovoltaic-wind based hybrid energy systems. Renewable and Sustainable Energy Reviews 50 (2015) 755-769.

[62] P. Hajela, C.Y. Lin. Genetic search strategies in multi-criterion optimal design. Structural and Multidisciplinary Optimization 4 (1992) 99-107.

[63] R. Dufo-López, J.L: Bernal-Agustín. Multi-objective design of PV-wind-diesel-hydrogen-battery systems. Renewable Energy 33 (2008) 2559–2572.

[64] R. Dufo-López, J.L. Bernal-Agustín, J.M. Yusta-Loyo, J. A. Domínguez-Navarro, I.J. Ramírez-Rosado, J. Lujano, et al.. Multi-objective optimization minimizing cost and life cycle emissions of stand-alone PV-wind-diesel systems with batteries storage. Applied Energy 88 (2011) 4033-4041.

[65] J.L. Bernal-Agustín, R. Dufo-López, D.M. Rivas-Ascaso. Design of isolated hybrid systems minimizing costs and pollutant emissions. Renewable Energy 44 (2012) 215-224.

[66] J.C. Rojas-Zerpa, J.M. Yusta. Methodologies, technologies and applications for electric supply planning in rural remote areas. Energy for Sustainable Development 20 (2014) 66-76.

[67] J.C. Rojas-Zerpa, J.M. Yusta. Application of multicriteria decision methods for electric supply planning in rural and remote areas. Renewable and Sustainable Energy Reviews 52 (2015) 557-571.

[68] V. Salas, W. Suponthana, R. a Salas. Overview of the off-grid photovoltaic diesel batteries systems with AC loads. Applied Energy 157 (2015) 195-216.

[69] A.D. Pasternak, Global Energy Futures and Human Development: a Framework for Analysis. U.S. Department of Energy (2000). UCRL-ID-140773.

[70] United Nations Development Program. Human Development Report 1999.

[71] United Nations Development Program. Human Development Report 2009. Overcoming Barriers: Human Mobility and Development.

[72] H. Belmili, M. Haddadi, S. Bacha, M.F. Almi, B. Bendib. Sizing stand-alone photovoltaic-wind hybrid system: techno-economic analysis and optimization. Renewable and Sustainable Energy Reviews 30 (2014) 821-832.

[73] O. Erdinc, M. Uzunoglu. Optimum design of hybrid renewable energy systems: overview of different approaches. Renewable and Sustainable Energy Reviews 16 (2012) 1412-1425.

[74] N.D. Nordin, H. Abdul Rahman. A novel optimization method for designing stand alone photovoltaic system. Renewable Energy 89 (2016) 706-715.

[75] I.G. Mason, A.J.V. Miller. Energetic and economic optimisation of islanded household-scale photovoltaic-plus-battery systems. Renewable Energy 96 (2016) 559-573.

[76] S. Mandelli, C. Brivio, E. Colombo, M. Merlo. A sizing methodology based on levelized cost of supplied and lost energy for off-grid rural electrification systems. Renewable Energy 89 (2016) 475-488.

[77] J.L. Bernal-Agustín, R. Dufo-Lopez. Efficient design of hybrid renewable energy systems using evolutionary algorithms. Energy Conversion and Management 50 (2009) 479-489.

[78] R. Dufo-Lopez, J.L. Bernal-Agustín, J. Contreras. Optimization of control strategies for stand-alone renewable energy systems with hydrogen storage. Renewable Energy 32 (2007) 1102-1126.

[79] D. Tsuanyo, Y. Azoumah, D. Aussel, P. Neveu. Modeling and optimization of batteryless hybrid PV (photovoltaic)/diesel systems for off-grid applications. Energy 86 (2015) 152-163.

[80] S. Rajanna, R.P. Saini. Modeling of integrated renewable energy system for electrification of a remote area in India. Renewable Energy 90 (2016) 175-187.

[81] S. Sanajaoba, E. Fernandez. Maiden application of Cuckoo search algorithm for optimal sizing of a remote hybrid renewable energy system. Renewable Energy 96 (2016) 1-10.

[82] P. Paliwal, N.P. Patidar, R.K. Nema. A novel method for reliability assessment of autonomous PV-wind-storage system using probabilistic storage model. International Journal of Electrical Power & Energy Systems 55 (2014) 692-703.

[83] P. Arun, R. Banerjee, S. Bandyopadhyay. Optimum sizing of photovoltaic battery systems incorporating uncertainty through design space approach. Solar Energy 83 (2009) 1013-1025.

[84] A. Kamjoo, A. Maheri, G. a. Putrus. Chance constrained programming using non-Gaussian joint distribution function in design of standalone hybrid renewable energy systems. Energy 66 (2014) 677-688.

[85] A. Kamjoo, A. Maheri, A.M. Dizqah, G. a. Putrus. Multi-objective design under uncertainties of hybrid renewable energy system using NSGA-II and chance constrained programming. International Journal of Electrical Power & Energy Systems 74 (2016) 187-194.

[86] A. Maheri. A critical evaluation of deterministic methods in size optimization of reliable and cost effective standalone hybrid renewable energy systems. Reliability Engineering & System Safety 130 (2014) 159-174.

[87] A. Maheri. Multi-objective design optimisation of standalone hybrid wind-PV-diesel systems under uncertainties. Renewable Energy 66 (2014) 650-661.

[88] W. Alharbi, K. Raahemifar. Probabilistic coordination of microgrid energy resources operation considering uncertainties. Electric Power Systems Research 128 (2015) 1-10.

[89] K.-H. Chang, G. Lin. Optimal design of hybrid renewable energy systems using simulation optimization. Simulation Modelling Practice and Theory 52 (2015) 40-51.

[90] I. Falconett, K. Nagasaka. Comparative analysis of support mechanisms for renewable energy technologies using probability distributions. Renewable Energy 35 (2010) 1135-1144.

[91] G.M. Tina, S. Gagliano. Probabilistic modelling of hybrid solar/wind power system with solar tracking system. Renewable Energy 36 (2011) 1719-1727.

[92] E.J.D.S. Pereira, J.T. Pinho, M.A.B. Galhardo, W.N. Macêdo. Methodology of risk analysis by Monte Carlo Method applied to power generation with renewable energy. Renewable Energy 69 (2014) 347-355.

[93] L.M. Carrasco, L. Narvarte, F. Martínez-Moreno, R. Moretón. In-field assessment of batteries and PV modules in a large photovoltaic rural electrification programme. Energy 75 (2014) 281-288.

[94] M. Tavana, Z. Li, M. Mobin, M. Komaki, E. Teymourian. Multi-objective control chart design optimization using NSGA-III and MOPSO enhanced with DEA and TOPSIS. Expert Systems with Applications 50 (2016) 17–39.

[95] O. Skarstein, K. Uhlen. Design Considerations with Respect to Long-Term Diesel Saving in Wind/Diesel Plants. Wind Energy 13 (1989) 72–87.

[96] M.H. Kalos, P. A. Whitlock. Monte Carlo Methods, 2008th ed. WILEY-VCH, 2008.

[97] L. Mendo, J.M. Hernando, A Simple Sequential Stopping Rule for Monte Carlo Simulation. IEEE Transactions on Communications 54 (2006) 231–241.

[98] J.-C. Chen, D. Lu, J.S. Sadowsky, K. Yao. On importance sampling in digital communications. I. Fundamentals, IEEE Journal on Selected Areas in Communications. 11 (1993) 300-308.

ANEXOS

Factor de impacto de las revistas y áreas temáticas correspondientes a las publicaciones que se recogen en la tesis.

ANEXO A.1

Revista: Energy Conversion and Management

Fuente: InCites Journal Citation Reports / Web of Science / THOMSHON REUTERS

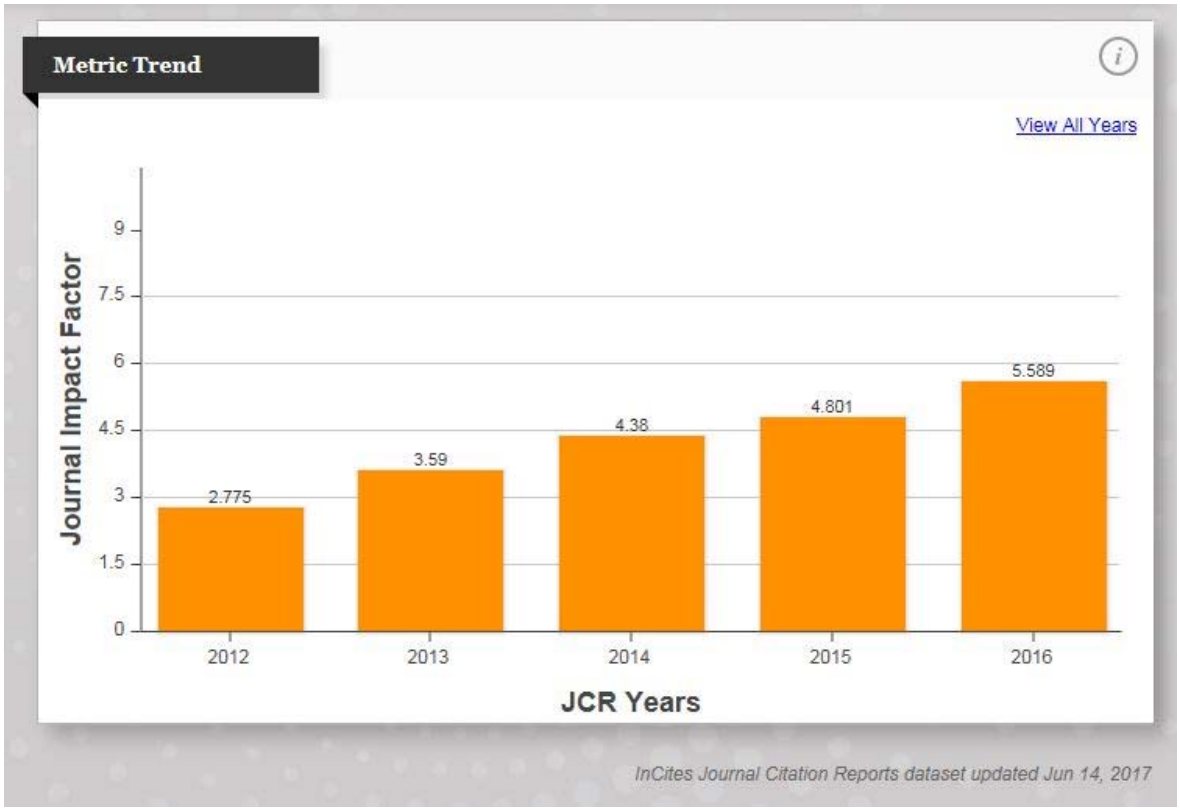

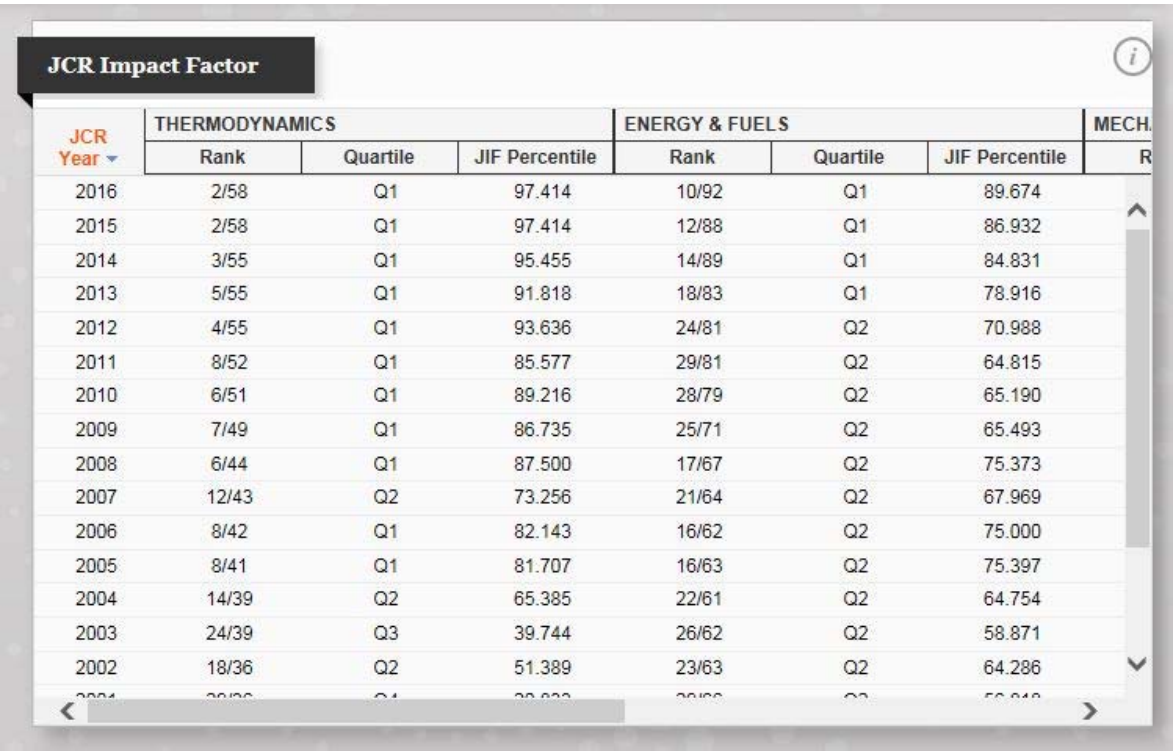

JCR Impact Factor

JCR Year	THERMODYNAMICS			ENERGY & FUELS			MECH.
	Rank	Quartile	JIF Percentile	Rank	Quartile	JIF Percentile	R
2016	2/58	Q1	97.414	10/92	Q1	89.674	
2015	2/58	Q1	97.414	12/88	Q1	86.932	
2014	3/55	Q1	95.455	14/89	Q1	84.831	
2013	5/55	Q1	91.818	18/83	Q1	78.916	
2012	4/55	Q1	93.636	24/81	Q2	70.988	
2011	8/52	Q1	85.577	29/81	Q2	64.815	
2010	6/51	Q1	89.216	28/79	Q2	65.190	
2009	7/49	Q1	86.735	25/71	Q2	65.493	
2008	6/44	Q1	87.500	17/67	Q2	75.373	
2007	12/43	Q2	73.256	21/64	Q2	67.969	
2006	8/42	Q1	82.143	16/62	Q2	75.000	
2005	8/41	Q1	81.707	16/63	Q2	75.397	
2004	14/39	Q2	65.385	22/61	Q2	64.754	
2003	24/39	Q3	39.744	26/62	Q2	58.871	
2002	18/36	Q2	51.389	23/63	Q2	64.286	

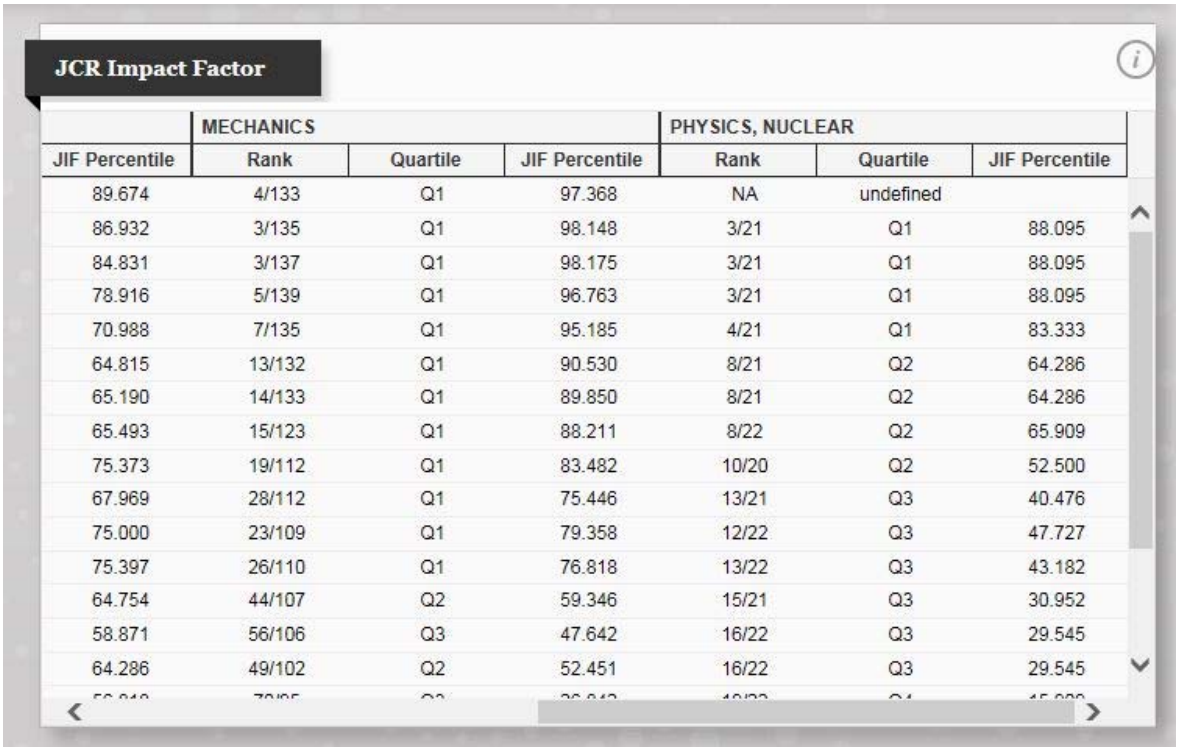

JCR Impact Factor

	MECHANICS			PHYSICS, NUCLEAR		
JIF Percentile	Rank	Quartile	JIF Percentile	Rank	Quartile	JIF Percentile
89.674	4/133	Q1	97.368	NA	undefined	
86.932	3/135	Q1	98.148	3/21	Q1	88.095
84.831	3/137	Q1	98.175	3/21	Q1	88.095
78.916	5/139	Q1	96.763	3/21	Q1	88.095
70.988	7/135	Q1	95.185	4/21	Q1	83.333
64.815	13/132	Q1	90.530	8/21	Q2	64.286
65.190	14/133	Q1	89.850	8/21	Q2	64.286
65.493	15/123	Q1	88.211	8/22	Q2	65.909
75.373	19/112	Q1	83.482	10/20	Q2	52.500
67.969	28/112	Q1	75.446	13/21	Q3	40.476
75.000	23/109	Q1	79.358	12/22	Q3	47.727
75.397	26/110	Q1	76.818	13/22	Q3	43.182
64.754	44/107	Q2	59.346	15/21	Q3	30.952
58.871	56/106	Q3	47.642	16/22	Q3	29.545
64.286	49/102	Q2	52.451	16/22	Q3	29.545

ANEXO A.2

Revista: Energy Conversion and Management

Fuente: Scimago Journal & Country Rank (SJR) / SCOPUS

Energy Conversion and Management

Country	United Kingdom
Subject Area and Category	Energy Energy Engineering and Power Technology Fuel Technology Nuclear Energy and Engineering Renewable Energy, Sustainability and the Environment
Publisher	Elsevier Ltd.
Publication type	Journals
ISSN	01968904
Coverage	1979-ongoing
Scope	The Journal provides a forum for publishing original contributions and comprehensive technical review articles of interdisciplinary and original research in static and dynamic energy conversion; energy efficiency and management; heat pipes; thermosyphons and capillary pumped loops; thermal management of spacecraft; space and terrestrial power systems; hydrogen production and storage; renewable energy; nuclear power; single and combined cycles; miniaturized energy conversion and power systems; fuel cells and advanced batteries; and water management and desalination. Papers of high technical merit addressing significant advances in the field and state-of-the-art developments are sought. (source)

139

H Index

SJR

2008	1.508
2009	1.339
2010	1.372
2011	1.292
2012	1.732
2013	1.669
2014	1.854
2015	2.090
2016	2.287

Quartiles

Energy Engineering and Power Technology	2008	Q1
Energy Engineering and Power Technology	2009	Q1
Energy Engineering and Power Technology	2010	Q1
Energy Engineering and Power Technology	2011	Q1
Energy Engineering and Power Technology	2012	Q1
Energy Engineering and Power Technology	2013	Q1
Energy Engineering and Power Technology	2014	Q1
Energy Engineering and Power Technology	2015	Q1
Energy Engineering and Power Technology	2016	Q1

Quartiles

Fuel Technology	2008	Q1
Fuel Technology	2009	Q1
Fuel Technology	2010	Q1
Fuel Technology	2011	Q1
Fuel Technology	2012	Q1
Fuel Technology	2013	Q1
Fuel Technology	2014	Q1
Fuel Technology	2015	Q1
Fuel Technology	2016	Q1

Quartiles

Nuclear Energy and Engineering	2008	Q1
Nuclear Energy and Engineering	2009	Q1
Nuclear Energy and Engineering	2010	Q1
Nuclear Energy and Engineering	2011	Q1
Nuclear Energy and Engineering	2012	Q1
Nuclear Energy and Engineering	2013	Q1
Nuclear Energy and Engineering	2014	Q1
Nuclear Energy and Engineering	2015	Q1
Nuclear Energy and Engineering	2016	Q1

Quartiles

Renewable Energy, Sustainability and the Environment	2008	Q1
Renewable Energy, Sustainability and the Environment	2009	Q1
Renewable Energy, Sustainability and the Environment	2010	Q1
Renewable Energy, Sustainability and the Environment	2011	Q1
Renewable Energy, Sustainability and the Environment	2012	Q1
Renewable Energy, Sustainability and the Environment	2013	Q1
Renewable Energy, Sustainability and the Environment	2014	Q1
Renewable Energy, Sustainability and the Environment	2015	Q1
Renewable Energy, Sustainability and the Environment	2016	Q1

ANEXO A.3

Revista: Renewable Energy

Fuente: InCites Journal Citation Reports / Web of Science / THOMSHON REUTERS

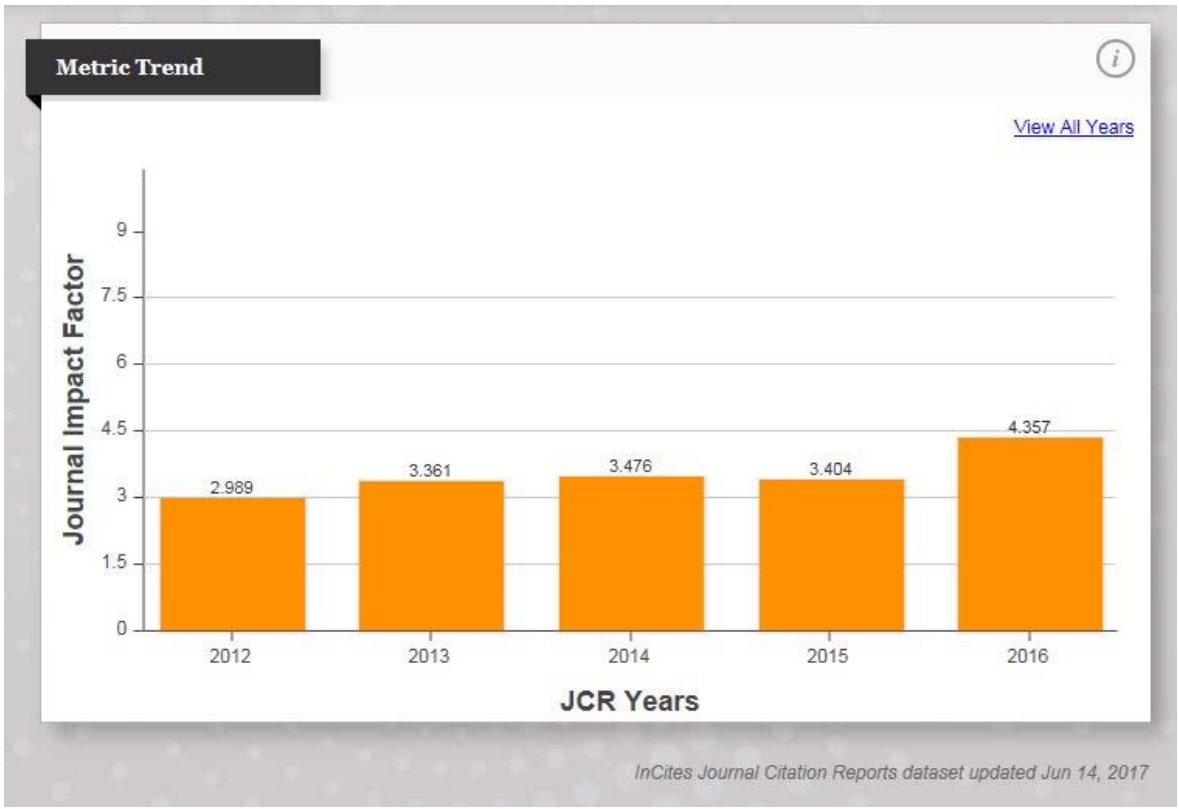

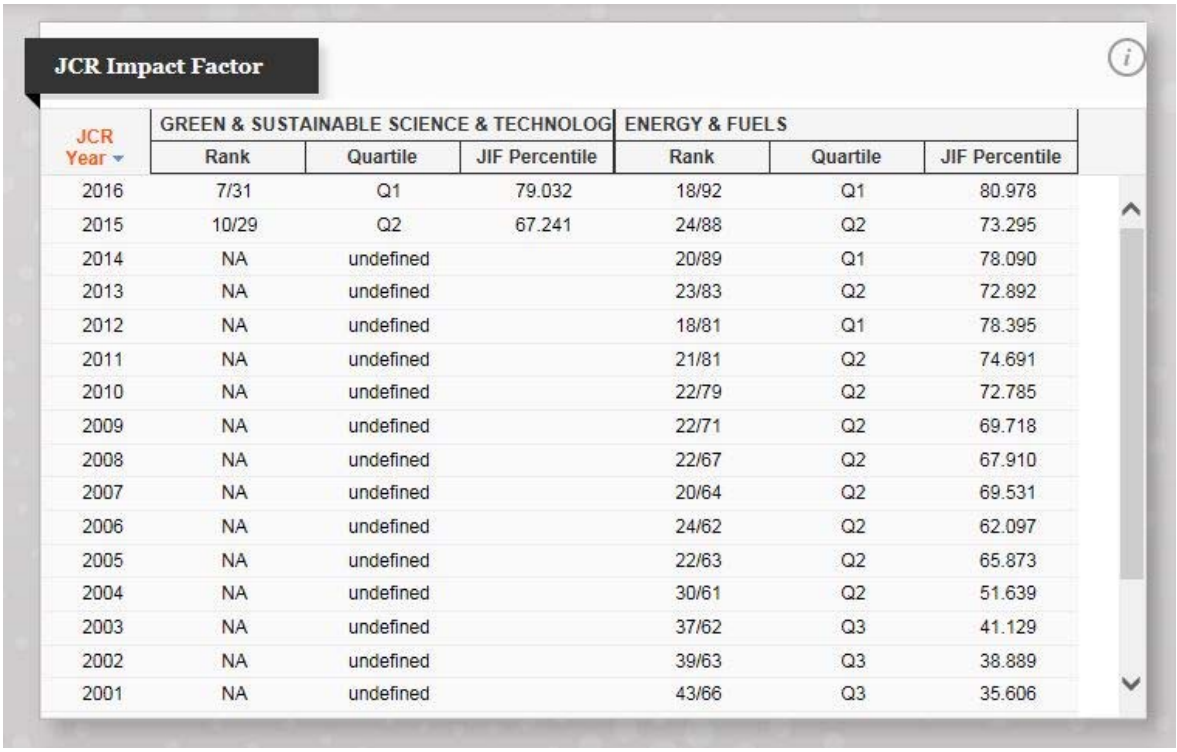

JCR Impact Factor

JCR Year	GREEN & SUSTAINABLE SCIENCE & TECHNOLOG			ENERGY & FUELS		
	Rank	Quartile	JIF Percentile	Rank	Quartile	JIF Percentile
2016	7/31	Q1	79.032	18/92	Q1	80.978
2015	10/29	Q2	67.241	24/88	Q2	73.295
2014	NA	undefined		20/89	Q1	78.090
2013	NA	undefined		23/83	Q2	72.892
2012	NA	undefined		18/81	Q1	78.395
2011	NA	undefined		21/81	Q2	74.691
2010	NA	undefined		22/79	Q2	72.785
2009	NA	undefined		22/71	Q2	69.718
2008	NA	undefined		22/67	Q2	67.910
2007	NA	undefined		20/64	Q2	69.531
2006	NA	undefined		24/62	Q2	62.097
2005	NA	undefined		22/63	Q2	65.873
2004	NA	undefined		30/61	Q2	51.639
2003	NA	undefined		37/62	Q3	41.129
2002	NA	undefined		39/63	Q3	38.889
2001	NA	undefined		43/66	Q3	35.606

ANEXO A.4

Revista: Renewable Energy

Fuente: Scimago Journal & Country Rank (SJR) / SCOPUS

Renewable Energy

Country	United Kingdom
Subject Area and Category	Energy Renewable Energy, Sustainability and the Environment
Publisher	Elsevier Ltd.
Publication type	Journals
ISSN	09601481
Coverage	1991-ongoing
Scope	The scope of the journal encompasses the following: Photovoltaic Technology Conversion, Solar Thermal Applications, Biomass Conversion, Wind Energy Technology, Materials Science Technology, Solar and Low Energy Architecture, Energy Conservation in Buildings, Climatology and Meteorology (Geothermal, Wave and Tide, Ocean Thermal Energies, Mini Hydro Power and Hydrogen Production Technology), Socio-economic and Energy Management. (source)

134

H Index

SJR

2008	1.449
2009	1.305
2010	1.494
2011	1.688
2012	1.852
2013	2.066
2014	1.983
2015	1.845
2016	1.697

Quartiles

Renewable Energy, Sustainability and the Environment	2008	Q1
Renewable Energy, Sustainability and the Environment	2009	Q1
Renewable Energy, Sustainability and the Environment	2010	Q1
Renewable Energy, Sustainability and the Environment	2011	Q1
Renewable Energy, Sustainability and the Environment	2012	Q1
Renewable Energy, Sustainability and the Environment	2013	Q1
Renewable Energy, Sustainability and the Environment	2014	Q1
Renewable Energy, Sustainability and the Environment	2015	Q1
Renewable Energy, Sustainability and the Environment	2016	Q1